LAPPEENRANTA-LAHTI UNIVERSITY OF TECHNOLOGY
School of Energy Systems
Master's Program in Bioenergy Technology

Master's Thesis

Pitch Control System for a Specific Arctic Wind Turbine

Lappeenranta, 15 June 2020

Afonso Julian Lugo

ABSTRACT

Lappeenranta University of Technology
LUT School of Energy Systems
Master's Program in Bioenergy Technology

Afonso Julian Lugo

Pitch Control System for a Specific Arctic Wind Turbine

Master's Thesis

2020

95 pages, 48 figures, 6 tables

Examiner: Professor Teemu Turunen-Saaresti
Supervisor: Professor Aki Grönman

Keywords: wind energy, wind turbines, pitch control, renewable energy, atmospheric ice

The expansion of renewable sources for energy generation is led by wind energy with 204.8 GW of cumulative installed capacity in Europe at the end of 2019. Regions of high altitude or latitude, such as Northern and Central Europe, Northern America and Asia have wind plants operating in cold climates and they are exposed to atmospheric ice, which causes problems for the wind turbine, such as increase of mechanical loads, premature shut down, reduction of lifetime of the components and power losses. Accumulation of ice on turbine's blades changes the airfoil's shape, rotor's balance and interaction between wind and blades. An investigation of the icing effects on power production is conducted to estimate power production losses and to propose a method to reduce losses and to improve energy efficiency under icing conditions based on the pitch control system. This strategy is applied in a study case for several locations in Finland and Russia, countries that have operational turbines and potential for new wind power in icing condition. Weather parameters data from MERRA2 and CFSv2 is used to simulate site operation. Conditions for atmospheric ice are set according to previous studies about ice accretion. Results show power losses between 21.2% and 28.5% for the region where pitch control is not actuating, and the optimization method reduced these losses from 15.7% and 15.3%, accordingly. In the study case, conditions for atmospheric ice varied from 1221 to 2596 hours of icing per year with yearly mean losses varying from 0.18% to 2.1%. The proposed optimization method decreased monthly mean losses up to 2.6% in severe cases. Power curve of the optimized case reduced the icing component and the power production was improved in comparison to the non-optimized case. This research contributed to the scientific field of wind energy with a new methodology to reduce power losses and to improve energy efficiency.

TABLE OF CONTENTS

NOMENCLATURE **4**

CHAPTER 1 – INTRODUCTION **5**

1.1 Introduction 5

1.2 Objectives 7

1.3 Methodology 7

1.4 Work structure 8

CHAPTER 2 - MODEL DESCRIPTIONS **9**

2.1 Wind 9

2.1.1 Wind Power *10*

2.2 Wind Turbine Aerodynamics 12

2.2.1 Power Coefficient *15*

2.3 Atmospheric Ice 16

2.3.1 Types of Ice *17*

Glaze Ice 17

Rime Ice 17

Mixed Ice 18

2.3.2 Conditions for Atmospheric Ice in this work *19*

CHAPTER 3 - AERODYNAMIC ANALYSIS **21**

3.1 Data Source 21

3.2 Data Extraction 21

3.3 Power Coefficient Curves 27

3.3.1 Summarized Results *35*

CHAPTER 4 – STUDY CASE **38**

4.1 Regions 38

4.2 Weather Data 39

4.3 Analysis of the Data 40

4.4 Results of Study Case 43

Jääräjoki, Finland *43*

Käsivarren, Finland *46*

Madetkoski, Finland *49*

Murmansk, Russia *52*

Olhava, Finland *55*

Yamalsky, Russia *58*

4.4.1 Summarized Results *61*

CHAPTER 5 - CONCLUSIONS AND RECOMMENDATIONS **63**

5.1 CONCLUSIONS 63

5.2 RECOMMENDATIONS FOR FUTURE WORK 65

REFERENCES **66**

APPENDIX A – WEATHER DATA **70**

A.1 – JÄÄRÄJOKI, FINLAND 70

A.2 – KÄSIVARREN, FINLAND 71

A.3 – MADETKOSKI, FINLAND 72

A.4 – MURMANSK, RUSSIA 73

A.5 – OLHAVA, FINLAND 74

A.5 – YAMALSKY, RUSSIA 75

APPENDIX B – CODE SCRIPTS **76**

B.1 – AERODYNAMIC ANALYSIS 76

B.2 – ENERGY YIELD 79

B.3 – POWER LOSSES 87

B.3.1 – Yearly Losses *87*

B.3.2 – Monthly Mean Losses *89*

TABLE OF FIGURES

FIGURE 1. ATMOSPHERIC CIRCULATION. (TONG, 2010) 9

FIGURE 2. AIR FLOW AT VELOCITY *U* THROUGH AREA *A*. (LETCHER, 2017) 10

FIGURE 3. SIZE EVOLUTION OF WIND TURBINES OVER TIME. (LANTZ, HAND, & WISER, 2012) 11

FIGURE 4. WIND TURBINE GENERAL STRUCTURE. (LETCHER, 2017) 12

FIGURE 5. INTERCONNECTION OF SUB-MODELS DESCRIBING THE CHARACTERISTICS OF THE WIND TURBINE. (THOMSEN, 2006) .. 13

FIGURE 6. PITCH OF THE BLADE, ANGLE OF ATTACK DEPENDENT OF THE WIND DIRECTION AND CHORD LINE, LIFT AND DRAG FORCES DEPENDENTS ON THE ANGLE FO ATTACK. (GIPE, 2004) 14

FIGURE 7. COMPARISON OF THE CURVES FOR MAXIMUM CP ACCORDING TO DIFFERENT AUTHORS. 15

FIGURE 8. GLAZE ICE FORMATION. (WIKIPEDIA, N.D.) 17

FIGURE 9. EXAMPLE OF RIME ICE ACCUMULATION. (GRIFFITH, WARD, & YORTY, 2016) 18

FIGURE 10. LOW TEMPERATURE AND ICING CLIMATE. (IEA WIND TASK 19, 2017) 19

FIGURE 11. DRAG COEFFICIENT (TOP LEFT), LIFT COEFFICIENT (TOP RIGHT) AND RATIO DRAG/LIFT (BOTTOM) FOR ICING AND CLEAN AIRFOIL BY HOMOLA ET AL. (2010). 22

FIGURE 12. DRAG COEFFICIENT (TOP LEFT), LIFT COEFFICIENT (TOP RIGHT) AND RATIO DRAG/LIFT (BOTTOM) FOR ICING AND CLEAN AIRFOIL BY ETEMADDAR ET AL. (2012). 23

FIGURE 13. DRAG COEFFICIENT (TOP LEFT), LIFT COEFFICIENT (TOP RIGHT) AND RATIO DRAG/LIFT (BOTTOM) FOR ICING AND CLEAN AIRFOIL BY TURKIA ET AL. (2013). 24

FIGURE 14. DRAG COEFFICIENT (TOP LEFT), LIFT COEFFICIENT (TOP RIGHT) AND RATIO DRAG/LIFT (BOTTOM) FOR ICING AND CLEAN AIRFOIL BY HUDECZ (2014). 25

FIGURE 15. DRAG COEFFICIENT (TOP LEFT), LIFT COEFFICIENT (TOP RIGHT) AND RATIO DRAG/LIFT (BOTTOM) FOR ICING AND CLEAN AIRFOIL BY GANTASALA ET AL. (2019). 26

FIGURE 16. CURVES OF POWER COEFFICIENT FOR CLEAN (LEFT) AND ICING (RIGHT) CASES FOR HOMOLA ET AL. (2010). 27

FIGURE 17. ANALYSIS OF THE OPTIMIZATION METHOD FOR HOMOLA ET AL. (2010). 28

FIGURE 18. CURVES OF POWER COEFFICIENT FOR CLEAN (LEFT) AND ICING (RIGHT) CASES FOR ETEMADDAR ET AL. (2012). 29

FIGURE 19. ANALYSIS OF THE OPTIMIZATION METHOD FOR ETEMADDAR ET AL. (2012) 30

FIGURE 20. CURVES OF POWER COEFFICIENT FOR CLEAN (LEFT) AND ICING (RIGHT) CASES FOR TURKIA ET AL. (2013). 30

FIGURE 21. ANALYSIS OF THE OPTIMIZATION METHOD FOR TURKIA ET AL. (2013). 31

FIGURE 22. CURVES OF POWER COEFFICIENT FOR CLEAN (LEFT) AND ICING (RIGHT) CASES FOR HUDECZ (2014). 32

FIGURE 23. ANALYSIS OF THE OPTIMIZATION METHOD FOR HUDECZ (2014). 33

FIGURE 24. CURVES OF POWER COEFFICIENT FOR CLEAN (LEFT) AND ICING (RIGHT) CASES FOR GANTASALA ET AL. (2019) 33

FIGURE 25. ANALYSIS OF THE OPTIMIZATION METHOD FOR GANTASALA ET AL. (2019). 34

FIGURE 26. COMBINED RESULTS OF THE POWER COEFFICIENTS WITH RESPECT TO WIND VELOCITY FOR THE FIVE REFERENCES 36

FIGURE 27. COMBINED AERODYNAMIC LOSSES OF THE ICING AND OPTIMIZED CASES WITH RESPECT TO THE WIND VELOCITY FOR ALL FIVE REFERENCES. 37

Figure 28. Location of the case studies in Finland and Russia. 38
Figure 29. Yearly losses for Jääräjoki, FI. 43
Figure 30. Monthly mean losses for Jääräjoki, FI. 44
Figure 31. Superposition of the power curves for Jääräjoki, FI. 45
Figure 32. Yearly losses for Käsivarren erämaa alue, FI. 46
Figure 33. Monthly mean losses for Käsivarren erämaa alue, FI. 47
Figure 34. Superposition of the power curves in Käsivarren erämaa alue, FI. 48
Figure 35. Yearly losses for Madetkoski, FI. 49
Figure 36. Monthly mean losses for Madetkoski, FI. 50
Figure 37. Superposition of the power curves in Madetkoski, FI. 51
Figure 38. Yearly losses for Murmansk, RU. 52
Figure 39. Monthly mean losses for Murmansk, RU. 53
Figure 40. Superposition of the power curves in Murmansk, RU. 54
Figure 41. Yearly losses for Olhava, FI. 55
Figure 42. Monthly mean losses for Olhava, FI. 56
Figure 43. Superposition of the power curves in Olhava, FI. 57
Figure 44. Yearly losses for Yamalsky, RU. 58
Figure 45. Monthly mean losses for Yamalsky, RU. 59
Figure 46. Superposition of the power curves in Yamalsky, RU. 60
Figure 47. Yearly mean losses for all locations in the study case. 62
Figure 48. January mean losses for all locations in the study case. 62

TABLES

Table 1. Conditions for Atmospheric Ice in this research. 20
Table 2. Data source and conditions for NACA 64618 airfoil. 21
Table 3. Summarized results of the power coefficient analysis for all five references given in Table 2. 35
Table 4. Coordinates of the locations from the study case. 39
Table 5. Annual statistical analysis of the six locations of the study case. 40
Table 6. Summarized results of the study case. 61

NOMENCLATURE

p	pressure	[bar], [Pa]
T	temperature	[ºC], [K]
V	volume	[m^3]
A	area	[m^2]
R	radius	[m]
Ke	kinetic energy	[J]
U	velocity	[m/s]
m	mass	[kg]
Tr	rotor's torque	[N.m]
Pr	rotor's power	[W]
ω_r	rotor's speed	[rad/s]
v	wind speed	[m/s]
c_p	power coefficient	-
λ	tip-to-speed ratio	-

Subscripts

opt	optimized case
clean	clean case
non-opt	non-optimized case

CHAPTER 1 – INTRODUCTION

1.1 Introduction

Wind energy is a renewable energy source with a fast global development, leading the expansion on the share of the electricity production from clean energy sources. Europe finished 2019 with a cumulative capacity of 204.8 GW with 14,1 GW of new capacity added that year. (Wind Europe, 2020)

Currently, there are wind turbines installed in cold climates in Northern and Central Europe, Northern America, and Asia. The artic region plays an important role of wind production in Scandinavia and the estimated potential for Finland is at least 3 GW, but it carries some challenges for its exploitation from the initial site assessment, during the construction of the wind plant and during its operation. (IEA Wind Task 19, 2017)

A wind turbine is designed to operate under predefined limits of torque in a range of ambient conditions. Due to the intermittency of the wind, a control system is required to maintain the machine operating under its designed limits, thus the equipment will not be damaged, and the lifetime will not be reduced. The pitch control system actuates to keep the rotational speed constant when the wind intensity is above the nominal wind speed of the turbine.

Wind turbines are exposed to ice formation in cold weather and this phenomenon causes a variety of problems to the machine, such as increasing of mechanical loads on the turbine's components and power production losses (Clausen & Giebel, 2017). Furthermore, icing increases possibility of ice throw and unbalance on the rotor, increasing the dynamics loads and noise level and it might lead to premature failure of the system and financial losses (Turkia, Huttunen, & Thomas, 2013) (IEA Wind Task 19, 2017).

In Finland, the availability of wind turbines caused by icing events decreased by 0.3% to 4.1% from 1996 to 2010 with 114 hours of average downtime. It corresponds to 1.4% of the annual operational hours, an average of 16 turbines reported downtime for icing problems per year. (IEA Wind Task 19, 2012)

Although the effects of icing in aircraft airfoils have been investigated since 1920s, only in the last 20 years studies were made focusing on the power loss production in wind turbines due to icing events. Super-cooled water droplets accrete to wind turbine's blades, changing

the surface roughness of the airfoil sections and degrading its performance, which is the main cause of lower power production. When the wind hits the blade one force is acting with two vectors: lift and drag. The lift force is perpendicular to the wind direction and it pulls the blade while the drag is in the same direction of the wind, hence, icing causes reduction of lift force and increase of drag force. (Clausen & Giebel, 2017)

Etemaddar et al. (2012) made a complete study about the effects of different parameters on the aerodynamics of the blade and it was pointed out that the difference between clean and iced blade profile increase with the increasing of the angle of attack, therefore in low wind speeds, when the angle of attack are larger than 5º the loss due to icing is higher than in higher wind speeds, when the angle of attack is below 5º (Etemaddar, Hansen, & Moan, 2012).

In freezing fog conditions, it was observed a 16% loss of airfoil lift and 190% increase of airfoil drag when the temperature is near 0 ℃ and for a freezing drizzle icing event, a 25% loss of airfoil lift and 220% of airfoil drag were observed and the conclusion was the differences in power loss are correlated to difference between clean and iced airfoil in: temperature, ice surface roughness and ice impingement length. (Blasco, Palacios, & Schmitz, 2016)

In cold climates the wind turbine is exposed to icing formation on the rotor, causing a variety of problems for the operation of the machine. For the loss of annual electricity production due to icing, some researchers with different approaches found results up to 10% loss without blade heating (Dierer, Oechslin, & Cattin, 2011), 22% loss using time series of wind speed and icing (Byrkjedal, 2009), while 25% loss was estimated in a wind plant in Sweden (Haaland, 2011).

Despite some authors discuss the effects of icing events on turbine's blades aerodynamics and on power productions, there is no concrete methodology to estimate annual power losses due to icing events in a wind plant. On top of that, a methodology to optimize the power production is valuable for wind plant developers and wind turbine manufacturers. Given these points, this investigation is conducted in the point of view of the pitch control system.

1.2 Objectives

This work aims to develop an arctic specific pitch control design program/method for optimizing the power production in various wind shear conditions.

1.3 Methodology

This research is divided into two parts. The first part investigates the behaviour of the aerodynamic coefficients of an airfoil with icing and discusses the optimization of aerodynamic performance. The second part proposes the methodology for the Optimized Annual Aerodynamic Performance.

For the evaluation of the aerodynamic losses, the power coefficient for an airfoil with ice formation and for a clean one will be estimated with data collected from previous works about icing formation/accretion for the same type of airfoil. One investigation is conducted in terms of the aerodynamic coefficients in order to get the main parameters that might contribute to the power loss. Once the analysis is performed, an optimization method is proposed to optimize the aerodynamic performance of the airfoil considering ice formation.

The ice formation does not occur all the time, but in some specific weather conditions which need to be considered for the estimation of the annual losses. Such conditions are assumed according to the literature about ice formation/accretion in airfoils and a methodology for estimating the annual energy production (AEP) considering icing on the blades will be proposed. The results are tested for several locations in Finland and Russia with wind data from the Modern-Era Retrospective analysis for Research and Application version 2 – MERRA2, from NASA, and weather data from the Climate Forecast System – CFS, from the National Centers for Environmental Prediction – NCEP.

Results of the study cases show the power production losses due to icing for the case with no optimization named “Icing Case”, and for the case with optimization named “Optimized Case”, and it is expected to show a reduction of the power losses due to this proposed method.

1.4 Work structure

In Chapter 1 the introduction of the thesis is presented, with the justification of the present research, objectives, methodology and description of the work structure presented in this report.

In Chapter 2, firstly the wind is described with its formation, actuating forces, global and local behaviours and the models of wind energy and wind power output are presented. Secondly, the aerodynamic forces are explained, focusing in the description of lift and drag coefficients and finally the power coefficient is discussed. Finally, the atmospheric ice is described, classified according to the norms and the conditions for its formation.

In Chapter 3 the proposed methodology is presented and data used in this research is extracted, visualized and discussed. Calculations of the power coefficient curves will be done according to the known literature and the strategy for the optimization method will be analysed.

In Chapter 4 the results from the previous chapter will be tested in several locations in Finland and Russia in which the icing phenomenon occurs. To have realistic results, weather data from MERRA2 and CSFv2 will be used for each location to simulate the wind conditions. A discussion to analyse the results comparing each location will be done in the last part of the chapter

In Chapter 5 the conclusions of this thesis are done in terms of the expected results for each step of the investigation. Observations of the strong and weak point of this research will be made and suggestions of future works will be proposed based in this experience.

The Appendix A – Weather Data shows a sample of the data used in this study because the entire dataset of each location has almost 80,000 timestep. The Appendix B – Code Scripts shows the codes written in Python programming language to perform all calculations described in this research.

CHAPTER 2 - MODEL DESCRIPTIONS

2.1 Wind

Wind can be defined as the atmospheric air in motion. The Sun heats up the Earth's surface through its irradiation and the spherical surface of the planet causes the irregular distribution of the solar irradiation. Regions in the equator, latitude 0º of the Earth, receive more energy from the Sun than the rest of the globe, causing difference of temperature (Letcher, 2017). This uneven distribution of heat through Earth's surface is converted to air motion. Hot air has a lower density than cold air, consequently it is lighter for the same volume. When the solar irradiation heats the surface (land or sea), the air will receive this energy from the surface and will rise up to the sky and when it reaches enough height it starts to spread to the poles (North and South) and descends in the subtropics. Wind energy is a result of the air pressure difference mainly explained due to the uneven distribution of solar irradiation on the different latitudes. (Emeis, 2013)

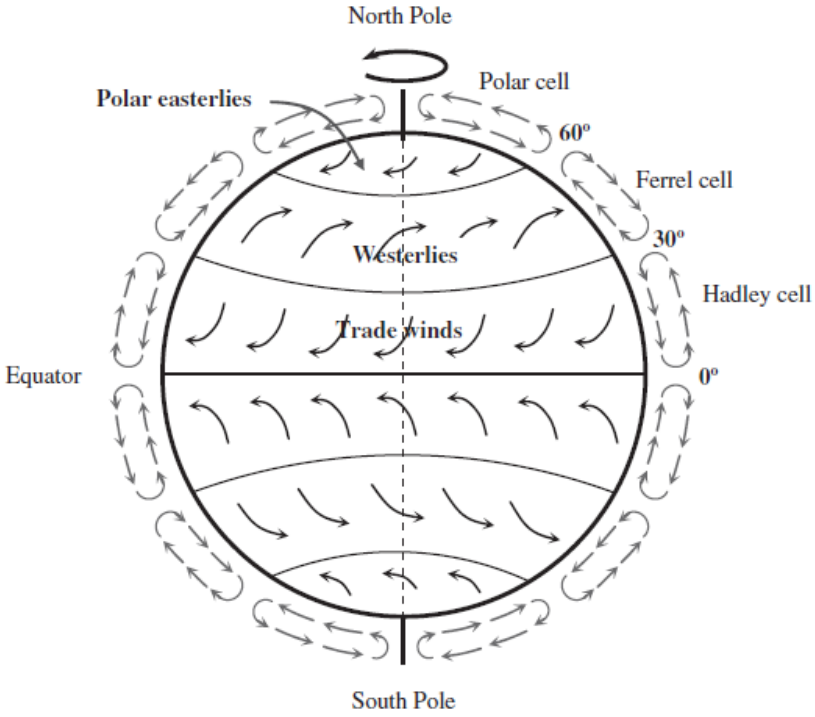

Figure 1. Atmospheric circulation. (Tong, 2010)

The Earth's self-rotation generates a force known as "Coriolis Force" and it impacts the path of the winds on the Earth's surface. This movement makes the atmospheric air that is moving from the equator to the poles or vice versa to bend in direction East-West. The combination of the Coriolis force and the uneven solar irradiation on the globe's surface causes this big

cell from the equator to the polar to break into three cells in each hemisphere: Hadley cell (between 0 and 30º latitudes), Ferrel cell (between 30º and 60º latitudes) and Polar cell (between 60º latitudes and north pole) (Tong, 2010). The north easterly winds are known as the trade winds, as illustrated in Figure 1, and these global wind cells have a spatial scale of 10,000 km. Temperature difference between ocean and continent and large north south oriented mountains modify the global wind system in a spatial scale of 1,000 km (Emeis, 2013).

2.1.1 Wind Power

Wind energy is a type of kinetic energy and it is defined as the energy of the air flow due to its motion and the expression is written as following:

$$Ke = \frac{1}{2}mU^2 \tag{1}$$

Wind power is a measure of the flux of wind energy flowing through an area of interest. (Letcher, 2017). Figure 2 is a schematic representation of a wind flow with velocity *U* through an area of interest *A*.

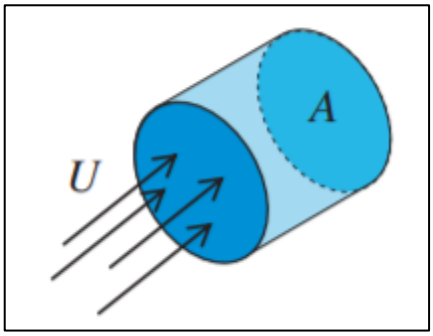

Figure 2. Air flow at velocity *U* through area *A*. (Letcher, 2017)

Considering the air density as ρ and *dt* as unit time, the mass flow rate represented in Figure 2 can be written as:

$$\frac{dm}{dt} = \rho AU \tag{2}$$

Substituting the flow rate from equation (2) in the mass of equation (1), the relation gives us the power of the wind:

$$P = \frac{1}{2}\rho A U^3 \tag{3}$$

This equation is known as the *Fundamental Equation of Wind Power*, and it has a nonlinear cubic dependence on the wind speed.

By analysing equation (3) it is possible to note that the main parameter to increase power is by increasing wind speed and it can be achieved with higher towers. The second parameter to increase wind power is area *A* and it can be achieved by increasing the size of the blades. Therefore, the modern wind turbines are getting taller with respect to tower hub height and bigger with respect to blade size, as illustrated in Figure 3.

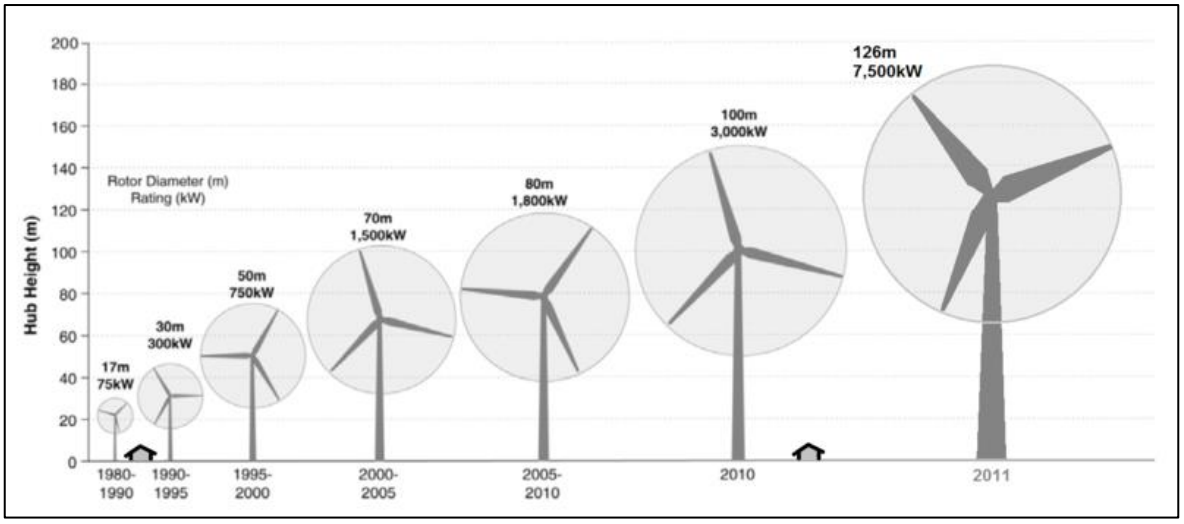

Figure 3. Size evolution of wind turbines over time. (Lantz, Hand, & Wiser, 2012)

When the wind hits a wind turbine, one part of the wind energy is extracted to move the rotor and the other part is deflected. The maximum amount of energy that can be extracted from the wind was defined as 16/27, or 59.3%, and this result was found by two scientists: Albertz Betz, from Germany and Nikolai Joukowsky, from Russia. Both published article in the year of 1920, so the result is called Betz-Joukowsky limit (Okulov & van Kuik, 2009).

A wind turbine is composed mainly by a support tower, a nacelle where the generator, motors for yaw and pitch control and other equipment are located, a hub to connect the blades with the generator and the blades to transform the kinetic energy from the wind into mechanical rotation. The general picture of a horizontal wind turbine is shown in Figure 4.

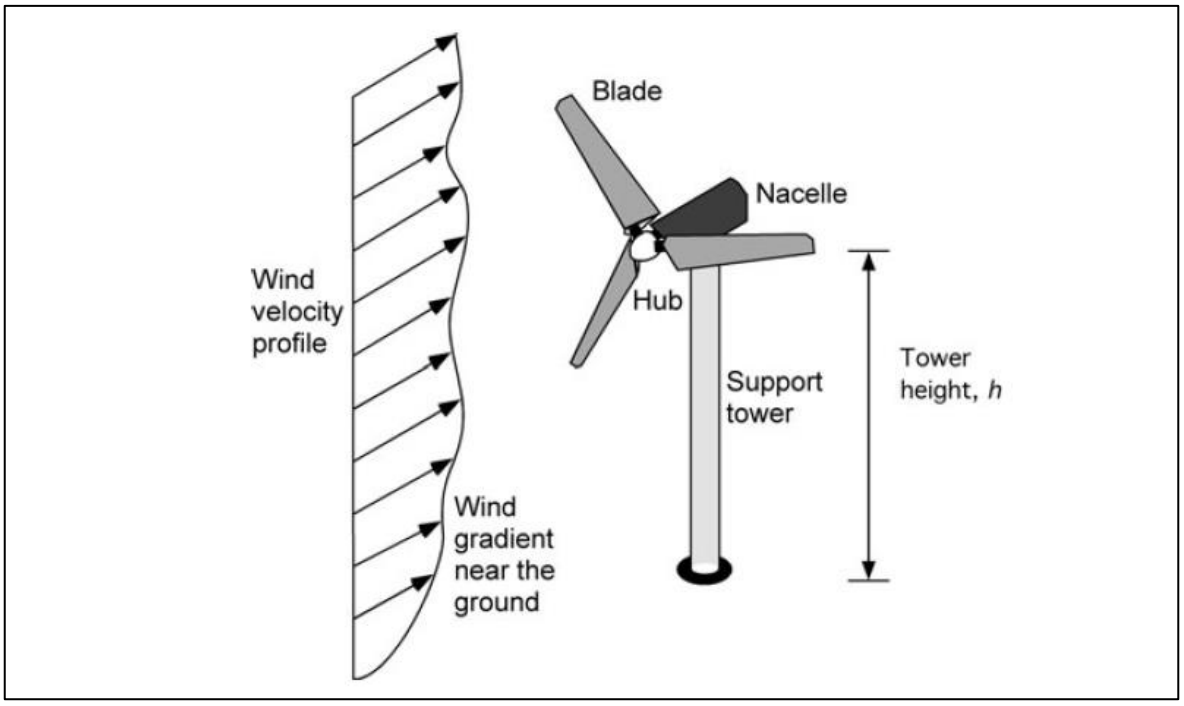

Figure 4. Wind turbine general structure. (Letcher, 2017)

For this research, the focus is on the aerodynamic parameters that affects the power production of the wind turbine. A detailed explanation of these parameters and how they related to the power production is presented on the next topic.

2.2 Wind Turbine Aerodynamics

A wind turbine is a complex system which can be described by subsystems according to its main characteristics: (Thomsen, 2006)

- Aerodynamics
- Mechanics
- Generator
- Actuator (pitch control)

These sub-models have their own characteristics, which are interconnected according to the parameters shown in Figure 5.

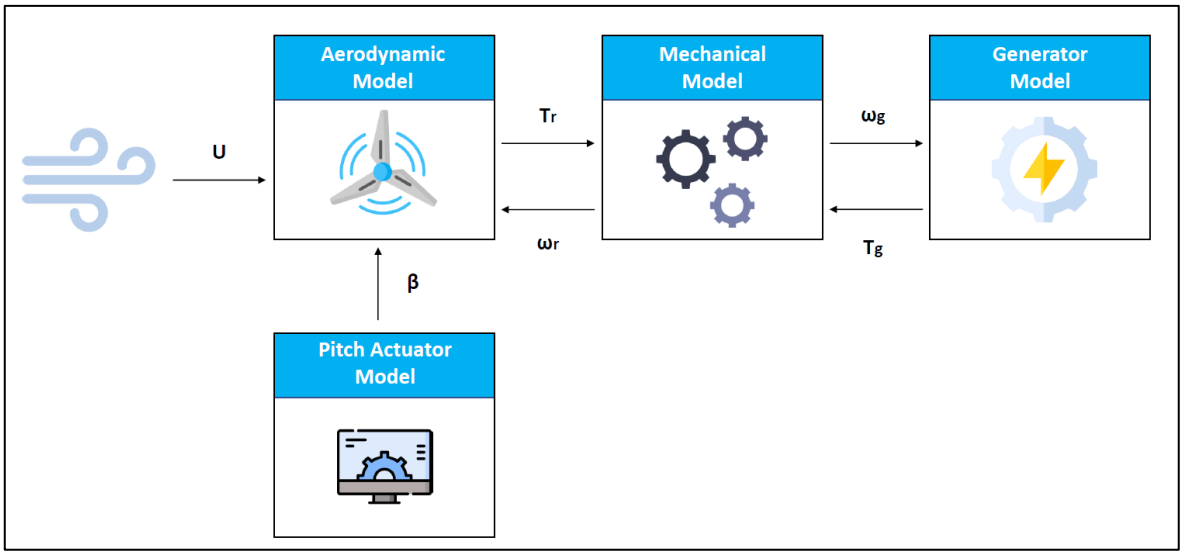

Figure 5. Interconnection of sub-models describing the characteristics of the wind turbine. (Thomsen, 2006)

Torque on the rotor can be calculated as a ratio between rotor's power and rotor's rotational speed:

$$T_r = \frac{P_r}{\omega_r} \tag{4}$$

The power of the rotor is given by the following relation:

$$P_r = \frac{1}{2}\rho\pi R^2 v^3 c_p(\lambda, \beta) \tag{5}$$

Where ρ is the air density, R is the blade radius, v is the wind speed and c_p is the power coefficient, which is a function of the tip-to-speed ratio λ and the blade pitch angle β. The tip-to-speed ratio is the ratio between the wind speed and the blade tip speed, described by the follow equation:

$$\lambda = \frac{v}{v_{tip}} = \frac{v}{R\omega_r} \tag{6}$$

Control designs use the derivative of c_p with respect to Tip-to-speed Ratio (λ) and pitch angle (β). The pitch control is used to change the intensity of lift and drag forces and regulate the power that comes from the rotor to optimize energy production and to ensure that mechanical loads do not exceed limitations. When the wind speed is below the rated operation, the pitch angle is 0º to optimize energy capture, and when the wind speed increases above the rated operation, the pitch control changes the angle to keep torque constant and maintain power and rotor speed at rated value (Mathew & Philip, 2011).

In Figure 6, the main parameters used in this study are shown on the cross-sectional shape of a blade (airfoil). Lift and drag forces are the components of the vector named ‘Force’ that moves the blade, and they are dependents on the angle of attack, that is the angle between the chord line of the airfoil and the relative wind. Pitch angle is between the chord line and the blade direction of travel, and it is possible to note that pitch and angle of attack have a negative relation, if one is increased, the other one is decreased.

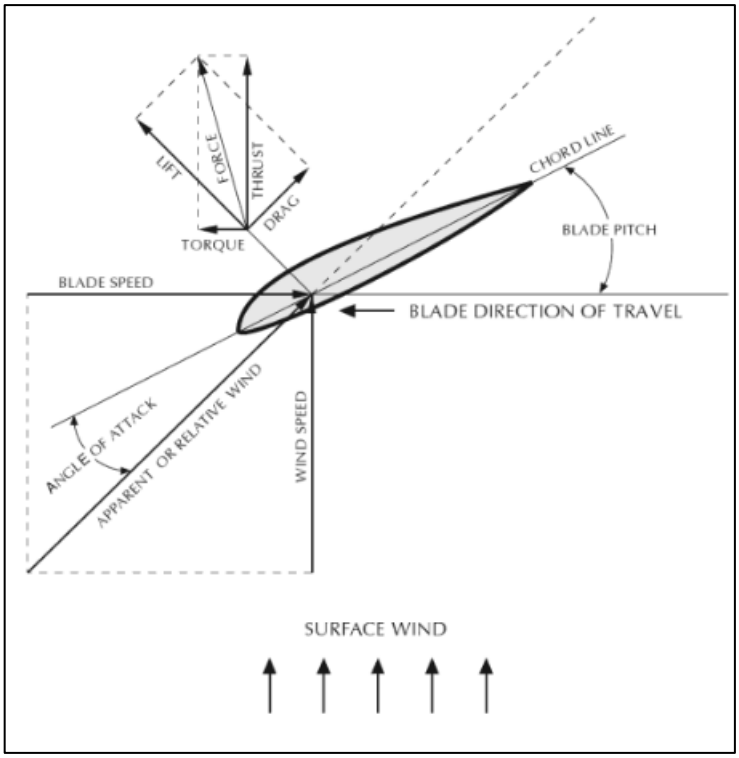

Figure 6. Pitch of the blade, angle of attack dependent of the wind direction and chord line, lift and drag forces dependents on the angle fo attack. (Gipe, 2004)

All wind turbines have their specific airfoil shape and one optimal angle of attack, where the aerodynamic performance of the blades are maximized, and the designers must calculate the optimal parameters for maximum energy production and to control mechanical loads on the machine. When the wind speed increases, the rotor must to spin faster to capture more energy, so relation between the tip of blade and wind speed at the hub is constant, in other words, the tip-to-speed ratio must be constant (Gipe, 2004).

The next topic provides the equations that correlates lift and drag coefficients (dependents on angle of attack) and the tip-to-speed ratio.

2.2.1 Power Coefficient

According to Wilson et al. (1976), it is possible to calculate the maximum power coefficient with the number of blades *B*, Tip-to-speed Ratio (λ) and lift and drag coefficients (C_l and C_d, respectively): (Wilson, Lissaman, & Walker, 1976)

$$C_{pmax} = \left(\frac{16}{27}\right)\lambda\left(\frac{B^{2/3}}{1.48 + (B^{2/3} - 0.04)\lambda + 0.0025\lambda^2} - \left(\frac{C_d}{C_l}\right)\frac{1.92B\lambda}{1 + 2B\lambda}\right) \quad (7)$$

On the other hand, Manwell et al. (2010), describes a slightly different way to calculate the maximum power coefficient with the same parameters: (Manwell, McGowan, & Rogers, 2010)

$$C_{pmax} = \left(\frac{16}{27}\right)\lambda\left[\lambda + \frac{1.32 + \left(\frac{\lambda - 8}{20}\right)^2}{B^{2/3}}\right]^{-1} - \frac{(0.57)\lambda^2}{\frac{C_l}{C_d}\left(\lambda + \frac{1}{2B}\right)} \quad (8)$$

The results of these equations are shown in Figure 7. When the Drag is zero, the maximum *Cp* is achieved, represented by the blue curve and it is possible to note that it is close the theoretical maximum from the *Betz' Law*.

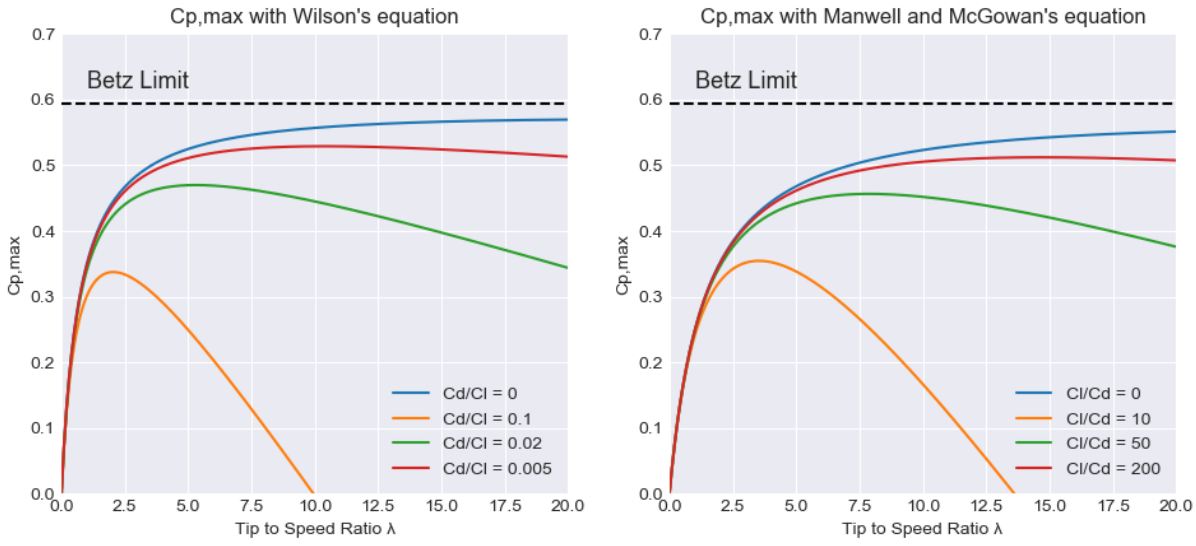

Figure 7. Comparison of the curves for maximum Cp according to different authors.

In this study, equation (7) from Wilson et at. (1976) is used because it is the most used equation for maximum power coefficient in the known literature.

2.3 Atmospheric Ice

In winter times, if the temperature is close to 0 ºC, it is common to see snow when the conditions are favourable. This snow can be a freezing rain, drizzle, or wet snow, and if the temperature decreases this accumulated wet snow will freeze and create ice. (Haaland, 2011)

The definition of atmospheric icing is the period where atmospheric conditions are favourable for the accretion of ice or snow on objects that are exposed to the atmosphere. (IEA Wind Task 19, 2017)

According to the Standard ISO 12494:2017, atmospheric ice can be classified in two types:

- In-cloud icing: formed by supercooled water droplets when the temperature is below 0 ºC. The types of ice for this event are rime ice, glaze ice and mixed ice.
- Precipitation icing: it comes from precipitation such as wet snow or freezing rain.

Ice formation depends in many factors involving the weather of the site:

"*The physical and mechanical characteristics of the accreted ice depend on different meteorological and characteristics of the accreted ice depends on meteorological and atmospheric parameters, such as the air liquid water content (LWC), median volume diameter (MVD), air temperature, relative humidity, wind speed, atmospheric pressure and air density.*" (Hudecz, 2014)

The type of ice depends on the heat balance at the surface during its accretion and this is mainly a function of temperature, air liquid water content and wind speed. (Davis, 2014)

For the wind turbine operation, in-cloud rime icing has more impact because it is formed in low temperatures and it get accreted on the rotor, changing its shape and mass, causing a variety of problems in the wind turbine such as power loss and increase of mechanical loads (IEA Wind Task 19, 2017).

2.3.1 Types of Ice

Glaze Ice

When the temperature is just below 0 ºC, the wind speed is increasing and the water content in the air is high, ice can be accreted on any surface, and it has a transparent appearance, glassy shiny surface or ice cubes and high density (Hudecz, 2014) and its appearance is seen in Figure 8.

Figure 8. Glaze ice formation. (Wikipedia, n.d.)

The droplet that hits the object does not freeze immediately, it spreads through the surface, making it wet and freezing it slowly, removing most of the air and giving a higher density for the ice when it is accreted. (Haaland, 2011)

Rime Ice

The rime ice occurs when the temperature is lower, usually lower than -4 ºC and higher than -20 ºC and the droplet freezes completely with the impact on the object, so it is not spread through the surface (IEA Wind Task 19, 2017). It is white, opaque, and streamlined

accretion, and it is more porous, therefore it has a lower density than glaze ice (Hudecz, 2014). This type of ice has two subdivisions:

- Soft rime: it is formed when droplets freeze immediately with the impact on the object, allowing air to be trapped during the freezing process, giving a lower density and a whiter appearance to the ice.
- Hard rime: it occurs when the droplets take a longer time to freeze on the surface of the object, giving a stronger adhesion, higher ice density and more opaque appearance.

Figure 9. Example of rime ice accumulation. (Griffith, Ward, & Yorty, 2016)

Mixed Ice

Mixed ice, as the name suggest, is a mix between glaze and rime ice and it forms when the temperature is decreasing and it has characteristics of glaze ice in the area of stagnation line, and characteristics of rime ice on both sides of the stagnation zone. (Addy, 2000)

2.3.2 Conditions for Atmospheric Ice in this work

According to the literature in this topic, there are several meteorological conditions for the formation of ice on structures and many experiments were conducted to simulate the ice accretion as close as possible to a real case. Some parameters used in previous researches are difficult to obtain from global information, such as air liquid water content and median volume diameter, but others are available from satellite data and forecast reanalysis observations, such as temperature, relative humidity and wind speed.

Firstly, the site is evaluated if it has conditions to be classified as Cold Climate (CC) by checking if it is a Low Temperature Climate (LTC) site and an Icing Climate (IC). Moreover, if temperature is lower than -20 ºC for more than 9 days in one year, the site can be defined as Low Temperature Climate (LTC) (IEA Wind Task 19, 2017).

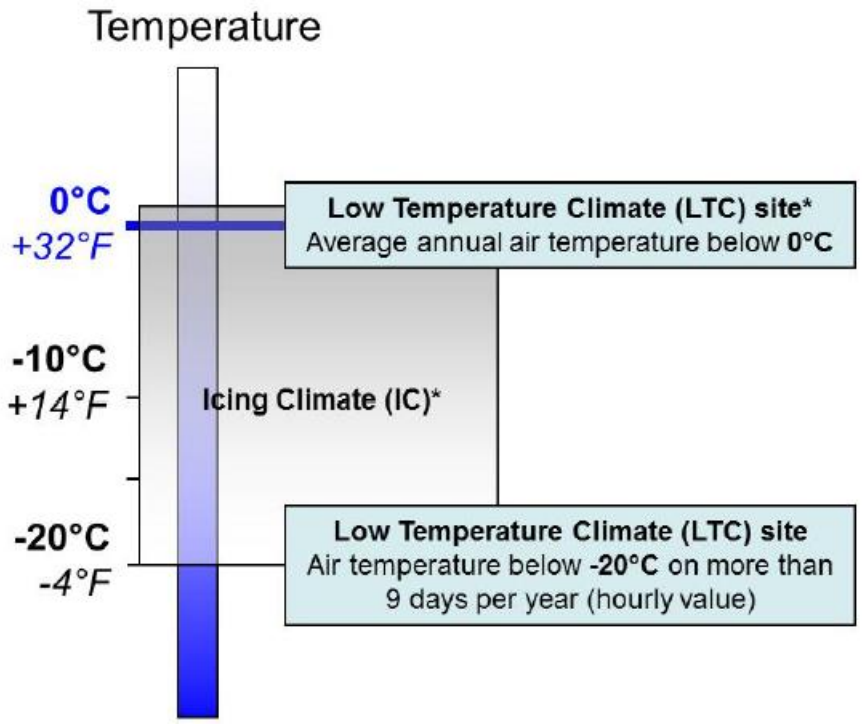

Figure 10. Low temperature and icing climate. (IEA Wind Task 19, 2017)

Most of the aerodynamic analysis of the effects of ice accretion on wind turbine's blades were done with rime ice and it occurs when temperature is lower than -4 ºC and higher than -20 ºC (Hudecz, 2014), so this range of values are used in this study.

The wind speed affects the ice accumulation and experiments were made with a variety of intensity values to evaluate the aerodynamic parameters. As most of modern wind turbines has the cut-in of 3 m/s, this value is used as the bottom parameter for atmospheric ice.

Air liquid water content is the third most import parameter for atmospheric ice formation (Davis, 2014) but it is difficult to find a global database for it. Freudenreich et al. (2016) used relative humidity higher than 90% in site measurements to determine icing events and they had accuracy of 90%. Within the cloud, the relative humidity is close to 100% or even higher, so the value of 90% might give false-positive results (Rast, Cattin, & Heimo, 2009).

Aerodynamic coefficients lift and drag for the icing and clean case used in this study and described in Chapter 3, were estimated for specific conditions, such as air temperature, air liquid content and droplet median volume diameter, meaning these coefficients would have variations by changing these conditions. Relative humidity has a significant impact when considered in ice formation and it reached up to 35% of annual hours of icing for some locations when 90% was considered. In this research, relative humidity is used with the value of 95% to have more realistic results.

For these reasons, the conditions for atmospheric ice formation used in this research are according to the Table 1.

Table 1. Conditions for Atmospheric Ice in this research.

Parameter	**Condition**
Wind Speed	$\geq$ 3 m/s
Temperature	- 4 ºC $\geq$ T $\geq$ -20 ºC
Relative Humidity	$\geq$ 95%

Parameters listed on Table 1 are available in different types, such as annual mean, monthly mean, daily mean, 6 hours mean and 1 hour mean. When it comes to wind micro-siting, the sorter the timestep of the variable, the more precise the analysis for power production and for this reason, the shortest timestep (1 hour) will be used.

CHAPTER 3 - AERODYNAMIC ANALYSIS

3.1 Data Source

For the analysis of the aerodynamic performance of a blade with ice accretion and to compare it with a clean blade, previous research on the topic was used. Some authors use different techniques to evaluate the effects of the ice on an airfoil of a wind turbine. The authors and the conditions are listed in the Table 2. The works were chosen because they provide data about lift and drag coefficients for the clean and icing cases for the same type of airfoil.

Table 2. Data source and conditions for NACA 64618 airfoil.

Author	**Type of Study**	**Year**	**Reynolds Number**	**Velocity at the hub [m/s]**
Homola et al.	Numerical	2010	$1.26 \cdot 10^6$	19.2
Etemaddar et al.	Numerical	2012	$2.0 \cdot 10^6$	6
Turkia et al.	Numerical	2013	$1{,}2 \cdot 10^6$	7.3
Hudecz	Experimental	2014	$1{,}0 \cdot 10^6$	3.2
Gantasala et al.	Numerical	2019	$1{,}85 \cdot 10^6$	2.2

The data collected for the analysis are lift and drag coefficients and wind speed, for iced and clean cases. These data will be used to apply models of wind turbine characteristics and calculate the power coefficient for each wind condition.

3.2 Data Extraction

As described in the previous chapters, the main parameters that affect the aerodynamic performance of a wind turbine are lift and drag coefficients. Data were extracted using digitizer tools to convert graph data to numeric data. Next images show drag and lift coefficients for angle of attack varying from 0 to 10º for the different authors. The third graph of each case is the ratio Drag/Lift per angle of attack, and it is important when analysing the equations for power coefficients. Results are slightly different because each

experiment was done in different conditions with different methods, but all of them follow the expected logical results.

Homola et al. (2010) made a numerical study of ice accretion using software TURBICE, with the results, a flow field characteristic was carried out for a 5 MW pitch-controlled wind turbine using CFD simulations with ANSYS FLUENT. The results for the aerodynamic coefficients are represented in Figure 11 with drag and lift (top images) and the ratio of drag per lift (bottom image).

It is possible to note that in lower angle of attack the effect of icing is higher, on the other hand for the lift, the icing effect is higher when the angle of attack is 10º. In the conclusions of their work, it was written that lift coefficient is reduced in a higher proportion when the icing causes “horn type of glazed icing shapes” and the accuracy would be improved when more atmospheric parameters are measured.

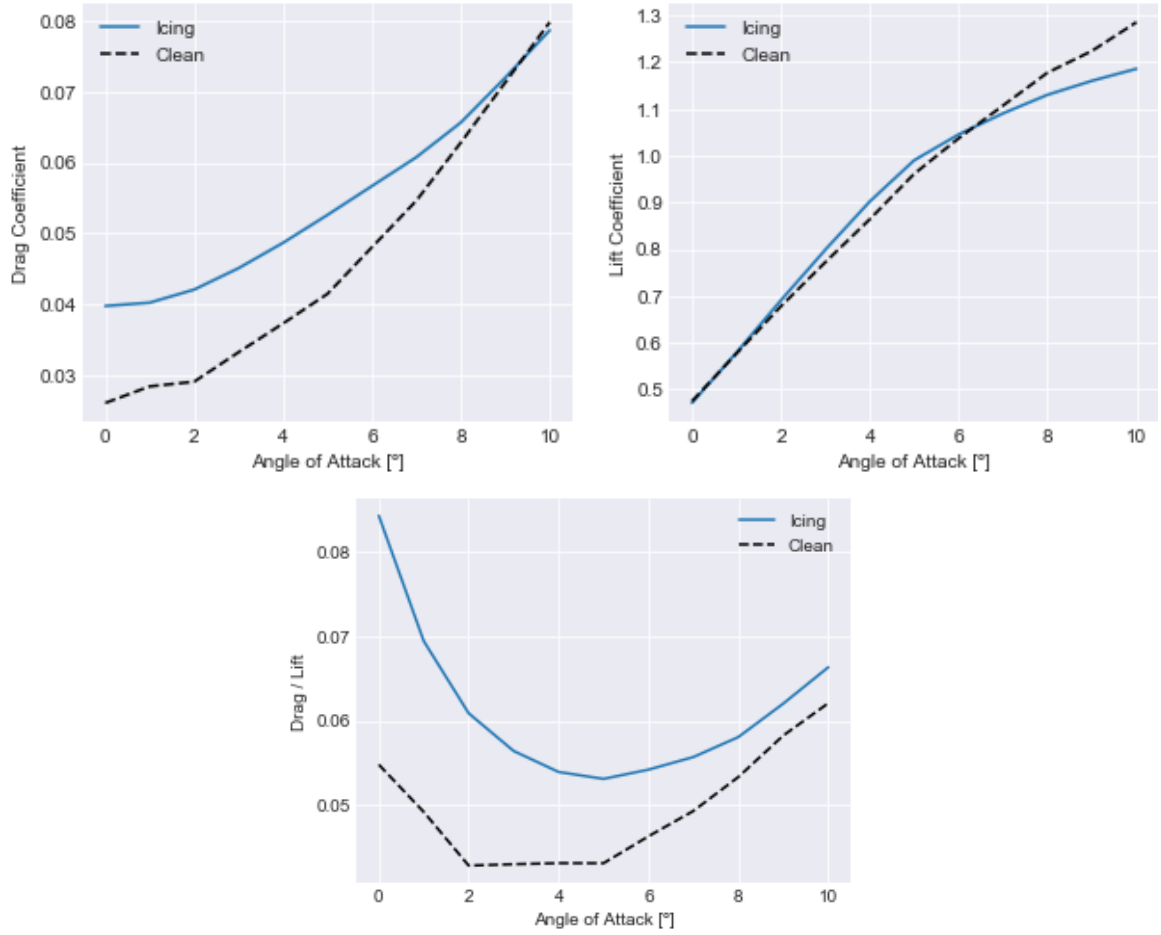

Figure 11. Drag coefficient (top left), lift coefficient (top right) and ratio drag/lift (bottom) for icing and clean airfoil by Homola et al. (2010).

Etemaddar et al. (2012) made a numerical study of ice accretion using the 2D ice accumulation software LEWICE and used computational fluid dynamics code FLUENT to estimate the aerodynamic coefficients of the blade.

Temperature and angle of attack are the two main parameters for ice geometry that change curvature of the blade, and when temperature is near zero Celsius degrees the ice profile has double peak (Etemaddar, Hansen, & Moan, 2012). The results for the aerodynamic coefficients are represented in Figure 12. For this case, both drag and lift are more affected by icing when the angle of attack is increasing.

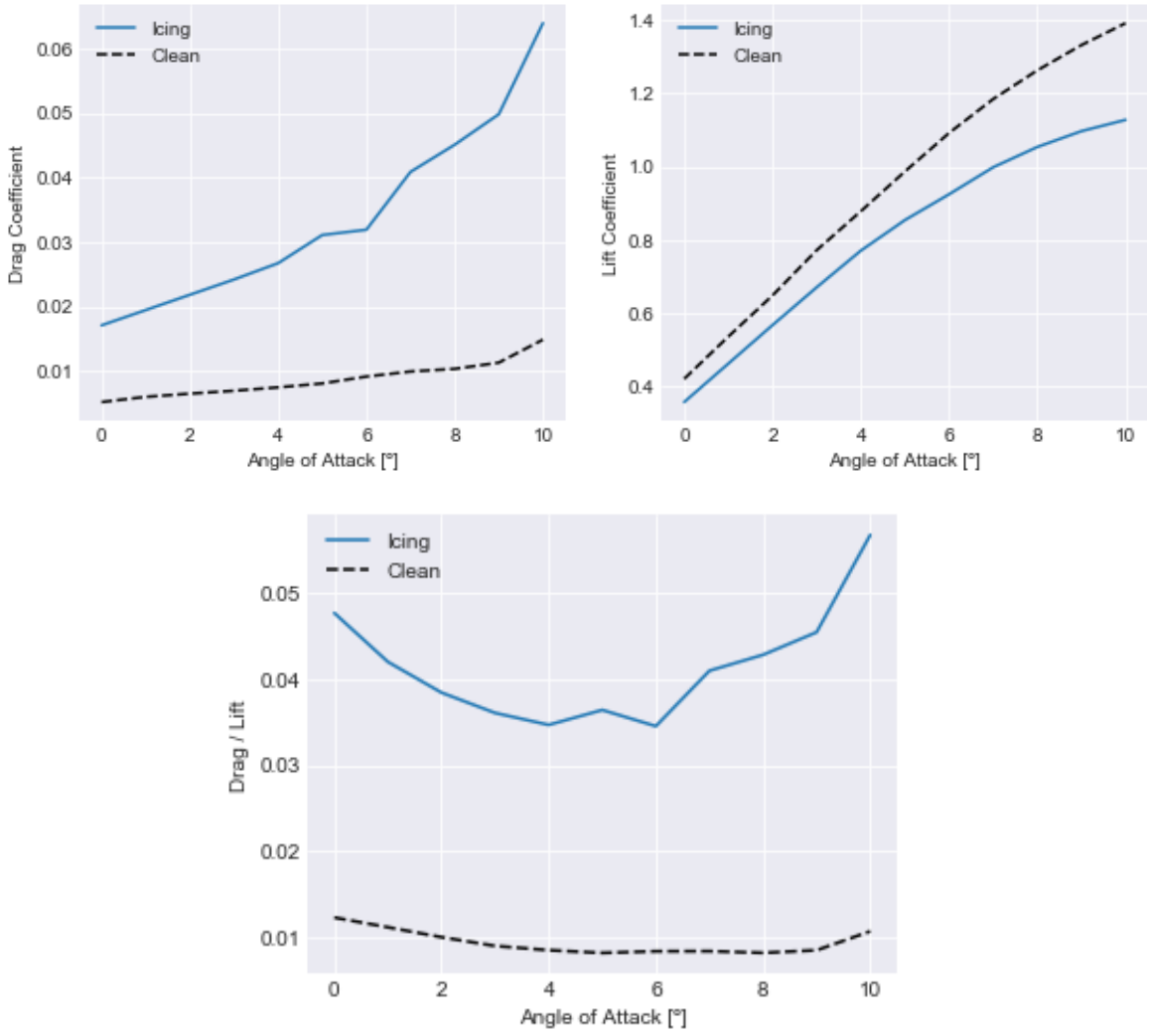

Figure 12. Drag coefficient (top left), lift coefficient (top right) and ratio drag/lift (bottom) for icing and clean airfoil by Etemaddar et al. (2012).

Turkia et al. (2013) made a numerical study of ice accretion using software TURBICE to model the ice with 3 different masses and solved the aerodynamic parameters using ANSYS FLUENT flow solver.

The ice shape and the large-scale surface roughness have a significant impact on drag coefficient but not significant effect on lift coefficient slope. “Results show decreasing production levels for iced up turbine. Main cause for the lower production levels was noticed to be the small-scale surface roughness that increases drag significantly”. Figure 13 shows drag and lift coefficient for Turkia et al. (2013).

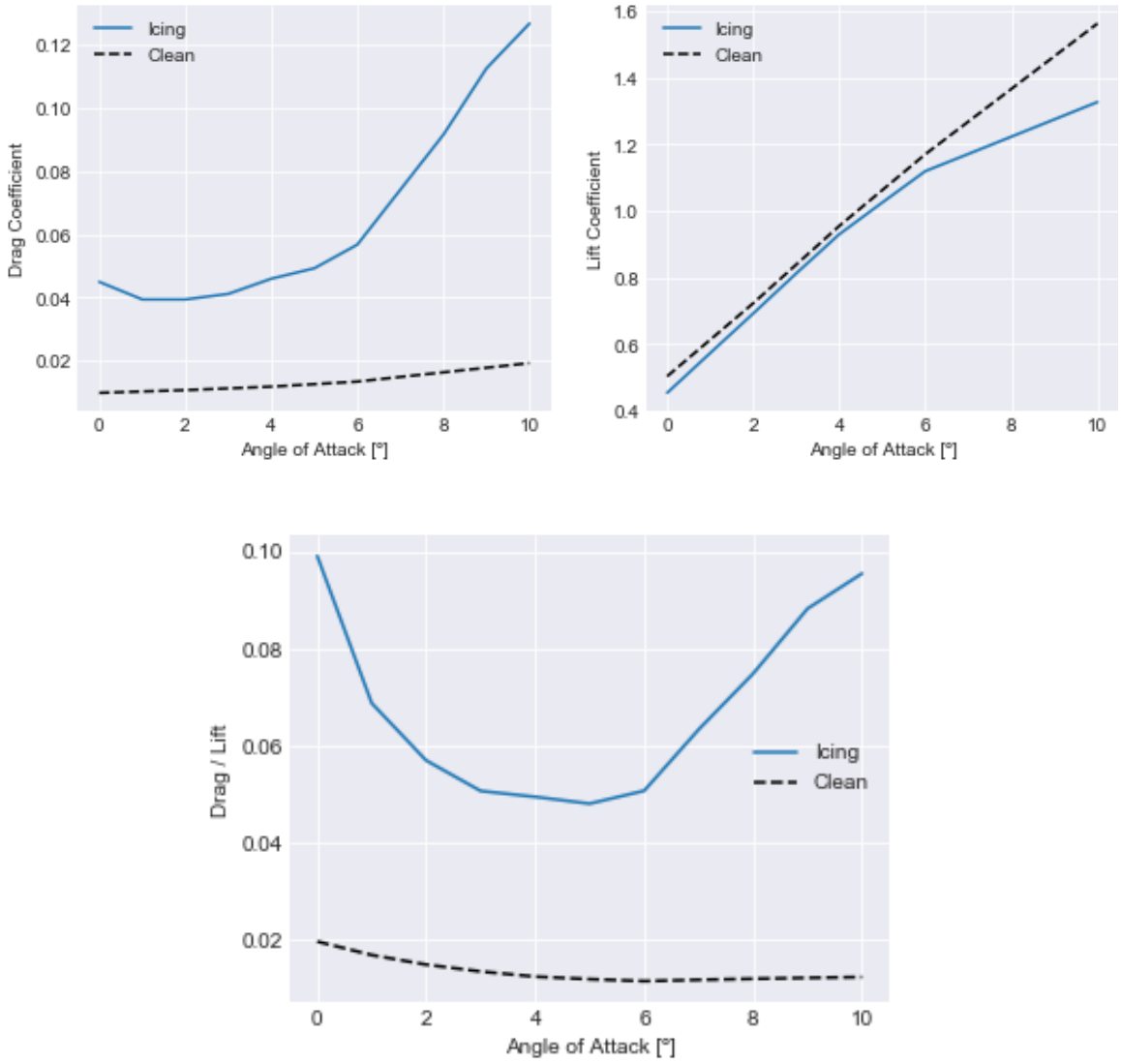

Figure 13. Drag coefficient (top left), lift coefficient (top right) and ratio drag/lift (bottom) for icing and clean airfoil by Turkia et al. (2013).

Hudecz (2014) made an experimental study of ice accretion in the Collaborative Climatic Wind Tunnel (CWT) located at FORCE Technology, in Kgs. Lyngby, Denmark. The ice accretion was performed for 1 hour, and right after that, aerodynamic coefficients were measured. The experiments were done for glaze, rime and mixed ice and the results on the next figures are only for rime ice, which is the focus of this research.

The results show that velocity decreases at the pressure side, thus ice accretion has influence on the flow field around the airfoil as angle of attack increases. Figure 14 shows drag and lift coefficients increasing with angle of attack. For the ratio Drag/Lift is possible to note that they are different for the clean and the icing case, indicating a possible different optimal operational point for each case.

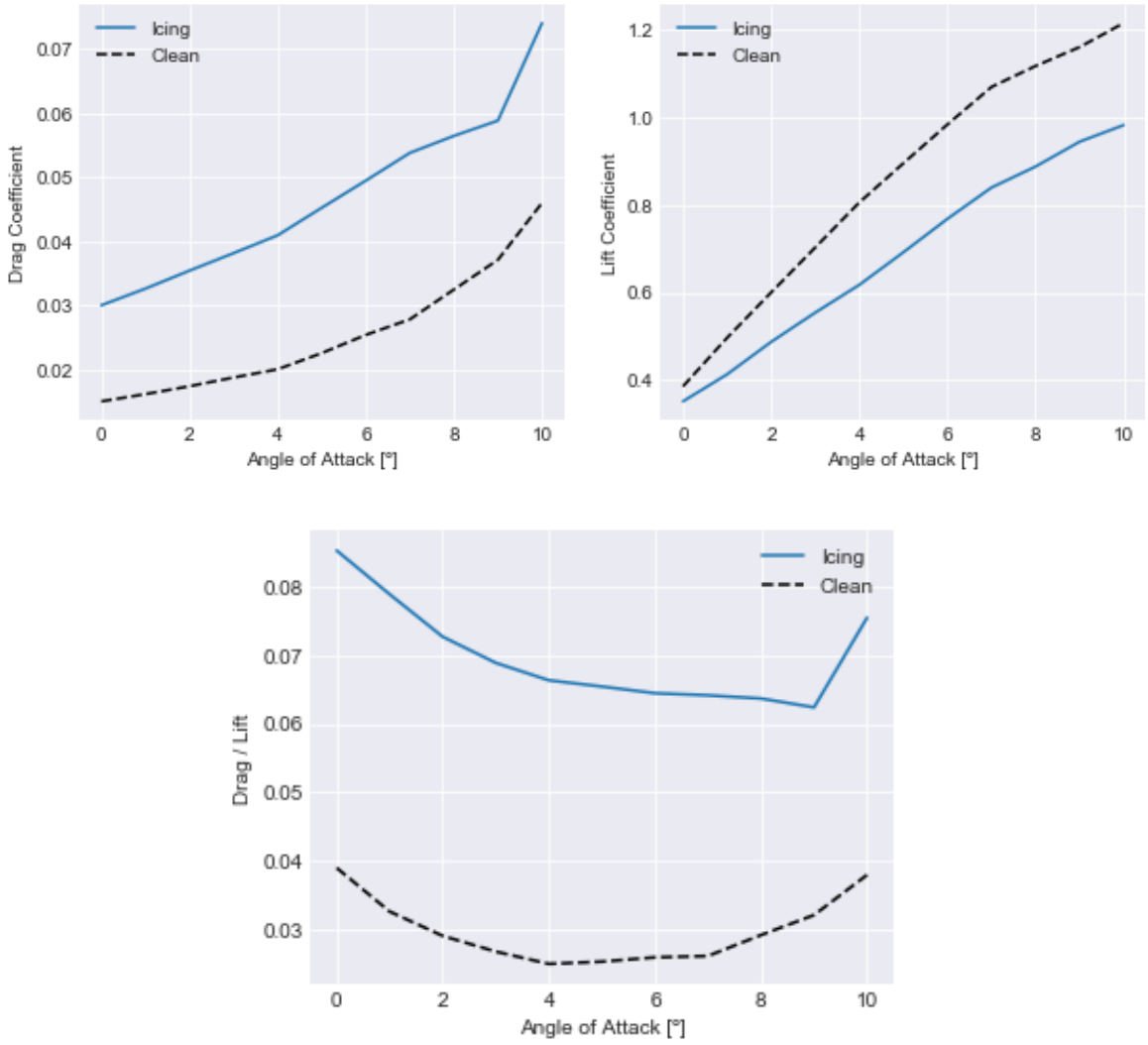

Figure 14. Drag coefficient (top left), lift coefficient (top right) and ratio drag/lift (bottom) for icing and clean airfoil by Hudecz (2014).

Gantasala et al. (2019) made a numerical study proposed by the authors to predict the ice accretion of several sections of a 5 MW pitch-controlled wind turbine. The results of ice accretion were solved using CFD simulation using ANSYS FLUENT to estimate aerodynamic coefficients.

Gantasala et al. (2019) performed investigation for 15 blade sections, and the section 9 of the blade (at 44.55 meters of radius) was used in this analysis because the third part of the blade has a higher impact in power production. Figure 15 shows drag and lift coefficients for Gantasala et al. (2019).

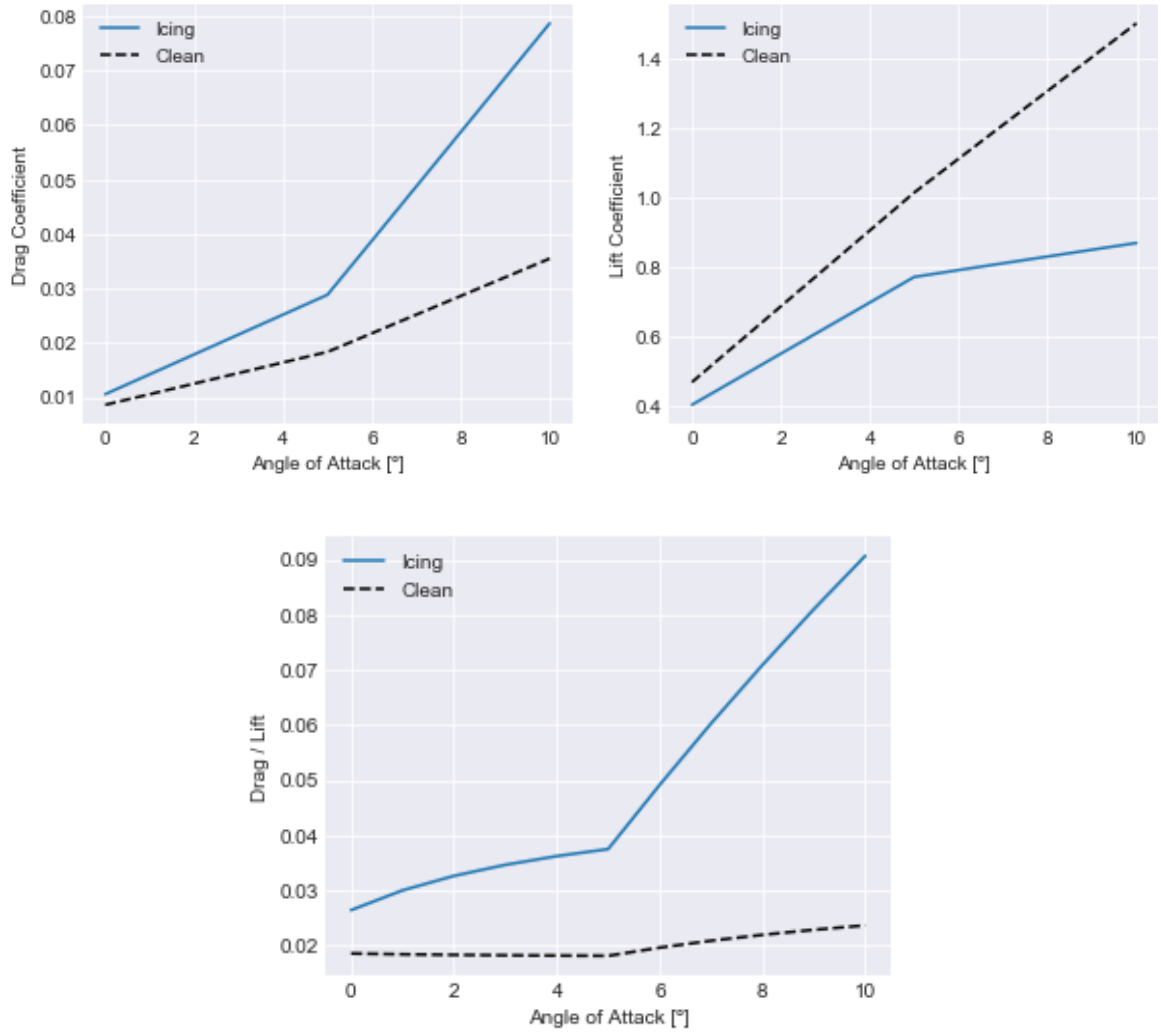

Figure 15. Drag coefficient (top left), lift coefficient (top right) and ratio drag/lift (bottom) for icing and clean airfoil by Gantasala et al. (2019).

The results show that icing decreases aerodynamic performance of the wind turbine when angle of attack is larger than 5º and it is according to existing trends in literature.

3.3 Power Coefficient Curves

With values of drag and lift coefficients varying from 0 to 10º, the maximum power coefficient is calculated according to the equation provided by Wilson et al. (1976) in equation (7).

For each angle of attack (α) there is a ratio drag / lift and the tip-to-speed ratio (λ) is varied from 0 to 20 so there is one curve for each combination of α and ratio. Each graph of the clean case has one maximum power coefficient for one combination of α and λ, which is the optimal operational point of the turbine. If there is ice on the blade, the optimum combination of α and λ changes and this is the new optimal operational point of the turbine with ice on its blades. When the values of α and λ of the clean case are applied to the icing case, loss of power production is observed. At the end of this section, a table with the main results will be shown together with graphs to analyse the parameters. The complete code for the power coefficient analysis is written in Appendix B.1 – Aerodynamic Analysis.

Three graphs for each reference are plotted, one for the clean case, one for the icing case, and one with the analysis of the optimized method.

Results of the power coefficient for Homola et al. (2010) are shown in Figure 16. For the clean case (graph on the left), the maximum power coefficient is $Cp_{clean} = 0.4173$, when $\alpha = 2^o$ and $\lambda = 3.5$. For the ice case (graph on the right), the maximum power coefficient is $Cp_{opt} = 0.3993$, when $\alpha = 5^o$ and $\lambda = 3.0$.

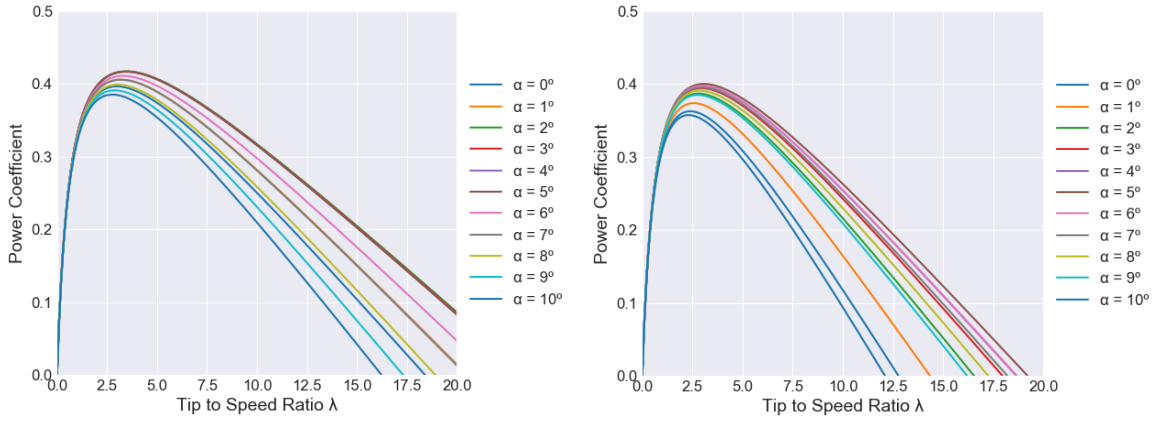

Figure 16. Curves of power coefficient for clean (left) and icing (right) cases for Homola et al. (2010).

Optimum α for the clean case is 2º and for the ice case is 5º and the power coefficient curves for these angles are plotted according to the ice case in Figure 17.

If the same conditions of α and λ of the clean case are applied for the ice case, the obtained power coefficient is $Cp,non\text{-}opt = 0.3829$, represented by the red mark. This value is the non-optimized configuration for the ice case (non-opt subscript).

If only α is optimized, the power coefficient is $Cp,\alpha\text{-}opt = 0.3989$, represented by the yellow mark. This value has optimization only in the angle α (α-opt subscript).

If α and λ are optimized, the power coefficient is $Cp,opt = 0.4002$ and it is represented by the green marks in Figure 17. This value is the optimum configuration for the icing case (opt subscript), with optimization in the angle α and in the tip-to-speed ratio λ.

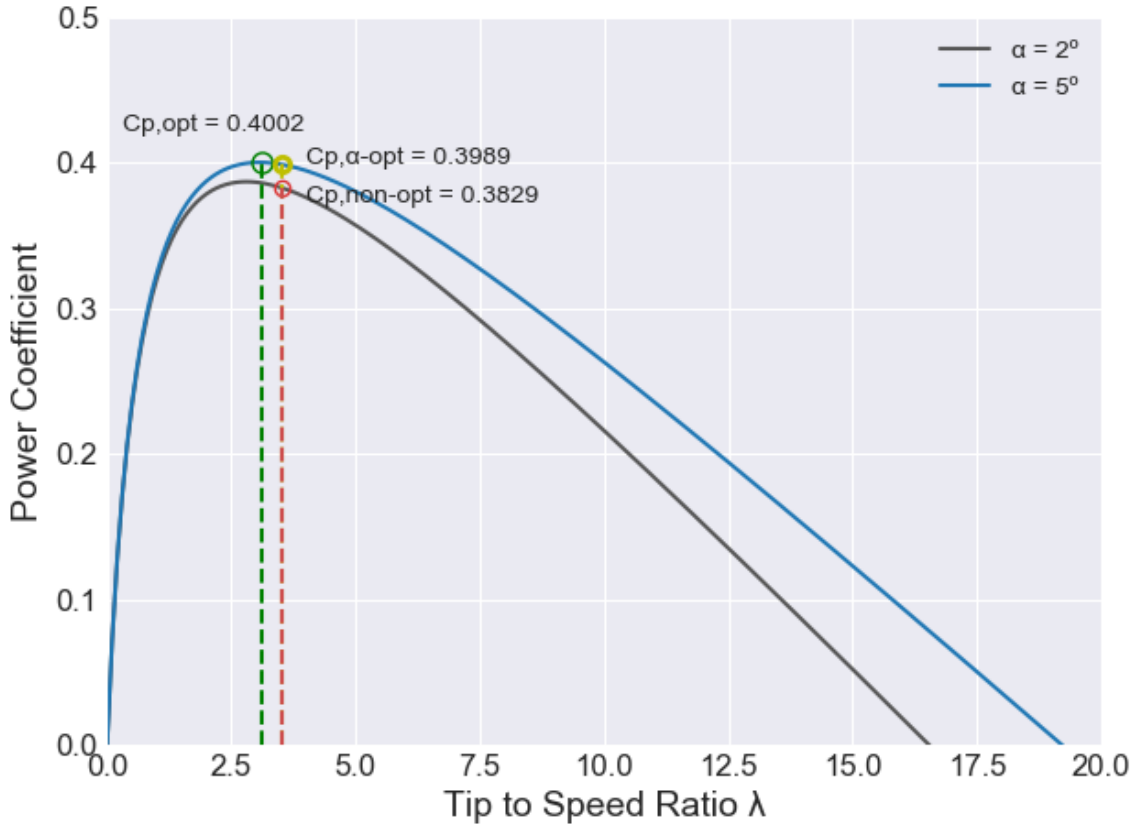

Figure 17. Analysis of the optimization method for Homola et al. (2010).

Results of the power coefficient for Etemadddar et al. (2012) are shown in Figure 18. For the clean airfoil (graph on the left), the maximum power coefficient is $Cp_{clean} = 0.5126$, when $\alpha = 5^o$ and $\lambda = 8.3$. For the icing case (graph on the right), the maximum power coefficient is $Cp_{opt} = 0.4340$, when $\alpha = 6^o$ and $\lambda = 3.9$.

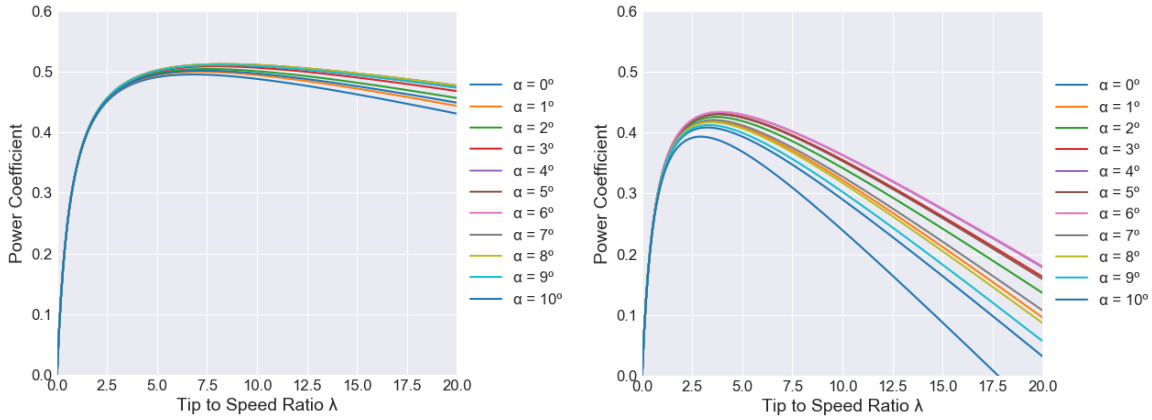

Figure 18. Curves of power coefficient for clean (left) and icing (right) cases for Etemaddar et al. (2012).

Optimum α for the clean case is 5º and for the ice case is 6º and the power coefficient curves for these angles are plotted according to the ice case in Figure 19.

If the same conditions of α and λ of the clean case are applied for the ice case, the obtained power coefficient is $Cp,non\text{-}opt = 0.3821$, represented by the red mark. This value is the non-optimized configuration for the ice case

If only α is optimized, the power coefficient is $Cp,\alpha\text{-}opt = 0.3907$, represented by the yellow mark. This value has optimization only in the angle α.

If α and λ are optimized, the power coefficient is $Cp,opt = 0.4340$ and it is represented by the green marks in Figure 19. This value is the optimum configuration for the icing case, with optimization in the angle α and in the tip-to-speed ratio λ.

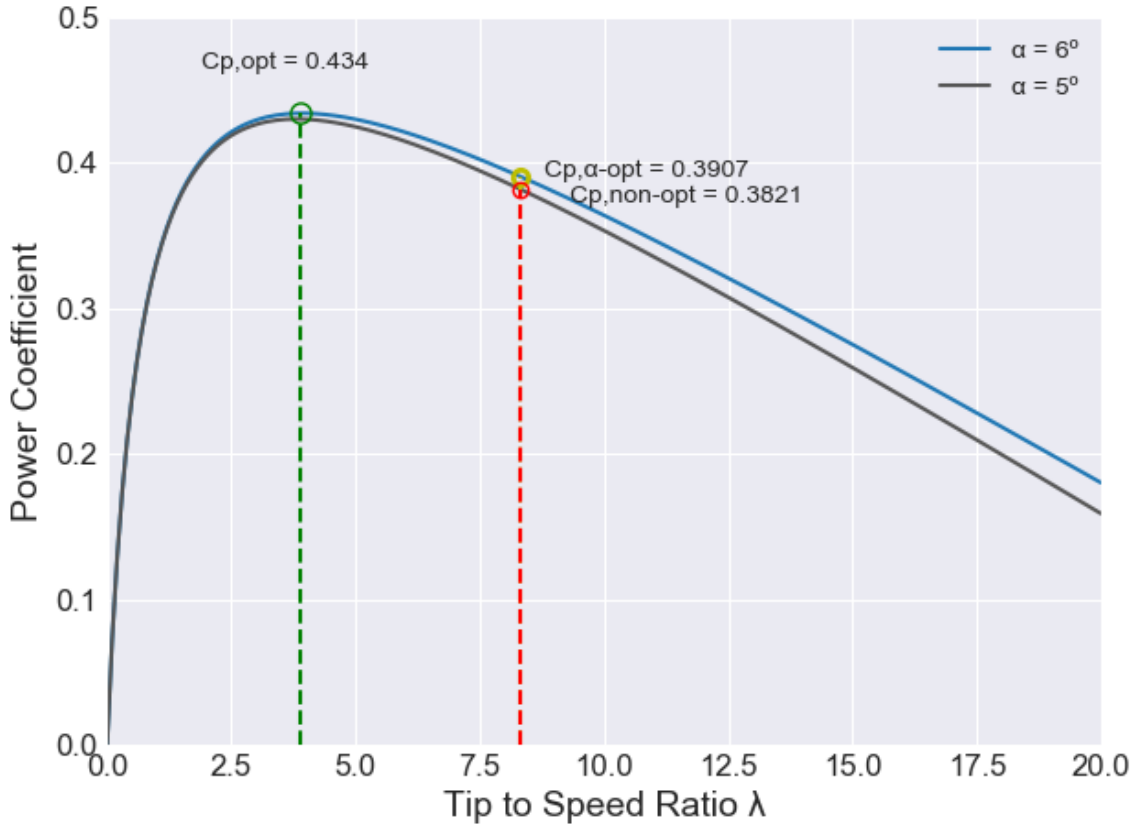

Figure 19. Analysis of the optimization method for Etemaddar et al. (2012).

Results of the power coefficient for Turkia et al. (2013) are shown in Figure 20. For the clean airfoil (graph on the left), the maximum power coefficient is $Cp_{clean} = 0.4984$, when $\alpha = 6^o$ and $\lambda = 7.0$. For the icing case (graph on the right), the maximum power coefficient is $Cp_{opt} = 0.4078$, when $\alpha = 5^o$ and $\lambda = 3.2$.

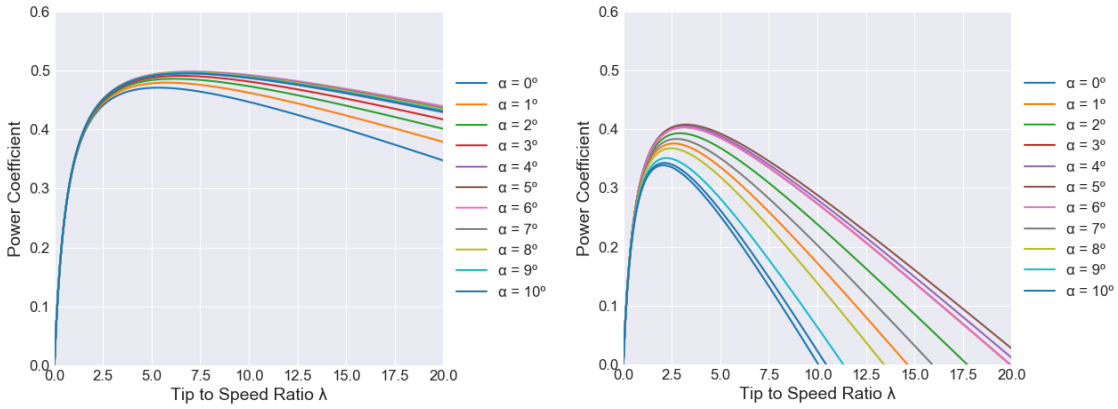

Figure 20. Curves of power coefficient for clean (left) and icing (right) cases for Turkia et al. (2013).

Optimum α for the clean case is 6º and for the ice case is 5º and the power coefficient curves for these angles are plotted according to the ice case in Figure 21.

If the same conditions of α and λ of the clean case are applied for the ice case, the obtained power coefficient is *Cp,non-opt = 0.3461*, represented by the red mark. This value is the non-optimized configuration for the ice case.

If only α is optimized, the power coefficient is *Cp,α-opt = 0.3564*, represented by the yellow mark. This value has optimization only in the angle α.

If α and λ are optimized, the power coefficient is *Cp,opt = 0.4078* and it is represented by the green marks in Figure 21. This value is the optimum configuration for the icing case, with optimization in the angle α and in the tip-to-speed ratio λ.

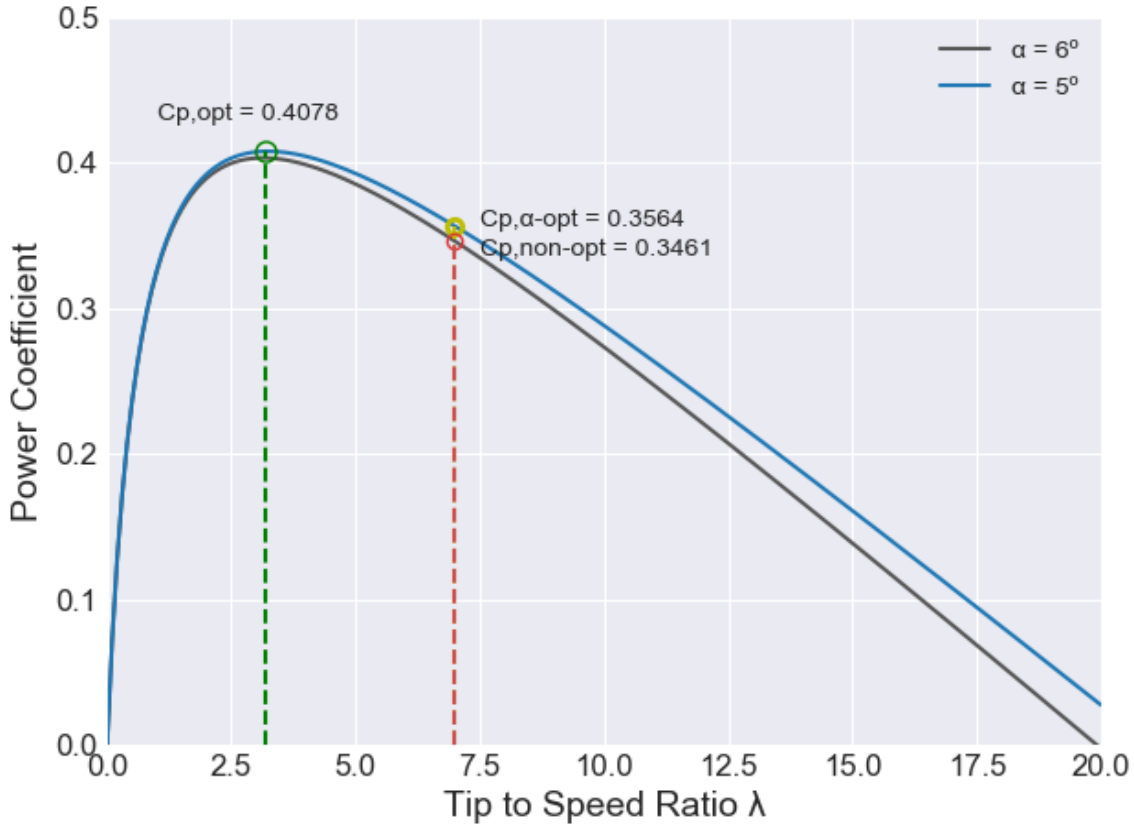

Figure 21. Analysis of the optimization method for Turkia et al. (2013).

Results of the power coefficient for Hudecz (2014) are shown in Figure 22. For the clean airfoil (graph on the left), the maximum power coefficient is $Cp_{clean} = 0.4565$, when $\alpha = 4^o$ and $\lambda = 4.7$. For the icing case (graph on the right), the maximum power coefficient is $Cp_{opt} = 0.3848$, when $\alpha = 9^o$ and $\lambda = 2.8$.

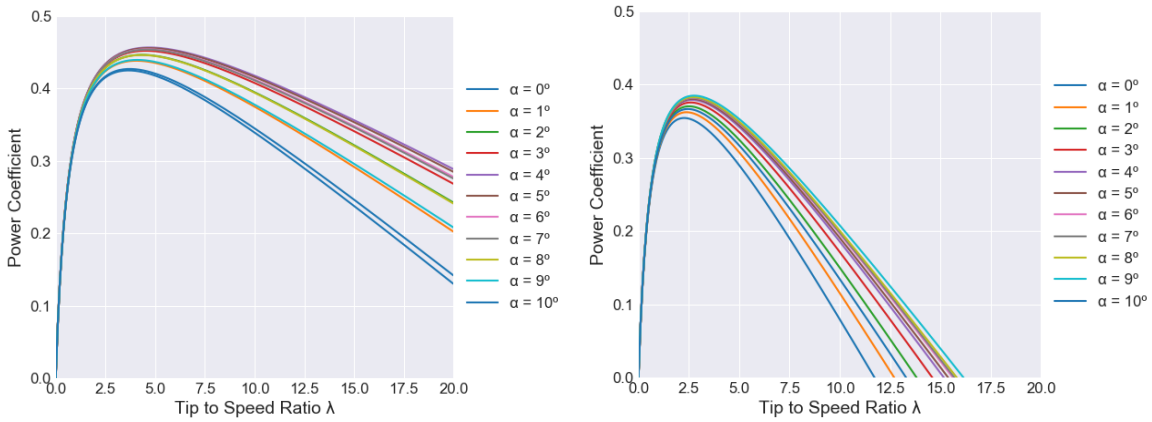

Figure 22. Curves of power coefficient for clean (left) and icing (right) cases for Hudecz (2014).

Optimum α for the clean case is 4º and for the ice case is 9º and the power coefficient curves for these angles are plotted according to the ice case in Figure 23.

If the same conditions of α and λ of the clean case are applied for the ice case, the obtained power coefficient is $Cp,non\text{-}opt = 0.3495$, represented by the red mark. This value is the non-optimized configuration for the ice case.

If only α is optimized, the power coefficient is $Cp,\alpha\text{-}opt = 0.3597$, represented by the yellow mark. This value has optimization only in the angle α.

If α and λ are optimized, the power coefficient is $Cp,opt = 0.3848$and it is represented by the green marks in Figure 23. This value is the optimum configuration for the icing case, with optimization in the angle α and in the tip-to-speed ratio λ.

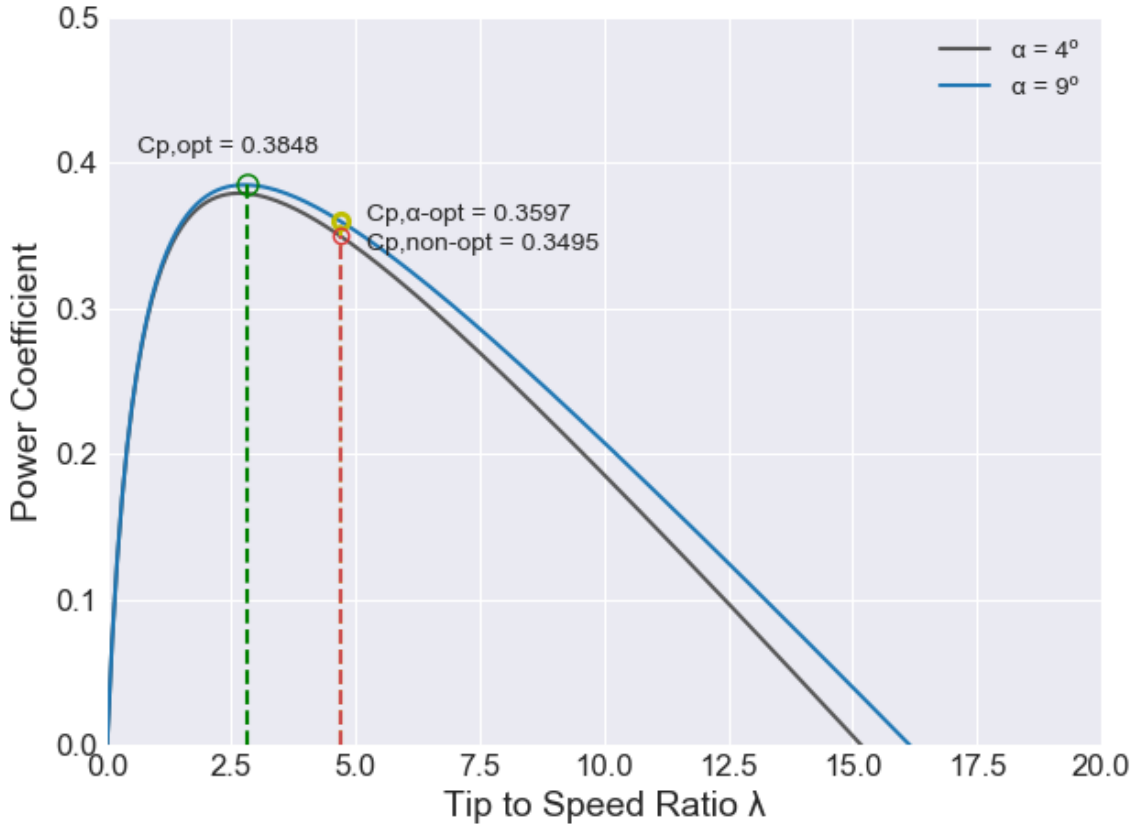

Figure 23. Analysis of the optimization method for Hudecz (2014).

Results of the power coefficient for Gantasala et al. (2019) are shown in Figure 24. For the clean airfoil (graph on the left), the maximum power coefficient is $Cp_{clean} = 0.4755$, when $\alpha = 5^o$ and $\lambda = 5.6$. For the icing case (graph on the right), the maximum power coefficient is $Cp_{opt} = 0.4526$, when $\alpha = 0^o$ and $\lambda = 4.6$.

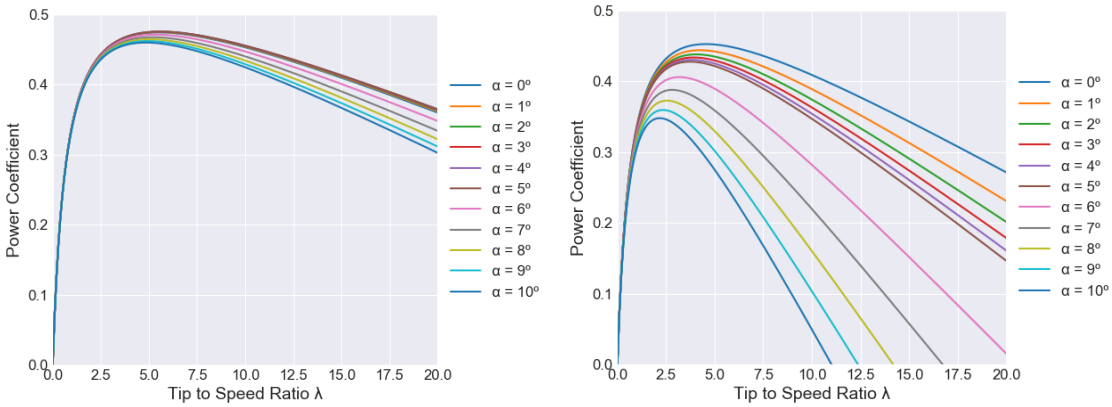

Figure 24. Curves of power coefficient for clean (left) and icing (right) cases for Gantasala et al. (2019)

Optimum α for the clean case is 5º and for the ice case is 0º and the power coefficient curves for these angles are plotted according to the ice case in Figure 25.

If the same conditions of α and λ of the clean case are applied for the ice case, the obtained power coefficient is *Cp,non-opt = 0.4157*, represented by the red mark. This value is the non-optimized configuration for the ice case.

If only α is optimized, the power coefficient is *Cp,α-opt = 0.4499*, represented by the yellow mark. This value has optimization only in the angle α.

If α and λ are optimized, the power coefficient is *Cp,opt = 0.4526* and it is represented by the green marks in Figure 25. This value is the optimum configuration for the icing case, with optimization in the angle α and in the tip-to-speed ratio λ.

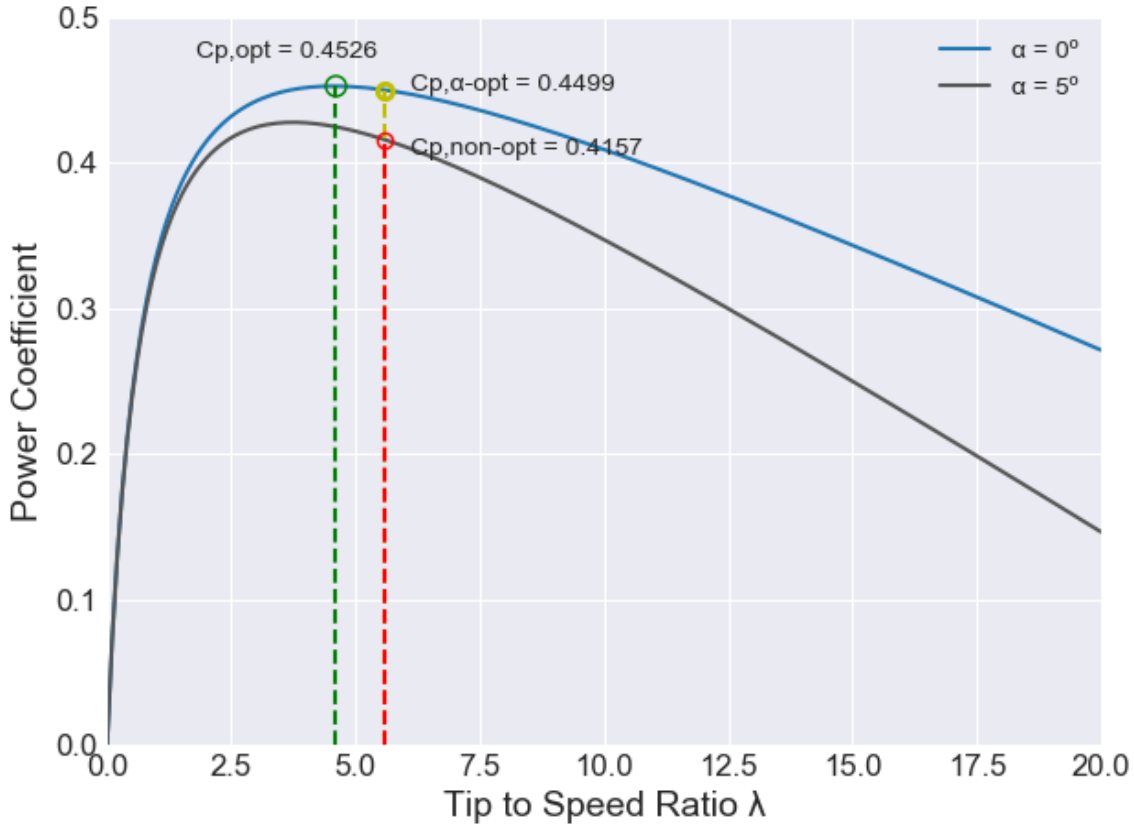

Figure 25. Analysis of the optimization method for Gantasala et al. (2019).

3.3.1 Summarized Results

The results of the power coefficient analysis show that angle of attack α alone does not provide the optimum optimization for power production, but when combined with tip-to-speed ratio λ, the new adjustment gives the highest power coefficient, so these are the two parameters that will be optimized to increase power production.

Results shown previously are summarized in Table 3, with the power coefficient, tip-to-speed ratio and angle of attack for the clean case (clean subscript) and for the icing case with optimization (opt subscript) and the power coefficient for the icing case with no optimization ($Cp_{non\text{-}opt}$). Each velocity corresponds to one reference, as described in Table 2.

Optimum angle of attack is different from the clean (α_{clean}) case to the icing case (α_{opt}) for all wind velocities, in some cases it is α_{clean} is higher than α_{opt} and in other cases it is lower, henceforth it does not show a clear relation.

Tip-to-speed ratio is a relation between the speed of the tip of the blade and the wind velocity at the hub of the turbine, according to equation (6), and its intensity was reduced from the clean case (λ_{clean}) to the icing case (λ_{opt}) for all wind velocities.

Table 3. Summarized results of the power coefficient analysis for all five references given in Table 2.

Velocity at the hub [m/s]	**Cp_{clean}**	**λ_{clean}**	**α_{clean}**	**Cp_{opt}**	**λ_{opt}**	**α_{opt}**	**$Cp_{non\text{-}opt}$**
2.2	0.4755	5.6	5º	0.4526	4.6	0º	0.4157
3.2	0.4565	4.7	4º	0.3848	2.8	9º	0.3495
6	0.5126	8.3	5º	0.4340	3.9	6º	0.3821
7.3	0.4984	7.0	6º	0.4078	3.2	5º	0.3461
19.2	0.4173	3.5	2º	0.4002	3.1	5º	0.3829

In a typical wind turbine IEC-Class III, the cut-in (minimum wind speed when the turbine begins to operate) is 3 m/s, the average wind speed is 7.5 m/s and the cut-off (maximum

wind speed) is 25 m/s (Zhang, 2015). The regions of the turbine are classified according to wind velocities: Region I (0 – 3 m/s); Region II (3 – 7.5 m/s); Region III (7.5 – 25 m/s).

Power coefficients from Table 3 with respect to the wind velocity are represented in Figure 26. The blue marks are the power coefficients for the clean case, the red marks are the power coefficients for the non-optimized icing case and the green marks between the red and blue are the power coefficients for the optimized icing case. For a pitch-controlled wind turbine, the Region II has a fixed angle and the control starts in Region III.

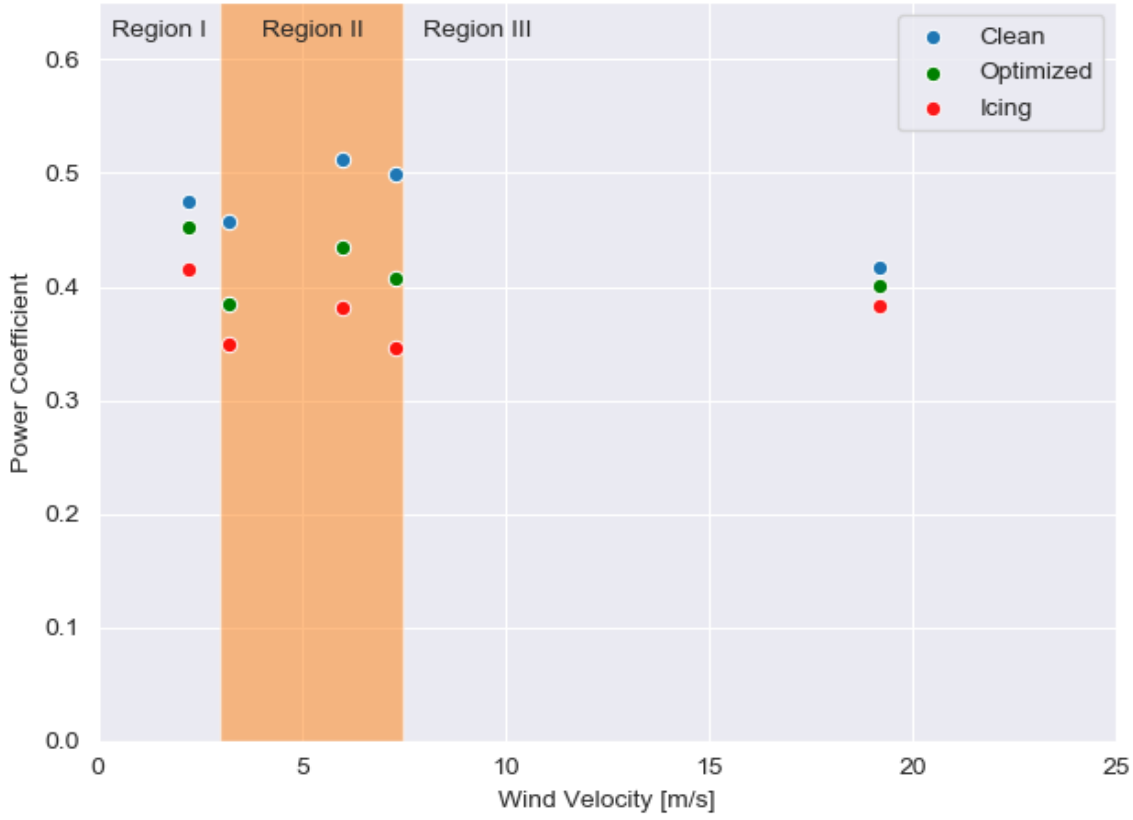

Figure 26. Combined results of the power coefficients with respect to wind velocity for the five references.

Aerodynamic loss is a relation between the analysed power coefficient (optimized or non-optimized) with the power coefficient of the clean case and it is defined according to the following equation:

$$Losses = 1 - \frac{C_{p,n}}{C_{p,clean}} \quad (9)$$

Where:

Cp,n is the power coefficient to be analysed (optimized or non-optimized)

Cp,clean is the power coefficient of the clean case

The losses for the five wind velocities are plotted in Figure 27, with the non-optimized case in red colour and the optimized case in green colour. It is possible to note the main losses when the wind velocity is higher than 3.2 m/s and close to 7.3 m/s. This range of wind speeds is the Region II, where pitch control is not actuating and in the transition region (between Regions II and III), where the pitch control starts to actuate in a wind turbine class III, a typical turbine in northern regions.

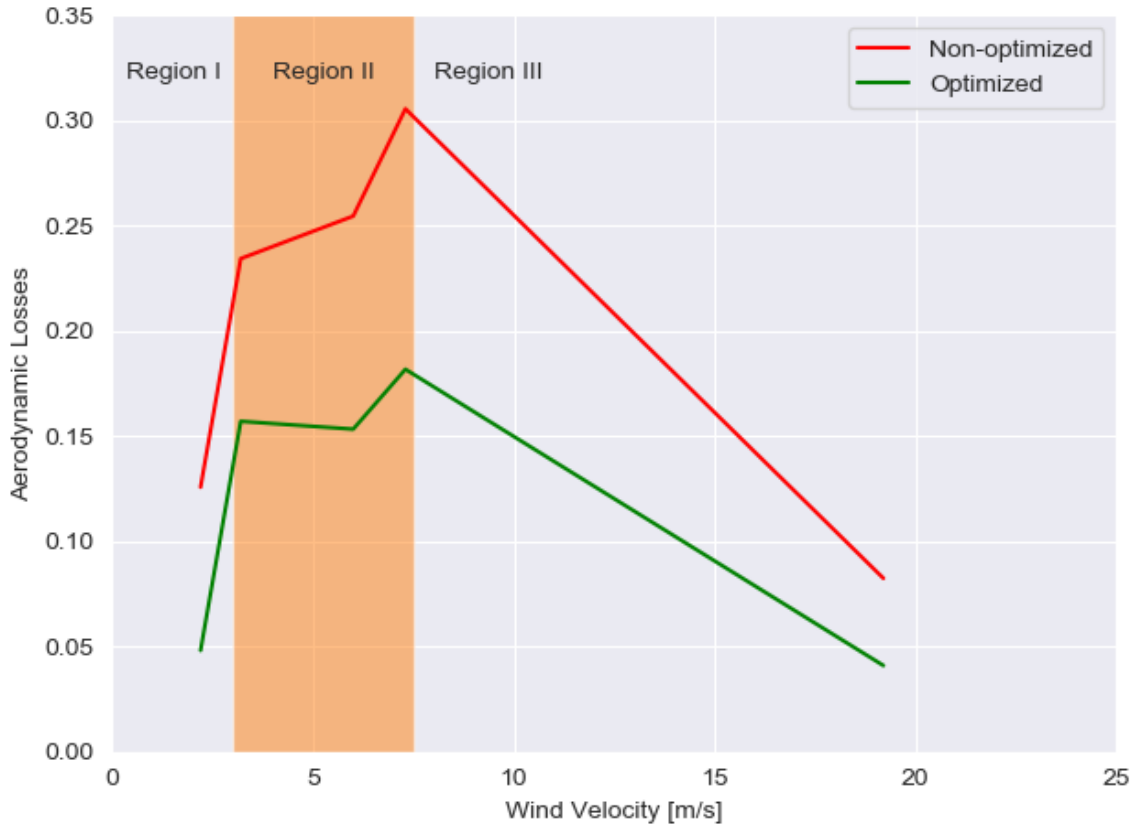

Figure 27. Combined aerodynamic losses of the icing and optimized cases with respect to the wind velocity for all five references.

Given the points presented in this chapter, two observations are made:

- The method to optimize power production is to adjust the angle of attack α and the tip-to-speed ratio λ combined.
- The highest losses occur when pitch control is not actuating (Region II) and in the transitional region, where pitch control starts to actuate (between Region II and III).

CHAPTER 4 – STUDY CASE

4.1 Regions

In order to study the proposed methodology, suitable regions were chosen according to its location and by analyzing wind maps from Finland and Russia, and according to the available datasets described in the next topic.

The Finnish Icing Atlas provided by Clausen & Giebel (2017) shows production losses due to icing and it was used to choose the locations in Finland.

Sites in Russia were chosen according to the wind power map provided by Elistratov et al. (2014) with latitudes close to the arctic region.

The six chosen locations are represented in the map in Figure 28.

Figure 28. Location of the case studies in Finland and Russia.

Geographical coordinates of the six locations are written in Table 4 in decimal degrees.

Table 4. Coordinates of the locations from the study case.

Name	Latitude	Longitude
Olhava, FI	65º N	25.333º E
Madetkoski, FI	68º N	26.667º E
Käsivarren Erämaa-Alue, FI	69º N	28.333º E
Jääräjoki, FI	70º N	28º E
Murmansk, RU	68.5º N	37.5º E
Yamalsky, RU	71º N	68.125º E

4.2 Weather Data

To validate the control strategy proposed in Chapter 3, data about the weather is going to be used in the study case.

For wind parameters, data from MERRA2 - The Modern-Era Retrospective analysis for Research and Applications, Version 2 is used. This dataset is the latest atmospheric reanalysis of the modern satellite era produced by NASA's Global Modelling and Assimilation Office (GMAO) and it provides data from 1980 on, in hourly timestep:

- Wind speed at 50 meters height
- Wind direction at 50 meters height
- Atmospheric pressure at ground level
- Temperature at 2- and 10-meters height

This dataset is widely used for long term series analysis in the development of wind projects and it is considered a reliable source of weather information.

Temperature alone cannot be used to define atmospheric icing (Homola, Virk, Wallenius, Nicklasson, & Sundsbø, 2010), but if combined with wind speed and air liquid water content the ice type can be determined (Davis, 2014).

Air liquid water content does not have a global dataset, and to refine this research, relative humidity is inserted in the analysis of icing using data from the Climate Forecast System version 2 – CFSv2, from the National Centers for Environmental Prediction – NCEP. This dataset provides data from 2011 on, in hourly timestep. (Saha, 2012)

4.3 Analysis of the Data

In this work, it is proposed that atmospheric ice occurs according to weather conditions described in Table 1, when wind speed is higher than 3 m/s, temperature is lower than -4 ºC and relative humidity is higher than 95%.

Before the methodology is applied to the study case, a statistical analysis of the compiled weather data is done to describe the conditions of each location. The summarized statistical analysis is written in Table 5.

Table 5. Annual statistical analysis of the six locations of the study case.

Name	**Wind Speed [m/s]**	**Temperature [ºC]**	**Relative Humidity [%]**	**Hours of Icing per year**
Jääräjoki, FI	5.58	-0.76	88.24	1,576
Käsivarren Eräma-Alue, FI	5.38	-2.43	89.89	2,113
Madetkoski, FI	4.52	-0.65	90.18	2,546
Murmansk, RU	7.45	0.15	88.28	1,221
Olhava, FI	4.57	2.39	88.21	1,598
Yamalsky, RU	7.14	-6.51	90.78	2,596
Average	5.77	-1,30	89,26	1,942

By analysing the Table 5 it is possible to conclude that any parameter alone cannot define the occurrence of atmospheric ice, but only a combination of the parameters is valid to determine condition for atmospheric ice.

Hours of icing per year by itself is not the parameter that will define the power production loss of a site, because depending on the wind regime, the losses can be higher or lower, so only a complete analysis will define the power losses.

Firstly, the results of power coefficients from Table 3 are interpolated with the wind speed of each location. Icing power coefficient will be applied when the temperature is lower than -4 ºC and higher than -20 ºC, relative humidity is higher than 95% and wind speed is higher than 3 m/s, if the conditions are not matched, the clean power coefficient is applied.

The results shown in Section 4.4 are plotted into graphs, with the red colour representing the icing case with no optimization and the green colour representing the icing case with optimization. There are 03 graphs for each location and they are shown from Figure 29 to Figure 46 and the description of the calculation for each graph is written below.

The first graph shows the yearly power production losses and it represents the power production losses of each year, with the average losses in the dashed lines. Yearly losses are calculated according to the following equation:

$$Yearly\ losses = 1 - \frac{\left(Power_{year,i}\right)_{icing\ case}}{\left(Power_{year,i}\right)_{clean\ case}} \tag{10}$$

The complete code is written in Appendix B.3.1 – Yearly Losses. Yearly losses are an important parameter to be analysed because it takes into consideration all the seasonality of the weather during the year and the comparison year by year shows the variation of the losses through the years. For all cases, the optimized strategy reduced the losses between 1 – 3.8% with respect to the icing case with no optimization.

The second graph is the monthly mean losses and it represents the mean power production losses of each month, from 2011 to 2019. Monthly mean losses are calculated according to the following equation:

$$Monthly\ mean\ losses = 1 - \frac{\left(\sum_{2011}^{2019} Power_{month,i}\right)_{icing\ case}}{\left(\sum_{2011}^{2019} Power_{month,i}\right)_{clean\ case}} \quad (11)$$

Where:

i = month being analysed

Equation (11) is applied to the 12 months of the year, and each month will have an average loss for the non-optimized ice case and for the optimized icing case. The complete code for the monthly mean losses is written in Appendix B.3.2 – Monthly Mean Losses.

During the analysis of the monthly mean losses, it is possible to note that January is the month with higher losses due to icing, reaching more than 29.6% in Madetkoski, Finland, where the optimization strategy reduced losses by 7.6% in this month (Figure 36).

The third graph is the power curves for the icing case with no optimization and the icing case with optimization. It was calculated according to the equation (5) $P_r = \frac{1}{2}\rho\pi R^2 v^3 c_p(\lambda, \alpha)$, considering between rotor and generator where:

- *R = 45 meters*
- $\rho = \frac{p}{RT}$, with *R = 287 J/kg.K*, *p* and *T* from the dataset
- v comes from the dataset
- $c_p$is interpolated with the velocity and the results of power coefficient from Table 3

It was chosen a theoretical wind turbine with rotor of 90 meters of diameter and rated power of 1,000 kW, and the air density was calculated for each timestep with air pressure, temperature, and gas constant. Moreover, the power curves for each location are presented, with the icing case with no optimization on the left (red curves) and the icing case with optimization on the right (green curves). The complete code for the power curves is written in Appendix B.2 – Energy Yield.

For all locations it is possible to note one component of the power curve for the clean case more to the left and one component of the icing case more to the right. The icing events cause a separation in the power curve because it decreases the power coefficient, being necessary a higher wind speed to reach the same power. For the optimization method, the

target is to reduce the space between the clean component and the icing component observed in the red curves and it was successfully achieved for all locations in the study case.

4.4 Results of Study Case

Jääräjoki, Finland

Jääräjoki is in the most north location in Finland, close to the border with Norway. It has an average wind speed of 5.58 m/s, average temperature of -0.76 ºC, average relative humidity of 88.24% and 1,576 hours of atmospheric ice per year. Even though Jääräjoki is the second highest latitude (70º N) of this study, it has the second fewest hours of atmospheric ice.

The year with the highest losses was 2012 with 9.2% and the minimum losses was 2017 with 4.9% of power losses for the icing case, reduced to 7% and 3% accordingly, with the optimization method. The average losses from 2011 to 2019 are 6.3% for the icing case and 4.3% for the optimized case and it is shown in Figure 29.

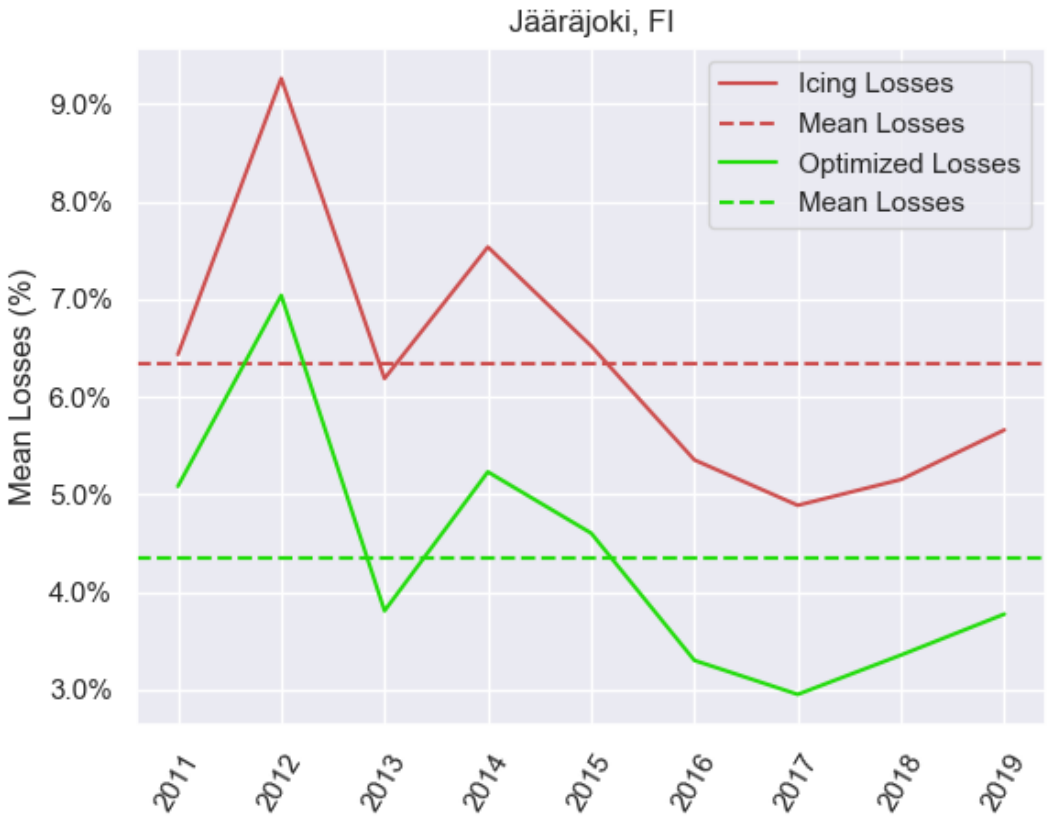

Figure 29. Yearly losses for Jääräjoki, FI.

According to Figure 30, January is the month with highest losses due to icing, with more than 16% of losses for the icing case and 12% of losses for the optimized case. May, the power losses due to icing are almost 0.5% and from June to September there are no conditions for atmospheric ice on wind turbines.

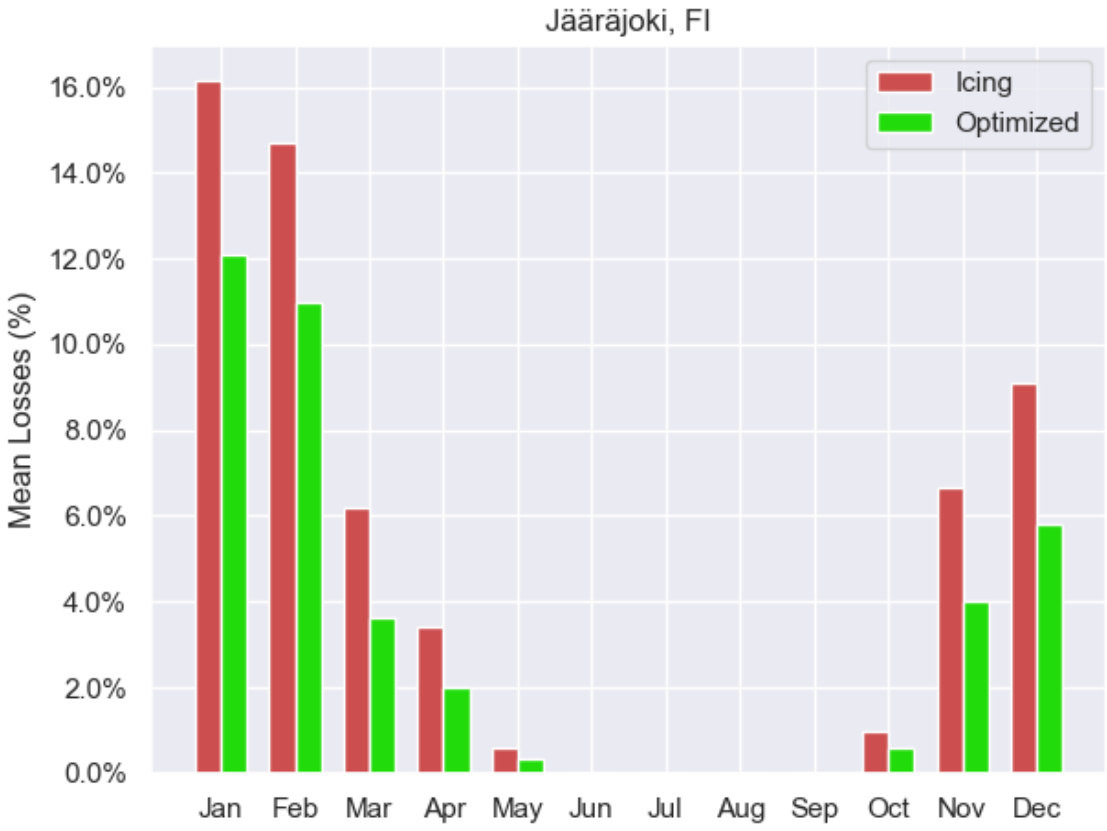

Figure 30. Monthly mean losses for Jääräjoki, FI.

The power curve of the cases were calculated and for a better visualization of the improvement made with the optimization method, a superposition of the power curves is shown in Figure 31.

The component of icing is represented by the red colour in the non-optimized case and by the green colour in the optimized case and the clean component is represented by the blue colour. The red dots are in the right adjacent and they represent the power produced with icing events with no optimization, and the objective of the presented method is to move these dots to the left adjacent, more close to the blue dots (clean case), so the same power is achieved with a lower wind speed.

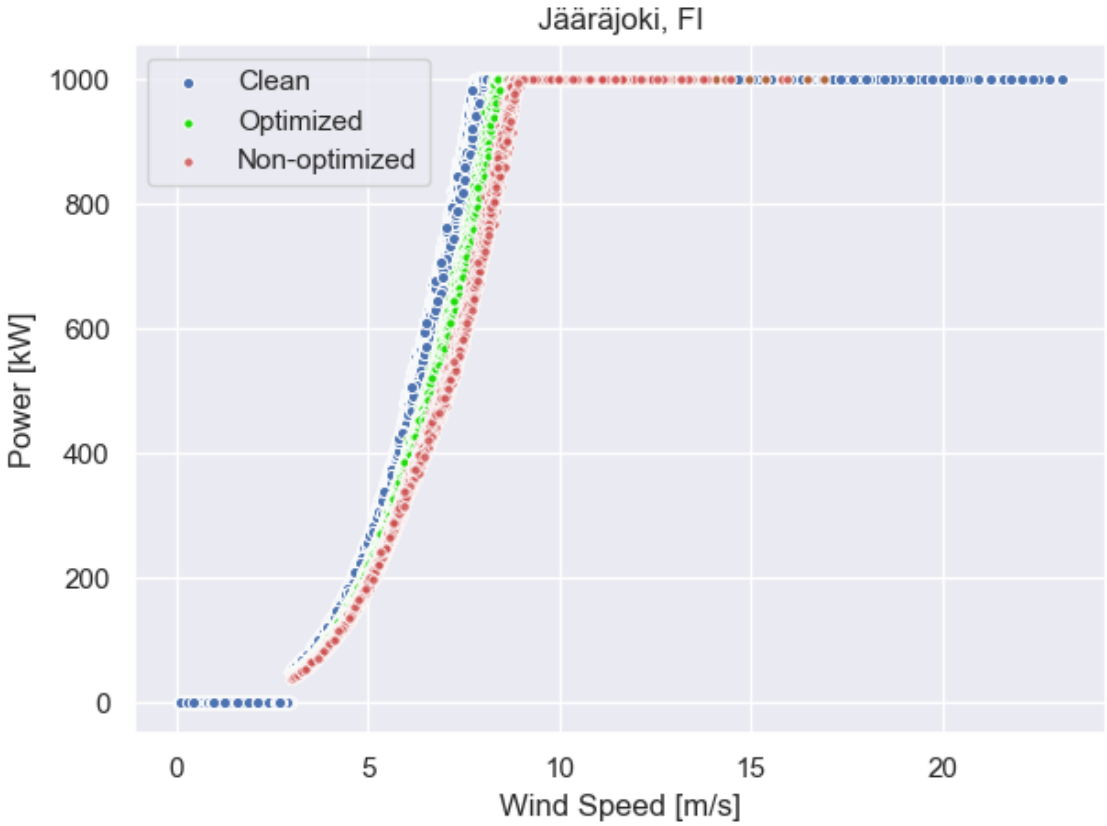

Figure 31. Superposition of the power curves for Jääräjoki, FI.

In summary, the main results for Jääräjoki are:

- Yearly mean losses:
  - Non-optimized case: 6.3%
  - Optimized case: 4.3%
- January mean losses:
  - Non-optimized case: 16.1%
  - Optimized case: 12.1%

Käsivarren, Finland

Käsivarren erämaa-alue is an environmental reserve on the northwest of Finland, close to the triple border between Finland, Norway, and Sweden. This region has an average wind speed of 5.38 m/s, average temperature of -2.43 ºC, average relative humidity of 89.89%, and more than 2,113 hours of atmospheric ice per year.

The analysis of the yearly losses shows a minimum of 7% in 2013 and maximum of 11% in 2012 and average of 9.1% for the icing case, values reduced to the minimum of 4.5%, maximum of 8.4% and average of 6.5% with the optimization method.

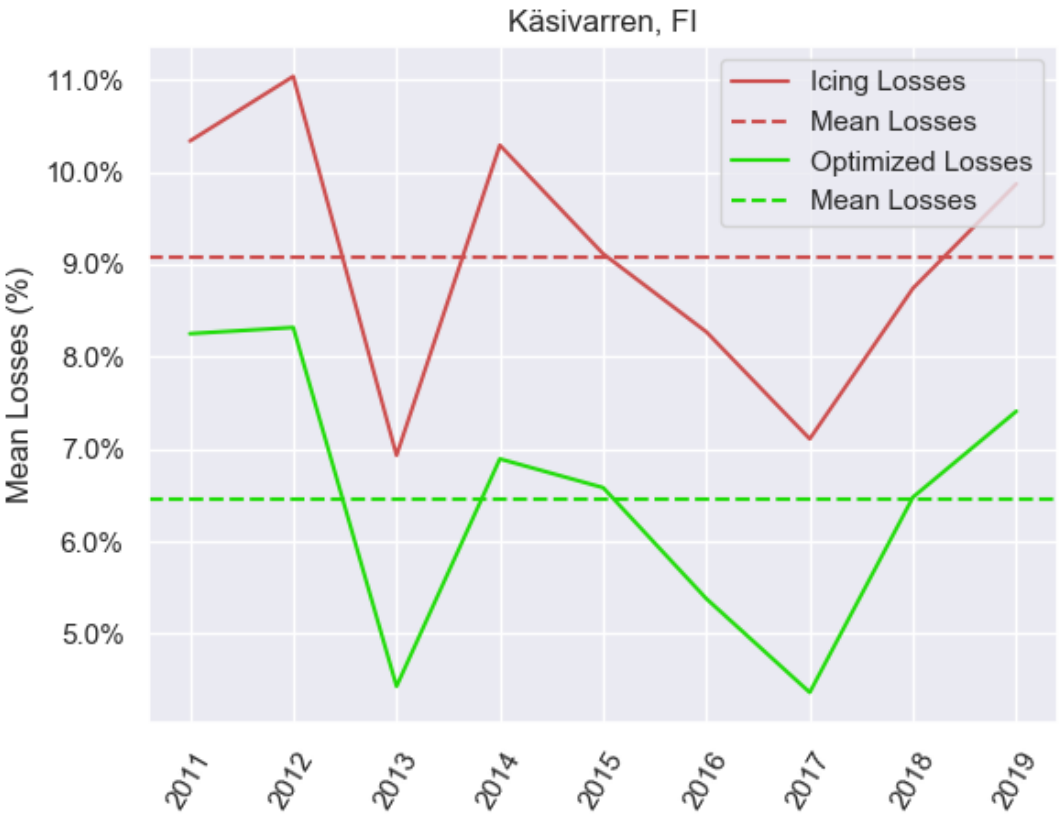

Figure 32. Yearly losses for Käsivarren erämaa alue, FI.

According the means of monthly mean losses in Figure 33, January with 23.5% and February with 21% of losses due to icing are the extreme months in Käsivarren erämaa alue, and these values were reduced to 18.5% and 16.5, accordingly. From June to September there is no conditions for atmospheric ice.

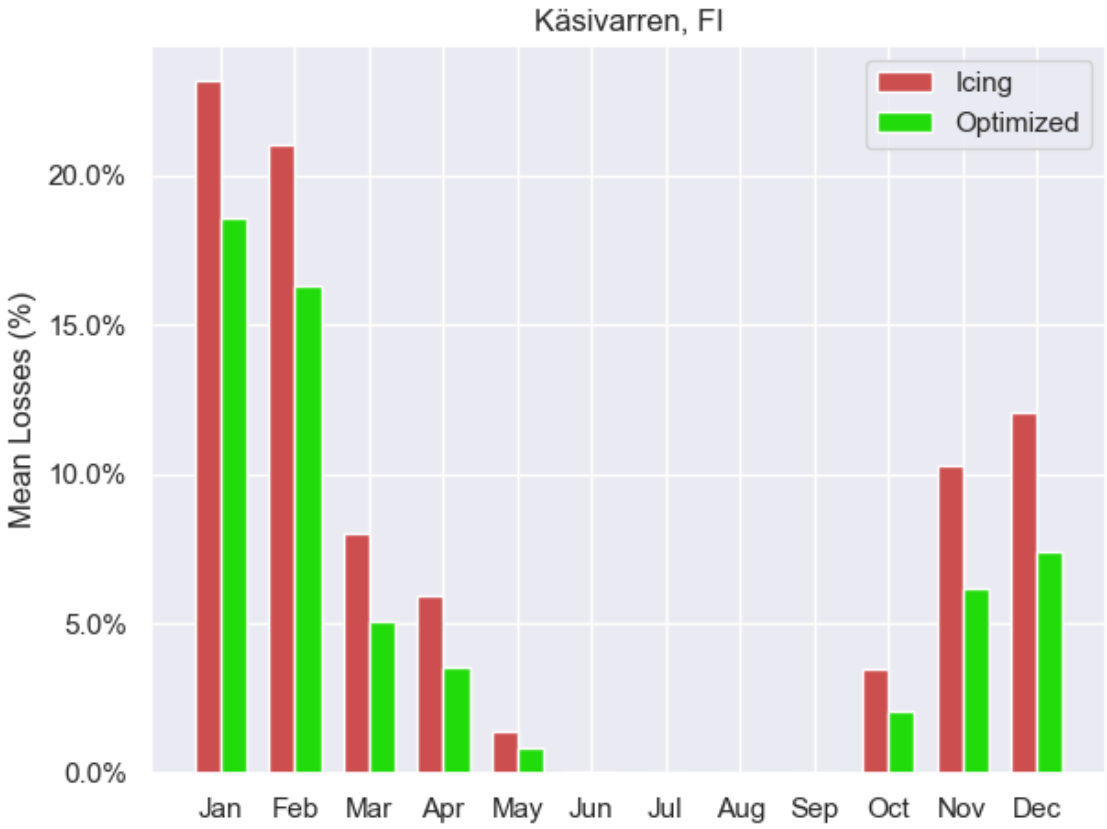

Figure 33. Monthly mean losses for Käsivarren erämaa alue, FI.

Furthermore, the power curves for Käsivarren are shown in Figure 34. It is possible to note that the green dots of the optimized case is more fitted than the red power curve of the icing case, meaning that they are more close to the blue dots of the clean case, and the same power is observed with a lower wind speed. As the dots from the optimized case are between the blue and red dots, this case shows the expected results for the optimization method.

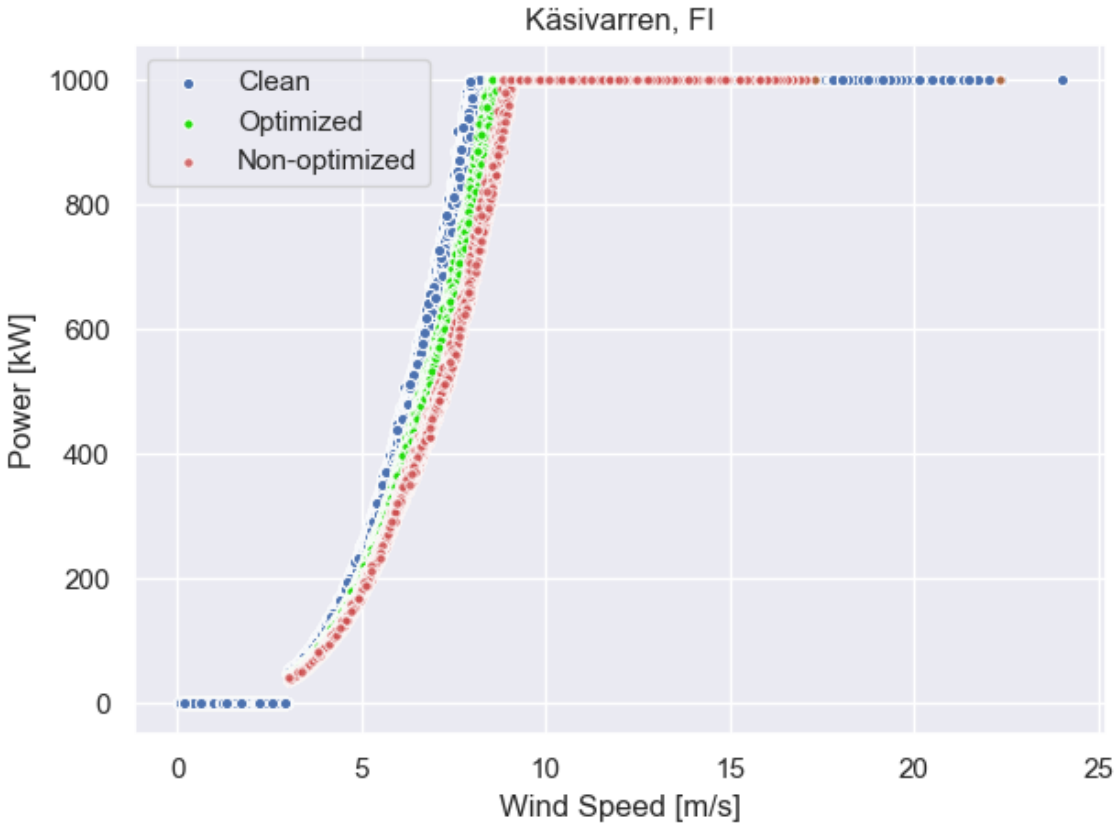

Figure 34. Superposition of the power curves in Käsivarren erämaa alue, FI.

In summary, the main results for Käsivarren erämaa alue are:

- Yearly mean losses:
  - Non-optimized case: 9.1%
  - Optimized case: 6.5%
- January mean losses:
  - Non-optimized case: 23.2%
  - Optimized case: 18.6%

Madetkoski, Finland

Madetkoski is in the middle of Lapland, in Finland, and it has an average wind speed of 4.52 m/s, average temperature of -0.65 ºC, average relative humidity of 90.18% and more than 2,546 hours of icing per year, the highest in this study case. This region was expected to have high amount of icing events because it is far away from the warm wind currents coming from the ocean.

Yearly losses in average were 12.4% from 2011 to 2019 and the highest losses were observed in 2012 with 16.3% for the icing case and it was reduced to 12.4% with the optimization method for that year and 8.6% of mean losses during the period.

Figure 35. Yearly losses for Madetkoski, FI.

January is the extreme month in Madetkoski with almost 30% of power losses due to icing, followed by February with 25%. The optimization method reduced these losses to 22% in January and 18% in February. From June to September there was no conditions for atmospheric ice.

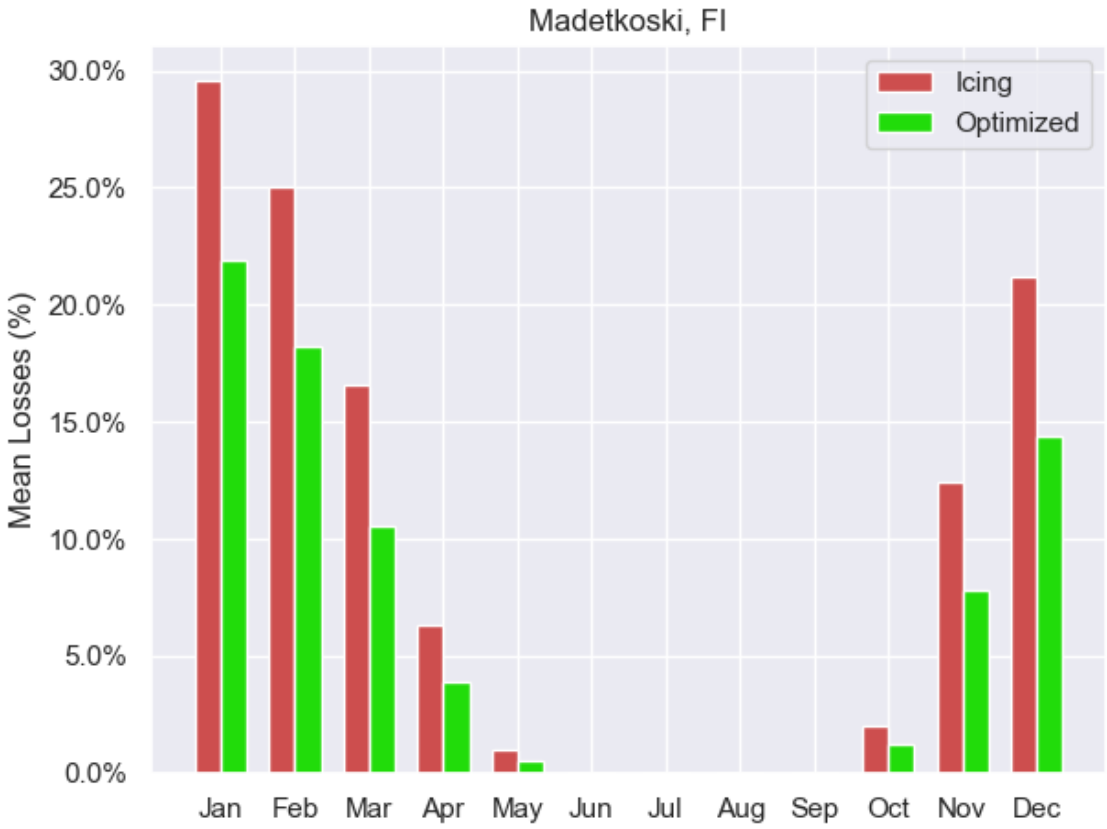

Figure 36. Monthly mean losses for Madetkoski, FI.

Moreover, the power curves for Madetkoski are shown in Figure 37 and it is possible to note that the green power curve of the optimized case is more fitted than the red power curve of the icing case. As it was expected, the optimization method (green dots) is between the clean (blue dots) and the non-optimized case (red dots), showing the improvement made by the presented method.

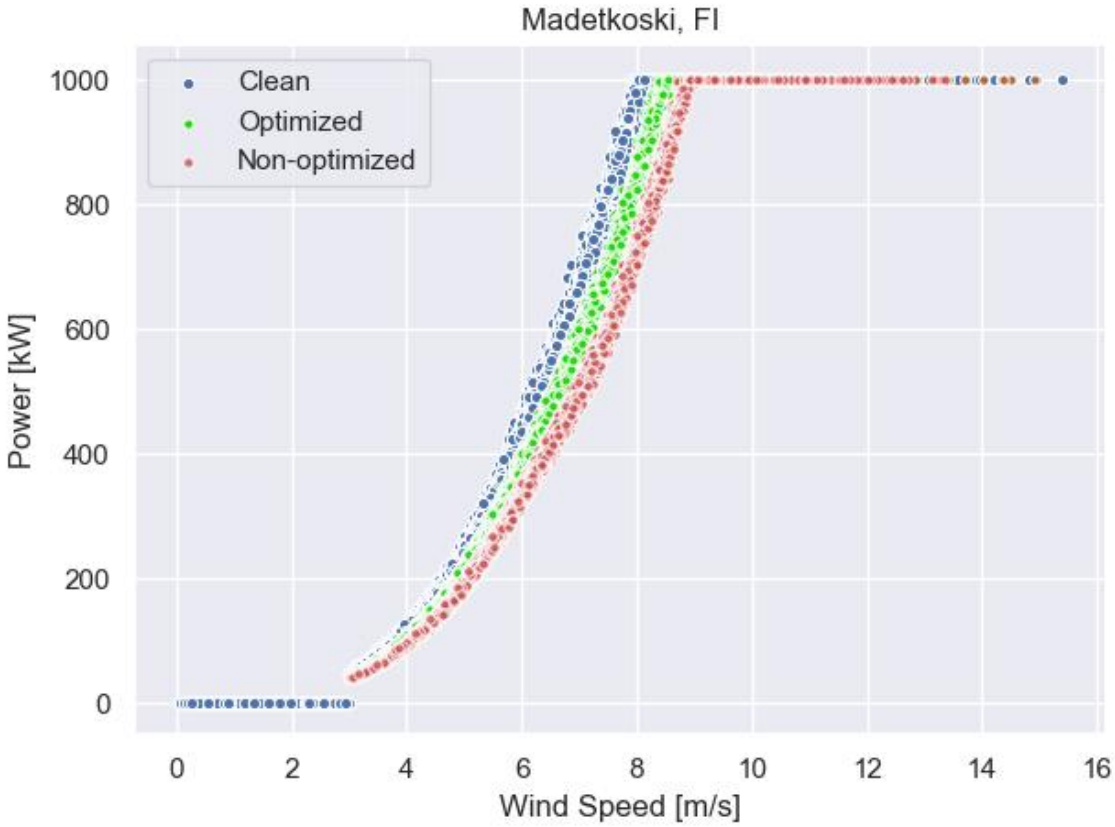

Figure 37. Superposition of the power curves in Madetkoski, FI.

In summary, the main results for Madetkoski are:

- Yearly mean losses:
  - Non-optimized case: 12.4%
  - Optimized case: 8.6%
- January mean losses:
  - Non-optimized case: 29.6%
  - Optimized case: 21.9%

Murmansk, Russia

Murmansk is located on the west side of Russia and it is the largest city at north of Arctic Circle. The average wind speed is 7.42 m/s, average temperature is 0.15 ºC, average relative humidity is 88.28% and it has 1,221 hours of conditions for atmospheric ice per year. Despite the relative high latitude (68.5º N), icing events are less frequent when compared to the other locations.

According to the top right graph in Figure 38, the yearly losses for the icing case varies from 1.6% to 3.7% with an average of 2.7% from 2011 to 2019 and it was reduced to 0.7% to 2.6% with an average of 1.7% for the optimized case.

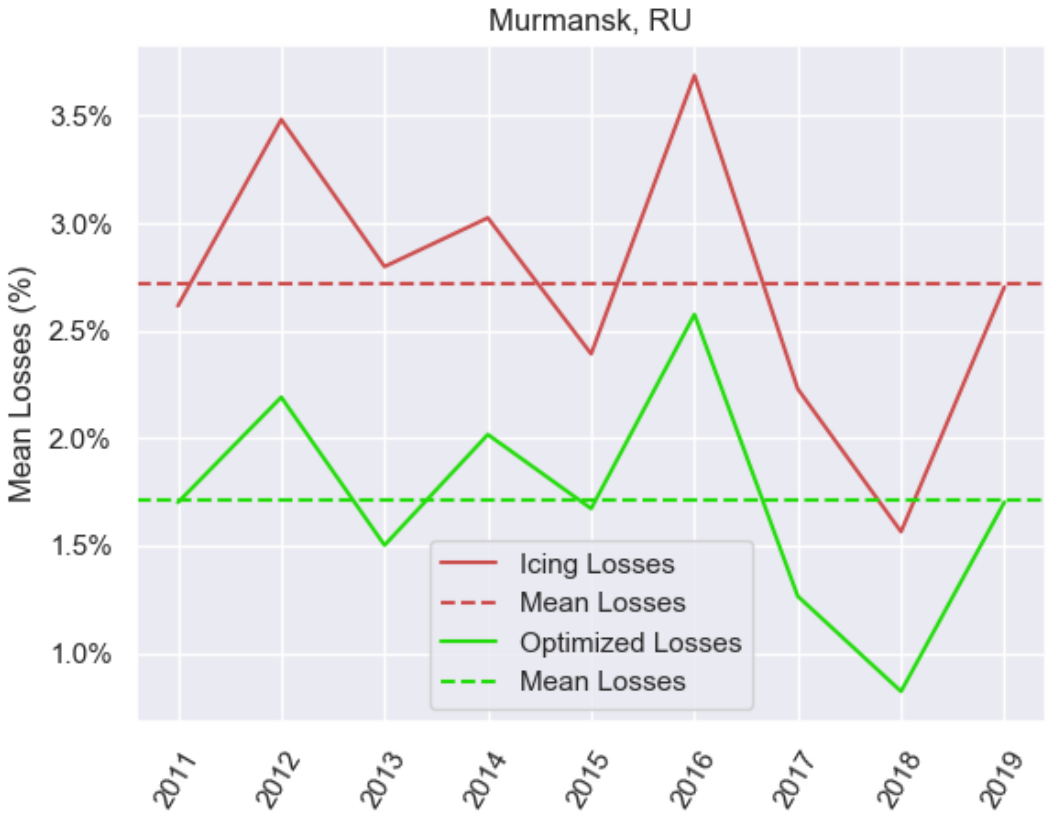

Figure 38. Yearly losses for Murmansk, RU.

Although the wind speed is higher in Murmansk, losses due to icing are not so severe as previous locations, and in January it is observed a mean losses of 9.5% for the icing case which is reduced to 7.8% with the optimization method. It is observed that conditions for atmospheric ice are not observed from May to September, according to Figure 39

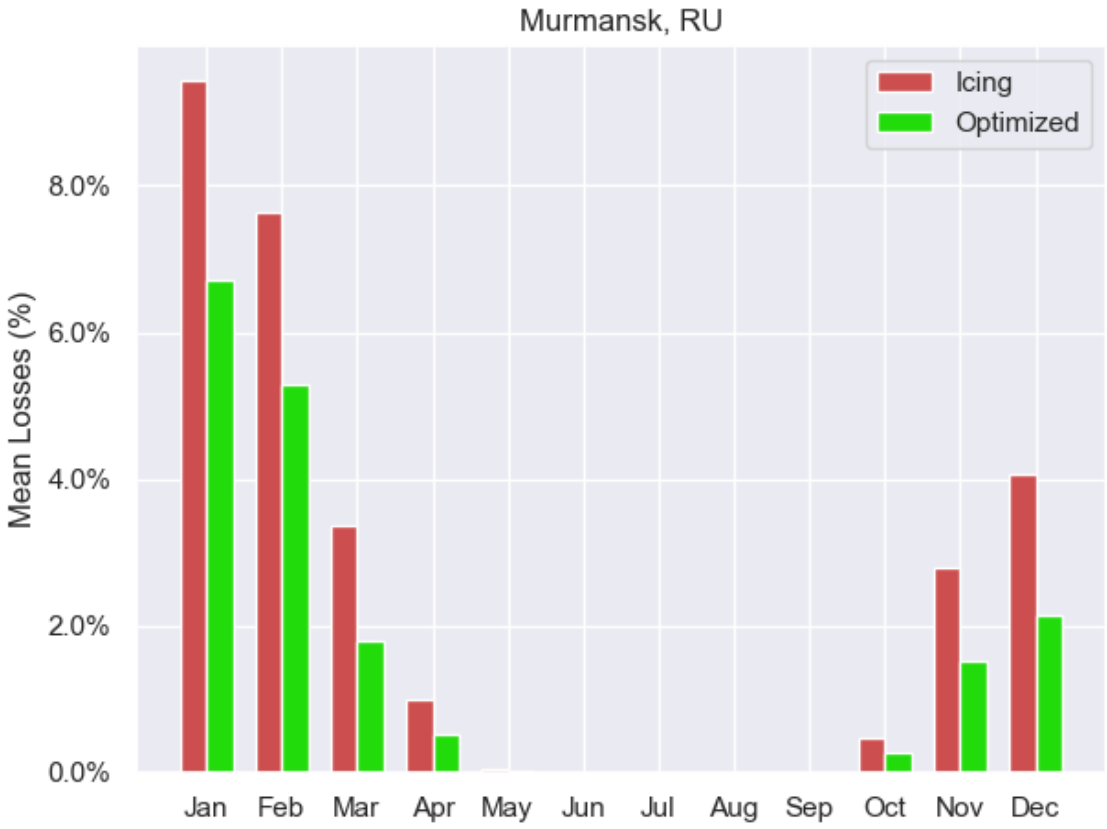

Figure 39. Monthly mean losses for Murmansk, RU.

The power curves for the icing case and for the optimized case are shown in the graphs in Figure 40 and it shows a small improvement made by the optimized method, with a less separation between the icing component and the clean component in the left graph. Even though this site has not many hours of icing per year, the average wind speed is close to the region with the highest losses shown in Figure 27 from Chapter 3. As it was expected, the optimization method (green dots) is between the clean (blue dots) and the non-optimized case (red dots), showing the improvement made by the presented method.

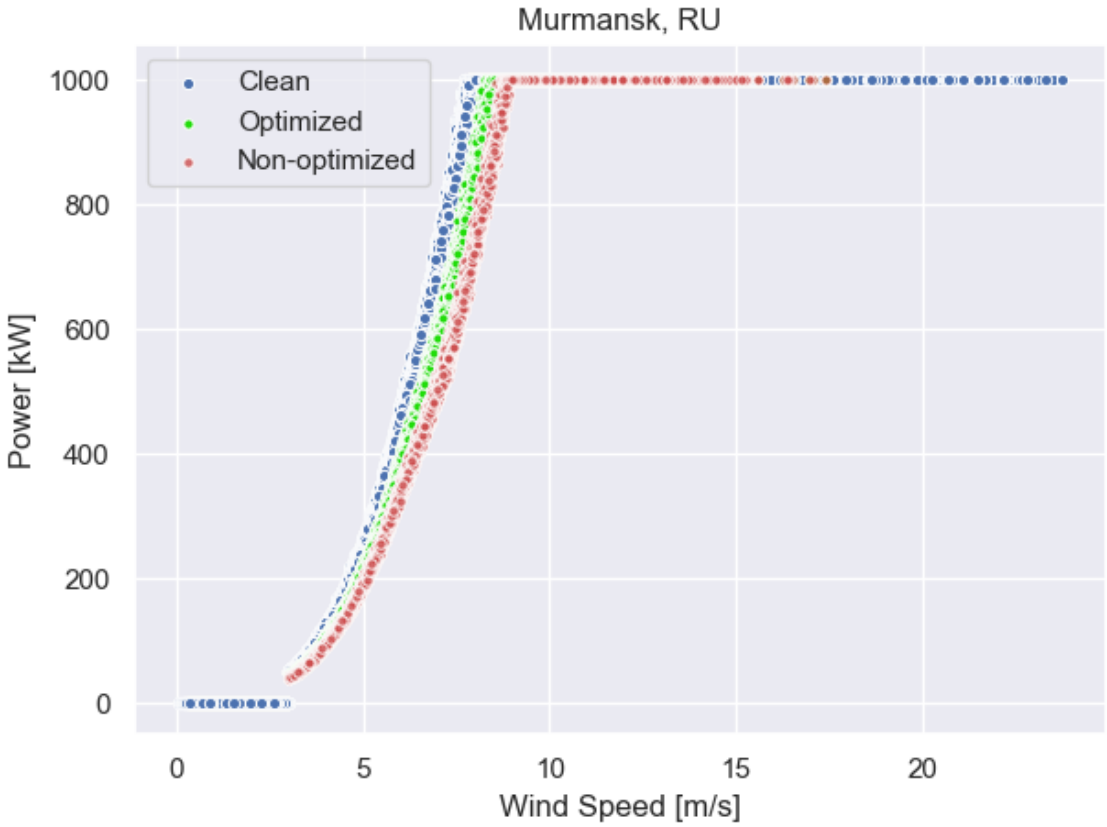

Figure 40. Superposition of the power curves in Murmansk, RU.

In summary, the main results for Murmansk are:

- Yearly mean losses:
  - Non-optimized case: 2.7%
  - Optimized case: 1.7%
- January mean losses:
  - Non-optimized case: 9.4%
  - Optimized case: 6.7%

Olhava, Finland

Olhava is in the middle Finland and is the most south location used in this study case, with an average wind speed of 4.57 m/s, average temperature of 2.39 ºC, average relative humidity of 88.21%, and 1,598 hours of icing per year. The region is known as a good area for wind plants and it has a high number of wind farms close by.

Yearly losses for Olhava shows an oscillation of power losses, varying from 4.3% to 10.6% with an average of 7.1% for the icing case and it is reduced from 2.8% to 7.6% with an average of 4.8% for the optimized case, according to Figure 41.

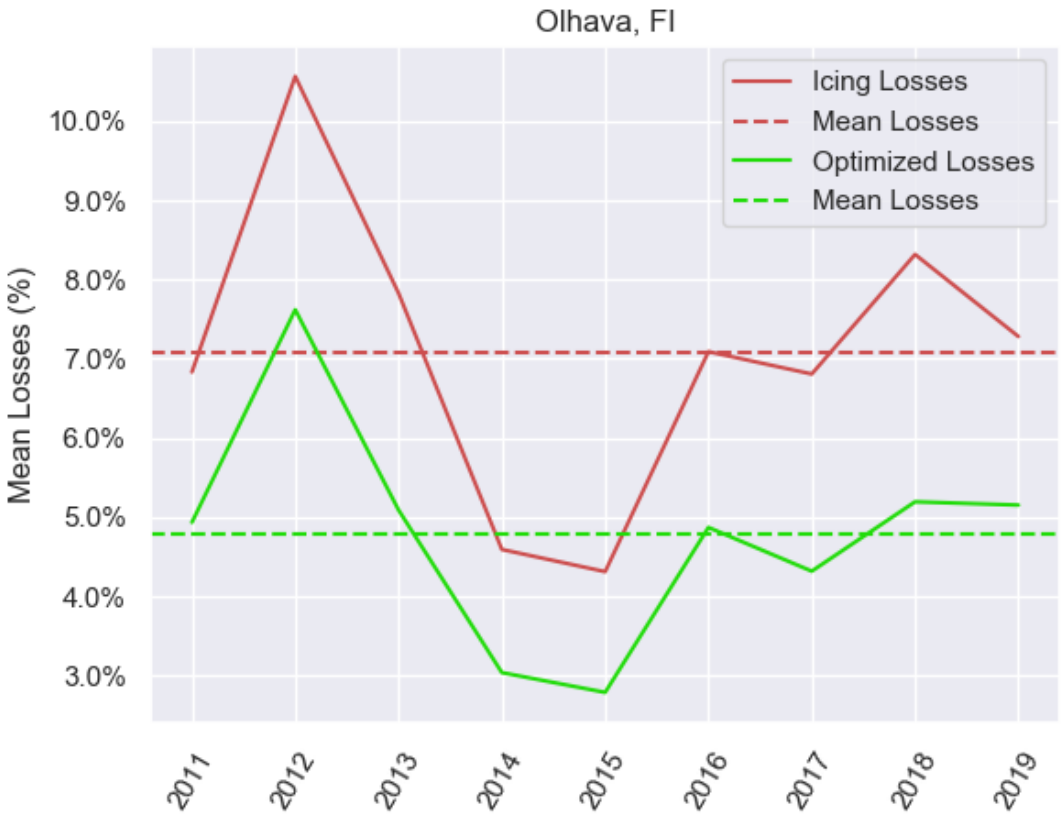

Figure 41. Yearly losses for Olhava, FI.

The monthly means of losses shows the highest losses of 23.1% in January for the icing case being reduced to 16.2% with the optimization method and no conditions for atmospheric ice from May to October, according to Figure 42. January, February, and March are months with severe power losses due to icing, with average losses between 12.5% and 23.1% with no optimization method.

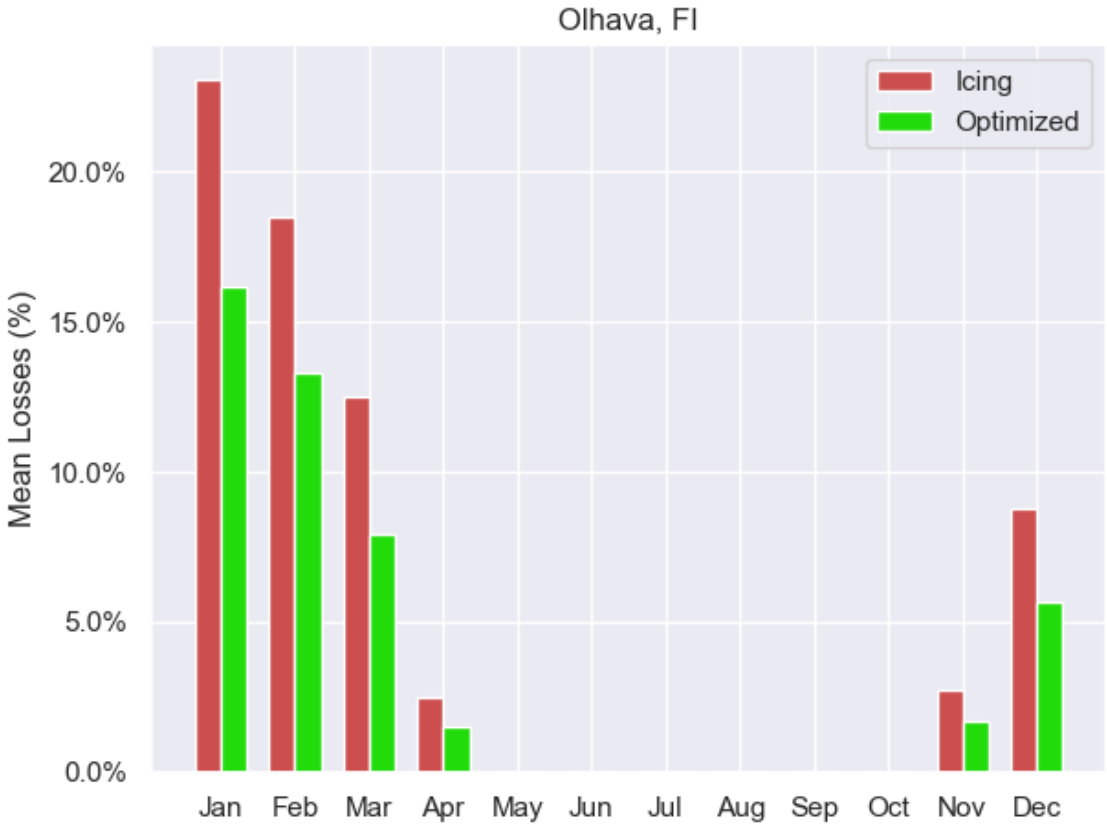

Figure 42. Monthly mean losses for Olhava, FI.

Furthermore, the power curves for Olhava are shown in Figure 43 and it is clearly visible that the icing component for the non-optimized case has a larger space separating it from the clean component. This space between the components is not visible in the optimized case, with the green dots almost together with the blue dots.

As it was expected, the optimization method (green dots) is between the clean (blue dots) and the non-optimized case (red dots), showing the improvement made by the presented method. The separation between the components is more visible in this case comparing to the others.

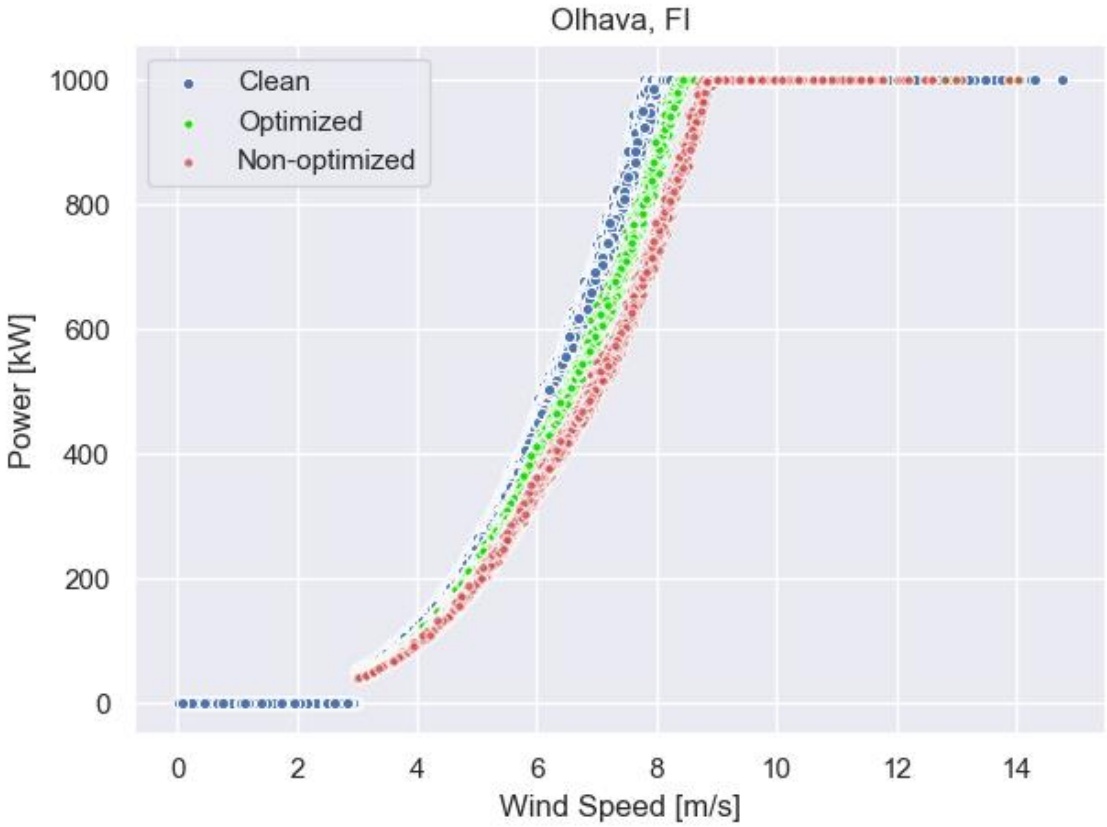

Figure 43. Superposition of the power curves in Olhava, FI.

In summary, the main results for Olhava are:

- Yearly mean losses:
  - Non-optimized case: 7.1%
  - Optimized case: 4.8%
- January mean losses:
  - Non-optimized case: 23.1%
  - Optimized case: 16.2%

Yamalsky, Russia

Yamalsky is in the north-west of Russia and it is the most north region of this study, with an average wind speed of 7.14 m/s, average temperature of -6.51 ºC, average relative humidity of 90.78%, and 2,596 hours of atmospheric ice per year. The site is in the most northern latitude in this study case, it has the lowest temperature, highest relative humidity, and it has the highest time of conditions for atmospheric ice per year.

The yearly losses in Yamalsky are 19.7% for the non-optimized case between 2011 and 2019, with a reduction to 17.8% with the optimization method. The highest losses occurred in 2014 when the losses reached 27% and the minimum were in 2012 with 11.2%, according to Figure 44.

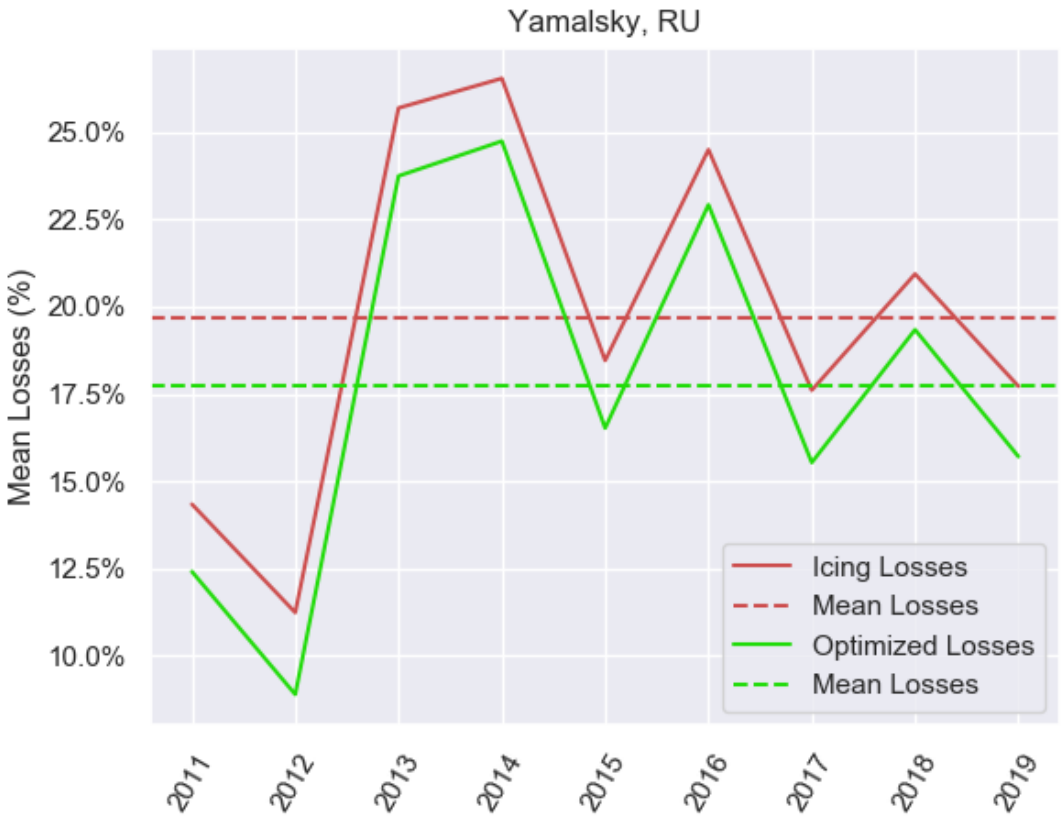

Figure 44. Yearly losses for Yamalsky, RU.

The monthly mean losses are presented in Figure 45, and it show the high losses in Yamalsky between November and April. The extreme month is January, with losses up to 57.1% for the non-optimized case, with a reduction to 55.2% with the optimization method. From June to September there are no conditions for atmospheric ice.

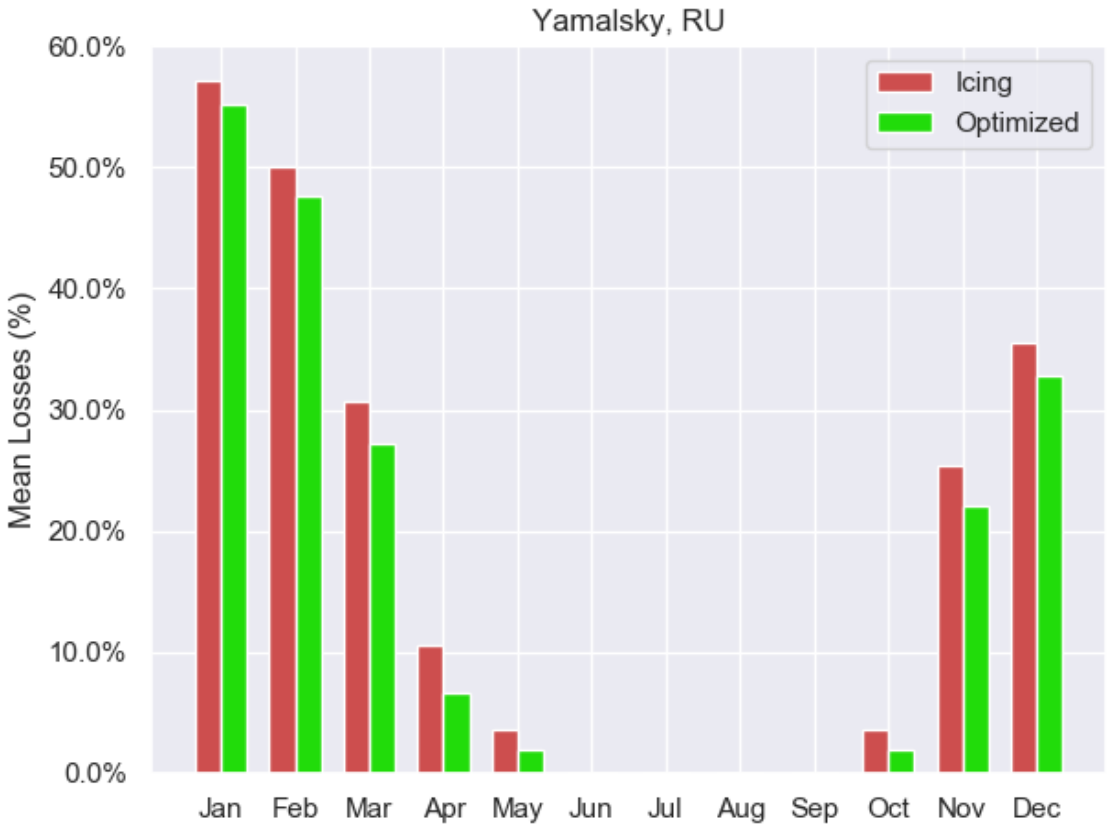

Figure 45. Monthly mean losses for Yamalsky, RU.

Finally, the power curves for Yamalsky are shown in Figure 46. The graph shows the improvement in the power curve for this location, with the non-optimized case at the right adjacent from the other cases.

As it was expected, the optimization method (green dots) is between the clean (blue dots) and the non-optimized case (red dots), showing the improvement made by the presented method.

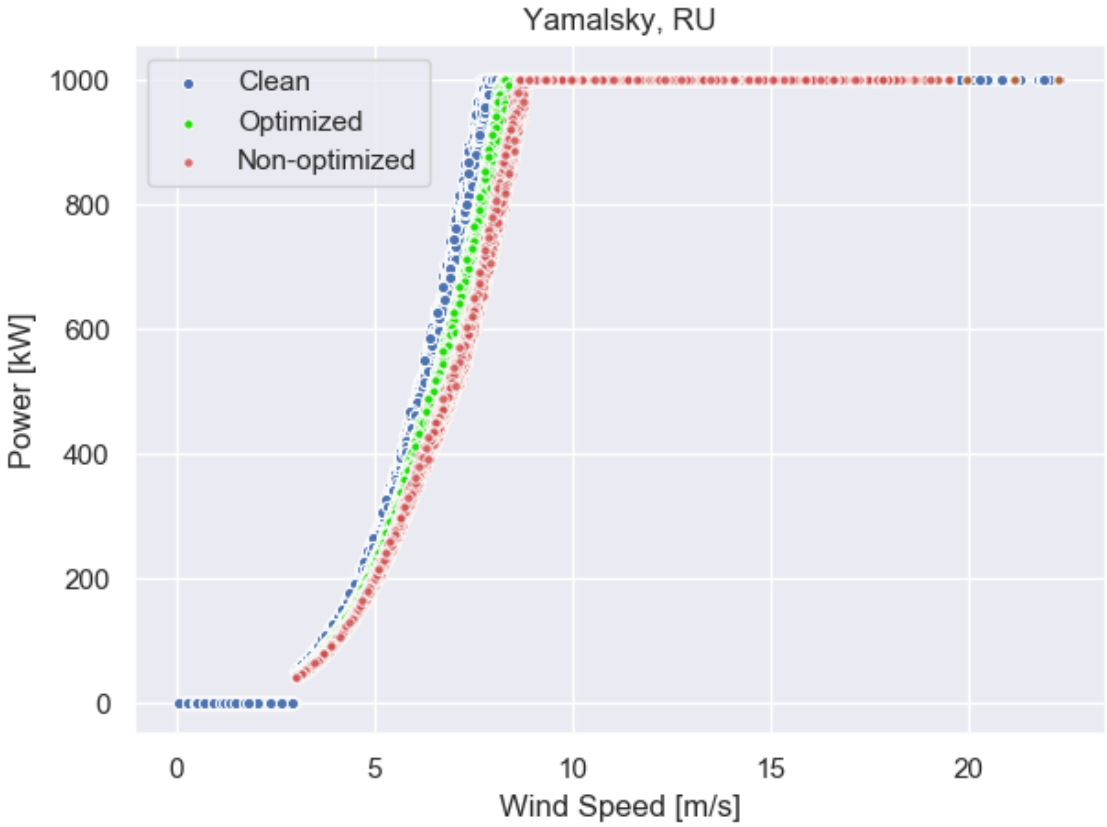

Figure 46. Superposition of the power curves in Yamalsky, RU.

In summary, the main results for Olhava are:

- Yearly mean losses:
  - Non-optimized case: 19.7%
  - Optimized case: 17.8%
- January mean losses:
  - Non-optimized case: 57.1%
  - Optimized case: 55.2%

4.4.1 Summarized Results

Results of the study cases are summarized in Table 6, with the average losses for the icing case, for the optimized case, and the improvement from the icing to the optimized case with the proposed control method for the entire period from 2011 to 2019 (Mean Yearly Losses) and for the most extreme month for the monthly mean losses.

The highest improvement in terms of mean yearly losses was observed in Madetkoski with 3.8%, and the highest improvement for mean monthly losses in January was observed in the same location, with 7.6% caused by the optimization method.

Table 6. Summarized results of the study case.

Location	**Mean Yearly Losses [%]**			**January Mean Losses [%]**		
	Non-Opt.	Optimized	Improvement	Non-Opt.	Optimized	Improvement
Jääräjoki, FI	6.3	4.3	2.0	16.1	12.1	4.0
Käsivarren, FI	9.1	6.5	2.6	23.2	18.6	4.6
Madetkoski, FI	12.4	8.6	3.8	29.6	21.9	7.6
Murmansk, RU	2.7	1.7	1.0	9.4	6.7	2.7
Olhava, FI	7.1	4.8	2.3	23.1	16.2	6.9
Yamalsky, RU	19.7	17.8	1.9	57.1	55.2	2.0

Results from Table 6 are plotted in Figure 47 for the yearly losses and in Figure 48 for the mean monthly losses of the extreme value of each location. As discussed before, the highest yearly losses were found in Yamalsky, Russia. In addition, the highest monthly mean losses occur in the same location in January.

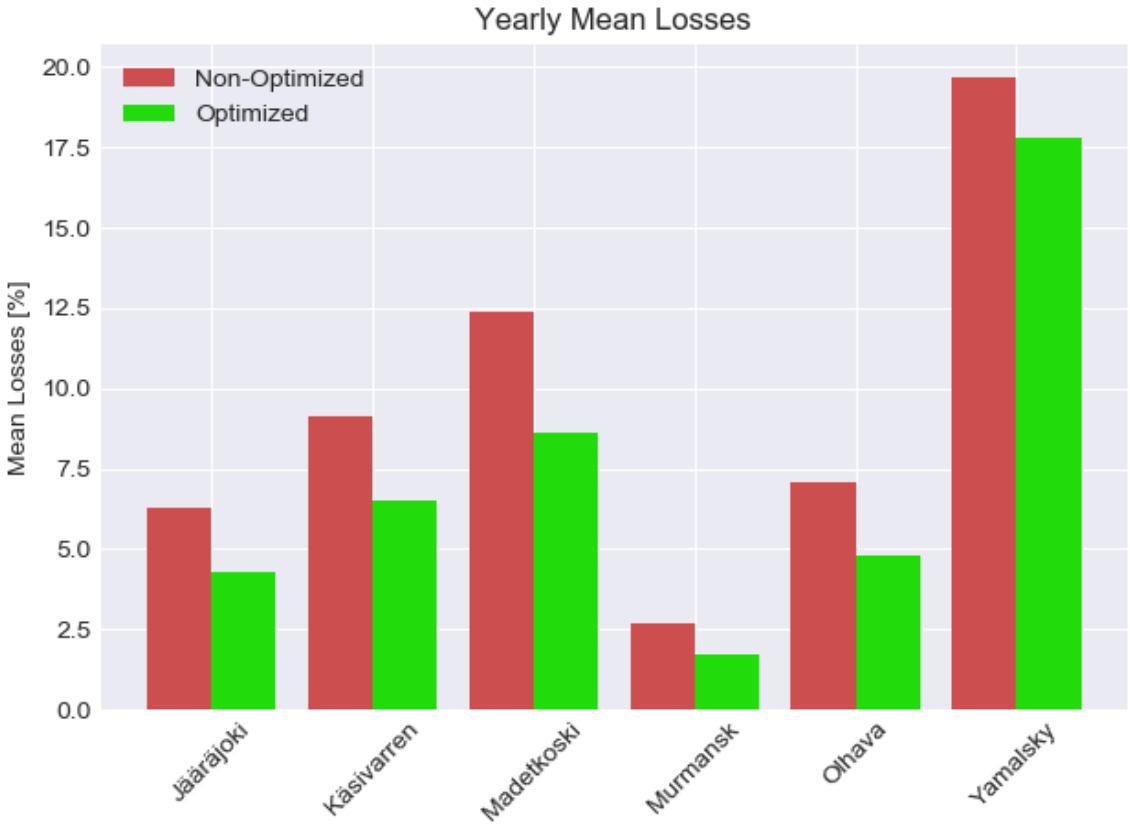

Figure 47. Yearly mean losses for all locations in the study case.

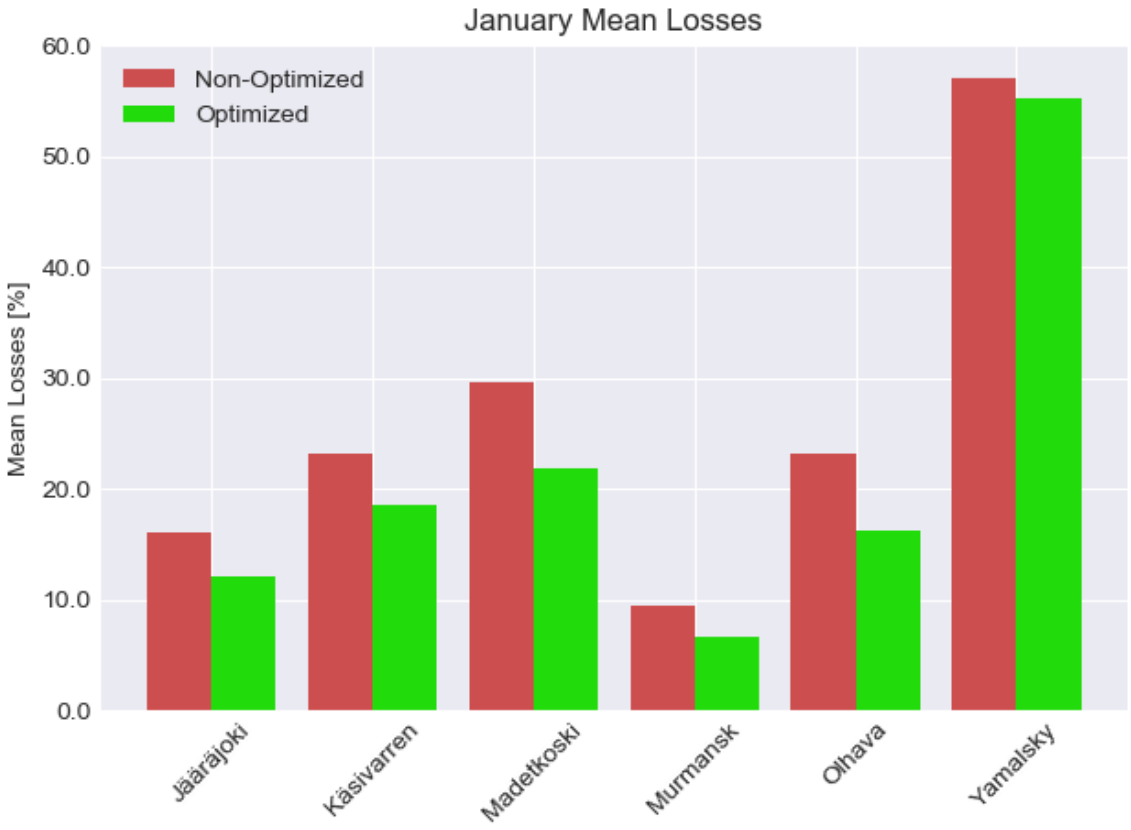

Figure 48. January mean losses for all locations in the study case.

CHAPTER 5 - CONCLUSIONS AND RECOMMENDATIONS

5.1 Conclusions

This master's thesis is part of EFREA Project (Energy-efficient systems based on renewable energy for Arctic conditions) a cross-border cooperation between Finland, represented by Lappeenranta-Lahti University of Technology and Russia, represented by Peter the Great St. Petersburg Polytechnic University and the National Research Centre "Kurchatov Institute", Central Research Institute of Structural Materials "Prometey". The research was carried out at the Laboratory of Energy Technology, LUT School of Energy Systems, Lappeenranta-Lahti University of Technology.

Calculations of the power coefficients of clean airfoils and airfoils with ice accumulation has been performed based on data extracted from previous papers, master's thesis and PhD studies that had in common the following information: lift and drag coefficients per angle of attack of clean airfoil and icing airfoil for the NACA 64618 airfoil series and the sources are listed in Table 2 from Chapter 3. This airfoil was chosen because it is widely used in wind turbines and it is part of the 5 MW Reference wind turbine from NREL (National Renewable Energy Laboratory). The information in the original studies is plotted in 2D graphs and a digitizer tool was used to convert the graphs to numerical data.

Comparing the studies used in this thesis, the first thing to notice is that they were performed using different software and methods to simulate the ice accretion and the aerodynamic coefficients. Homola et al. (2010) and Turkia et al. (2013) simulated the ice accretion with TURBICE software and used ANSYS software to estimate aerodynamic coefficients, while Etemaddar et al. (2012) used LEWICE software and Gantasala et al. (2019) proposed a new method to simulate ice accretion. On the other hand, Hudecz (2014) performed an experimental study using a wind tunnel to simulate ice accretion and measured the aerodynamic coefficients. Different software and methods to estimate drag and lift coefficients might lead to different results, but they are all supported by the scientific methodology. Secondly, the aerodynamic coefficients had different intensities, but they followed the general trend of forces on an airfoil with ice, that for higher values of angle of attack, for the lift coefficient there is a separation between the clean and the icing case and for the drag coefficient the separation occurs for angle of attack close to zero degrees.

Power coefficient curves were calculated according to equation (7) provided by Wilson et al. (1976) for angle of attack (α) varying from 0º to 10º and tip-to-speed ratio (λ) varying from 0 to 20 in order to find to optimal combination between α and λ for the clean and icing cases. Table 3 from section 3.3.1 Summarized Results shows the results obtained in this proposed methodology for the data extracted from the 5 references sources. Figure 27 provides a visualization of the results showing the higher power losses when the wind is higher than 3.2 m/s and lower than 7.3 m/s, which is the region where the pitch control system is not actuating in wind turbines class III (typical wind turbines in northern region). In other words, the configuration of the pitch control is not on its optimum operational point, and without the optimization method it is losing power production.

Locations in Finland and Russia were chosen according to wind and icing maps of the countries. Data of wind speed, temperature and pressure was downloaded from MERRA2 and data of relative humidity was downloaded from CFSv2. Conditions for atmospheric ice formation were defined as wind speed higher than 3 m/s, temperature lower than -4 ºC and higher than -20 ºC, and relative humidity higher than 95%, according to definitions by the literature. Statistics of the data are written in Table 5 and it shows an average of 1,942 hours of icing between the 6 locations, with Murmansk, in Russia, having less atmospheric ice with 1,221 hours and Murmansk, also in Russia, the highest with 2,596 hours of atmospheric ice per year. The highest average temperature is 2.39 ºC and the lowest relative humidity is 88.21% in Olhava, but it is not the less affected in power production due to icing, because parameters need to analyzed together and icing events depend on local profile, as discussed before by some authors (Davis, 2014) (Turkia, Huttunen, & Thomas, 2013) (Hudecz, 2014).

The yearly losses show the variation of power losses by year and it is important to point out the variation of atmospheric ice formation each year. The optimized method reduced the losses for all locations, with 1% of improvement for Murmansk and 3.8% for Madetkoski. For the icing case, yearly losses varied from 2.7% to 19.7%. This parameter is useful for wind plants developers for the estimation of annual energy production.

Monthly mean losses are an indicator of when the optimization strategy must by applied and how much of power is estimated to be lost due to icing. For all cases January was the most severe month in terms of power losses due to icing, but it depends on local weather. The optimization method decreased between 2.0 - 7.6% the power losses. For all locations there

is a period with no conditions for atmospheric ice in the summer season, with 5 months in Olhava and Murmansk, and 4 months for the other locations with no icing events. In fact, atmospheric ice may occur during more than half of the months of the year.

Finally, the power curve shows the component produced when there is no icing more on the left adjacent of the graph and the component on the right adjacent, when there is icing formation. In theory, the icing component should move to the left, close to the clean component when the optimization method is applied, and this fact was observed in all cases.

This thesis was performed to investigate icing effects on wind turbines and to propose a method to optimize power production of a wind turbine with ice accreted on the blades. The power coefficient of a wind turbine had losses up to 28.5% in wind speed of 7.3 m/s and the proposed method reduced it to 15.3%. The power losses were reduced from 29.6% to 21.9% in a typical month of January in Madetkoski, Finland, and the yearly losses were reduced from 12.4% to 8.6% in the same location.

5.2 Recommendations for Future Work

Despite of the results achieved in this research, some suggestions of future are proposed:

- In-site measurements of parameters are more precise than satellite data used in this study
- Deeper investigation about the conditions for atmospheric ice formation
- Experiments of ice accretion for different types of ice
- More experiments to estimate lift and drag coefficients for as many wind speeds as possible
- Improvement of the method to estimate the power coefficient of a wind turbine
- Improvement in the methodology of AEP considering icing events

REFERENCES

Byrkjedal, Ø. (2009). Estimating wind power production loss due to icing. *International Workshop on Atmospheric Icing of Structures.* Kjeller, Norway. Retrieved from https://www.compusult.com/html/IWAIS_Proceedings/IWAIS_2009/Session_5_wind_energy/session_5_byrkjedal.pdf

Addy, H. E. (2000). *Ice Accretions and Icing Effects for Modern Airfoils.* NASA STI Program Office, Glenn Research Center, Ohio. Retrieved from https://ntrs.nasa.gov/archive/nasa/casi.ntrs.nasa.gov/20000044552.pdf

Blasco, P., Palacios, J., & Schmitz, S. (2016). *Effect of icing roughness on wind turbine power production.* PA 16801, USA: Department of Aerospace Engineering, The Pennsylvania State University, State College.

Clausen, N.-E., & Giebel, G. (2017). *IceWind final scientific report.* Copenhagen: DTU Wind Energy.

Davis, N. (2014). *Icing Impacts on Wind Energy Production.* Doctoral Thesis, Technical University of Denmark, DTU Wind Energy, Copenhagen. Fonte: https://backend.orbit.dtu.dk/ws/portalfiles/portal/104279722/Icing_Impacts_on_Wind_Energy_Production_final.pdf

Dierer, S., Oechslin, R., & Cattin, R. (2011, September 6). Wind turbines in icing conditions: performance and prediction. *Advances in Science and Research, 6,* 245–250. doi:https://doi.org/10.5194/asr-6-245-2011

Elistratov, V. V., Knežević, M., Denisov, R., & Konishchev, M. (2014). PROBLEMS OF CONSTRUCTING WIND-DIESEL POWER PLANTS IN HARSH CLIMATIC CONDITIONS. *Journal of Applied Engineering Science, 12,* 8. doi:10.5937/jaes12-5632

Emeis, S. (2013). *Wind Energy Meteorology.* Garmisch-Partenkirchen, Germany: Springer. doi: 10.1007/978-3-642-30523-8

Etemaddar, M., Hansen, M. O., & Moan, T. (2012, November 22). Wind turbine aerodynamic response under atmospheric icing conditions. *Wind Energy, 17,* 241-265. doi:10.1002/we.1573

Freudenreich, K., Steiniger, M., Khadiri-Yazami, Z., Tang, T., & Säger, T. (2016). Site assessment for a type certification icing class. *WindEurope Summit 2016,* (p. 10). Hamburg. Retrieved from

https://windeurope.org/summit2016/conference/allfiles2/240_WindEurope2016presentation.pdf

Gantasala, S., Tabatabaei, N., Cervantes, M., & Aidanpää, J.-O. (2019). Numerical Investigation of the Aeroelastic Behavior of a Wind Turbine with Iced Blades. *Energies, 2422*, 12. doi:doi.org/10.3390/en12122422

Gipe, P. (2004). *Wind Power, Renewable Energy for Home, Farm and Business* (2nd edition ed.). United States: Chelsea Green Publishing Company.

Griffith, D. A., Ward, S. M., & Yorty, D. P. (April de 2016). Analysis Of Ice Detector Observations At Mount Crested Butte, Colorado During The 2014-2015 Winter Season. *Journal of Weather Modification, 48*, 17.

Haaland, S. S. (2011). *Estimating Production Loss due to Icing on Wind Turbines.* University of Tromsø, Department of Physics and Technology. Tromsø: Faculty of Science and Technology. Retrieved from https://munin.uit.no/handle/10037/3814

Homola, M. C., Virk, M. S., Wallenius, T., Nicklasson, P. J., & Sundsbø, P. A. (2010, August 7). Effect of atmospheric temperature and droplet size variation on ice accretion of wind turbine blades. *Journal of Wind Engineering*. doi:10.1016/j.jweia.2010.06.007

Hudecz, A. (2014). *Icing Problems of Wind Turbine Blades in Cold Climates.* Doctoral Thesis, Technical University of Denmark, Department of Wind Energy, Copenhagen. Retrieved from https://orbit.dtu.dk/en/publications/icing-problems-of-wind-turbine-blades-in-cold-climates

IEA Wind Task 19. (2012). *State-of-the-Art of Wind Energy in Cold Climates.* Retrieved from https://community.ieawind.org/task19/viewdocument/iea-wind-tcp-task-19-state-of-the-1?CommunityKey=b1ba65c9-bf79-4b55-98cd-cf324c26f76f&tab=librarydocuments

IEA Wind Task 19. (2017). *Wind Energy Projects in Cold Climate.* IEA Wind TCP Recommended Practice 13 2nd Edition: Wind Energy in Cold Climates. Fonte: https://community.ieawind.org/task19/viewdocument/iea-wind-tcp-task-19-recommended-pr?CommunityKey=b1ba65c9-bf79-4b55-98cd-cf324c26f76f&tab=librarydocuments

Lantz, E., Hand, M., & Wiser, R. (2012). The Past and Future Cost of Wind Energy. *World Renewable Energy Forum.* Denver: National Renewable Energy Laboratory. Retrieved from https://www.nrel.gov/docs/fy12osti/54526.pdf

Letcher, T. M. (2017). *Wind Energy Engineering.* London, United Kingdom: Elsevier. doi:10.1016/B978-0-12-809451-8.00002-3

Manwell, J. F., McGowan, J. G., & Rogers, A. L. (2010). *Wind energy explained: theory, design and application.* John Wiley & Sons.

Mathew, S., & Philip, G. S. (2011). *Advances in Wind Energy Conversion Technology* (1 ed.). New York: Springer-Verlag Berlin Heidelberg. doi:10.1007/978-3-540-88258-9

Okulov, V., & van Kuik, G. A. (2009). The Betz-Joukowsky limit for the maximum power coefficient of wind turbines. *International Scientific Journal for Alternative Energy and Ecology, 9*, 106-111. Retrieved from http://isjaee.hydrogen.ru/?pid=1845

Rast, J., Cattin, R., & Heimo, A. (2009). Icing Indices: a good solution? *International Workshop on Atmospheric Icing of Structures - IWAS.* Bern. Retrieved from https://www.compusult.com/html/IWAIS_Proceedings/IWAIS_2009/Session_4_cost_727_wg2/session_4_rast.pdf

Saha, S. M. (2012). *NCEP Climate Forecast System Version 2 (CFSv2) Monthly Products.* Computational and Information Systems Laboratory. Research Data Archive at the National Center for Atmospheric Research. doi:https://doi.org/10.5065/D69021ZF

Thomsen, S. C. (2006). *Nonlinear Control of a Wind Turbine.* Technical University of Denmark, Informatics and Mathematical Modelling, Kongens Lyngby. Retrieved from http://www2.imm.dtu.dk/pubdb/views/edoc_download.php/4813/pdf/imm4813.pdf

Tong, W. (2010). *Wind Power Generation and Wind Power Generation and Wind Turbine Design Wind Turbine Design.* Ashurst, Southampton, UK: WIT Press. Retrieved from https://www.witpress.com/images/stories/content_images/contents/c42051.pdf

Turkia, V., Huttunen, S., & Thomas, W. (2013). *Method for estimating wind turbine production losses due to icing.* VTT Technical Research Centre of Finland. Espoo: VTT Technology, No. 114.

Wikipedia. (n.d.). *Glaze (ice)*. Retrieved April 24, 2020, from Wikipedia, the free encyclopedia: https://en.wikipedia.org/wiki/Glaze_(ice)

Wilson, R. E., Lissaman, P. B., & Walker, S. N. (1976). *Aerodynamic Performance of Wind Turbines.* Oregon State University. Oregon: Energy Research and Development Administration, Technical Information Center. Fonte:

https://nwtc.nrel.gov/system/files/WilsonLissamanWalker_AerodynamicPerformanceOfWindTurbines%281976%29.pdf

Wind Europe. (2020). *Wind energy in Europe in 2019.* Brussels: Wind Europe.

Zhang, M. H. (2015). *Wind Resource Assessment and Micro-siting: Science and Engineering.* John Wiley & Sons Singapore Pte Ltd.

APPENDIX A – Weather Data

A.1 – Jääräjoki, Finland

Date/time [UTC]	Speed 50m [m/s]	Direction 50m [degrees]	Temperature 10m [degrees C]	Temperature 2m [degrees C]	Pressure 0m [kPa]	RH 2m [%]
2011-01-01T00:00:00	6.28	214.2	-12.4	-12.8	95.9	97.5
2011-01-01T01:00:00	5.96	219.8	-12.1	-12.6	95.9	97.5
2011-01-01T02:00:00	5.56	223.6	-11.7	-12.4	95.9	97.5
2011-01-01T03:00:00	5.21	225.4	-11.2	-12.1	95.9	97.6
2011-01-01T04:00:00	4.87	225.9	-10.7	-11.8	95.9	97.6
2011-01-01T05:00:00	4.42	226	-10.1	-11.5	96	97.6
2011-01-01T06:00:00	4.02	224.1	-9.8	-11.3	96	97.4
2011-01-01T07:00:00	3.64	222.2	-9.6	-11	96.1	97.2
2011-01-01T08:00:00	3.16	221	-9.3	-10.5	96.1	96.7
2011-01-01T09:00:00	2.64	215.9	-9.2	-10.2	96.2	96.3
2011-01-01T10:00:00	2.23	205.7	-9.1	-10.2	96.2	96.2
2011-01-01T11:00:00	1.85	196.5	-9.3	-10.4	96.3	96
2011-01-01T12:00:00	1.33	187.2	-9.5	-10.8	96.4	96.1
2011-01-01T13:00:00	0.69	157.9	-9.9	-11.5	96.5	96.1
2011-01-01T14:00:00	0.77	89.7	-10.2	-11.7	96.5	96.7
2011-01-01T15:00:00	1.3	62.6	-10.3	-11.6	96.6	97.4
2011-01-01T16:00:00	1.47	50.8	-10.3	-11.4	96.7	97.3
2011-01-01T17:00:00	1.43	36.1	-10.2	-11.3	96.7	98.8
2011-01-01T18:00:00	1.43	17	-10	-11.3	96.8	100

A.2 – Käsivarren, Finland

Date/time [UTC]	Speed 50m [m/s]	Direction 50m [degrees]	Temperature 10m [degrees C]	Temperature 2m [degrees C]	Pressure 0m [kPa]	RH 2m [%]
2011-01-01T00:00:00	6.82	305.2	-7.9	-8.7	91	100
2011-01-01T01:00:00	7.15	299.7	-8.1	-8.8	91	100
2011-01-01T02:00:00	7.25	296.3	-8.2	-8.9	91	100
2011-01-01T03:00:00	7.2	294.5	-8.2	-8.9	91.1	100
2011-01-01T04:00:00	7.04	293.9	-8	-9	91.1	100
2011-01-01T05:00:00	6.75	297.3	-7.9	-9.1	91.1	100
2011-01-01T06:00:00	6.35	305.9	-7.9	-9.3	91.1	100
2011-01-01T07:00:00	6.18	317.2	-7.5	-9.2	91.2	100
2011-01-01T08:00:00	6.44	325.4	-7.1	-8.5	91.2	98.6
2011-01-01T09:00:00	6.78	331.9	-6.6	-7.7	91.3	97.2
2011-01-01T10:00:00	7.06	334.2	-6.1	-6.9	91.3	100
2011-01-01T11:00:00	7.27	336.6	-5.5	-6.1	91.4	100
2011-01-01T12:00:00	7.22	339.6	-5.4	-5.9	91.4	98.7
2011-01-01T13:00:00	6.74	339.1	-5.6	-6.2	91.5	95.5
2011-01-01T14:00:00	6.77	340.3	-5.7	-6.4	91.5	96.5
2011-01-01T15:00:00	6.55	343.9	-5.6	-6.4	91.6	96.2
2011-01-01T16:00:00	6.25	348.5	-5.7	-6.6	91.6	95.4
2011-01-01T17:00:00	5.66	350.7	-5.8	-7	91.7	94.6
2011-01-01T18:00:00	5.43	354.2	-5.9	-7.4	91.8	94.5

A.3 – Madetkoski, Finland

Date/time [UTC]	Speed 50m [m/s]	Direction 50m [degrees]	Temperature 10m [degrees C]	Temperature 2m [degrees C]	Pressure 0m [kPa]	RH 2m [%]
2011-01-01T00:00:00	4.87	211.3	-16.9	-17.3	95.9	99.3
2011-01-01T01:00:00	4.79	213.3	-16.8	-17.2	95.9	99.3
2011-01-01T02:00:00	4.62	214.4	-16.6	-16.8	95.9	99.4
2011-01-01T03:00:00	4.38	213.4	-16.4	-16.6	95.9	99.5
2011-01-01T04:00:00	4.25	211.8	-16.4	-16.5	95.9	99.5
2011-01-01T05:00:00	4.33	216.7	-16.3	-16.4	96	99.4
2011-01-01T06:00:00	4.53	221.9	-16.2	-16.4	96	99.4
2011-01-01T07:00:00	4.81	223.9	-16.3	-16.6	96.1	99.4
2011-01-01T08:00:00	4.73	219.1	-16.6	-16.8	96.1	99.3
2011-01-01T09:00:00	4.85	217.6	-16.8	-17.1	96.1	99.3
2011-01-01T10:00:00	4.79	215.5	-17.1	-17.3	96.2	99.3
2011-01-01T11:00:00	4.7	213.3	-17.3	-17.5	96.2	99.3
2011-01-01T12:00:00	4.62	212.2	-17.3	-17.6	96.2	99.3
2011-01-01T13:00:00	4.56	209.5	-17.4	-17.6	96.3	99.3
2011-01-01T14:00:00	4.54	205.3	-17.4	-17.7	96.3	99.4
2011-01-01T15:00:00	4.51	204.1	-17.5	-17.7	96.4	99.4
2011-01-01T16:00:00	4.42	203.9	-17.6	-17.9	96.4	99.5
2011-01-01T17:00:00	4.34	202.4	-17.7	-18.1	96.5	99.6
2011-01-01T18:00:00	4.11	200.8	-17.8	-18.3	96.5	99.6

A.4 – Murmansk, Russia

Date/time [UTC]	Speed 50m [m/s]	Direction 50m [degrees]	Temperature 10m [degrees C]	Temperature 2m [degrees C]	Pressure 0m [kPa]	RH 2m [%]
2011-01-01T00:00:00	7.5	208.5	-12.5	-12.5	97.6	94.7
2011-01-01T01:00:00	7.65	211.5	-12.4	-12.4	97.6	94.7
2011-01-01T02:00:00	7.92	212.1	-12.5	-12.4	97.6	94.5
2011-01-01T03:00:00	8.48	211	-12.6	-12.5	97.6	94.1
2011-01-01T04:00:00	9.24	209.8	-12.8	-12.7	97.7	94.1
2011-01-01T05:00:00	10.25	209.2	-12.9	-12.9	97.7	94.1
2011-01-01T06:00:00	11.54	210.5	-12.7	-12.7	97.8	94.2
2011-01-01T07:00:00	11.37	208.4	-12.6	-12.6	97.8	93.9
2011-01-01T08:00:00	11.7	206.3	-12.4	-12.3	97.9	93.7
2011-01-01T09:00:00	11.99	204.5	-12.1	-12	97.9	93.3
2011-01-01T10:00:00	11.88	203	-12	-11.9	98	93
2011-01-01T11:00:00	11.53	201.3	-12.1	-12	98	92.8
2011-01-01T12:00:00	11.09	199.1	-12.2	-12.1	98.1	92.8
2011-01-01T13:00:00	10.7	196.2	-12.2	-12.1	98.1	92.9
2011-01-01T14:00:00	10.42	193.2	-12.2	-12.1	98.2	93.2
2011-01-01T15:00:00	10.48	191.5	-12.2	-12.1	98.2	93.5
2011-01-01T16:00:00	10.21	188.6	-12.2	-12.1	98.3	93.6
2011-01-01T17:00:00	10.24	187.4	-12.3	-12.2	98.3	93.7
2011-01-01T18:00:00	10.31	187.1	-12.4	-12.3	98.3	93.9

A.5 – Olhava, Finland

Date/time [UTC]	Speed 50m [m/s]	Direction 50m [degrees]	Temperature 10m [degrees C]	Temperature 2m [degrees C]	Pressure 0m [kPa]	RH 2m [%]
2011-01-01T00:00:00	3.6	125.2	-14.5	-14.7	98.6	99.3
2011-01-01T01:00:00	3.74	122.6	-14.9	-15	98.6	99.3
2011-01-01T02:00:00	3.78	118.1	-15.1	-15.2	98.6	99.3
2011-01-01T03:00:00	3.5	116.8	-15	-15.1	98.7	99.4
2011-01-01T04:00:00	3.2	116.1	-14.9	-15	98.7	99.4
2011-01-01T05:00:00	3.08	116.6	-14.7	-14.8	98.8	99.4
2011-01-01T06:00:00	3.11	122.6	-14.6	-14.7	98.8	99.5
2011-01-01T07:00:00	3.12	126.5	-14.4	-14.5	98.9	99.5
2011-01-01T08:00:00	2.99	129.4	-14.2	-14.3	98.9	99.5
2011-01-01T09:00:00	2.84	127.4	-14.1	-14.2	98.9	99.5
2011-01-01T10:00:00	2.67	125.3	-14	-14.1	98.9	99.5
2011-01-01T11:00:00	2.6	125.6	-14	-14.2	99	99.5
2011-01-01T12:00:00	2.69	128.4	-14	-14.4	99	99.4
2011-01-01T13:00:00	2.7	133.3	-14	-14.5	99	99.5
2011-01-01T14:00:00	2.74	137.1	-14	-14.6	99.1	99.6
2011-01-01T15:00:00	2.9	141.1	-14.1	-14.8	99.1	99.6
2011-01-01T16:00:00	3.07	146.9	-14.2	-15.1	99.1	99.6
2011-01-01T17:00:00	3.02	152.6	-14.3	-15.6	99.2	99.5
2011-01-01T18:00:00	2.75	156	-14.1	-15.8	99.2	99.4

A.5 – Yamalsky, Russia

Date/time [UTC]	Speed 50m [m/s]	Direction 50m [degrees]	Temperature 10m [degrees C]	Temperature 2m [degrees C]	Pressure 0m [kPa]	RH 2m [%]
2011-01-01T00:00:00	13.58	178.8	-18.3	-18.6	102.1	89.1
2011-01-01T01:00:00	13.71	178.9	-18.8	-19	102	89.2
2011-01-01T02:00:00	13.75	179.4	-19	-19.3	102	89.9
2011-01-01T03:00:00	13.57	180.2	-19.1	-19.4	102	91.7
2011-01-01T04:00:00	13.25	181.6	-19.3	-19.5	102	92.3
2011-01-01T05:00:00	12.83	183.4	-19.5	-19.7	102	92
2011-01-01T06:00:00	12.33	184.3	-19.8	-20	102.1	91.4
2011-01-01T07:00:00	11.83	184.8	-20.1	-20.3	102.1	91.3
2011-01-01T08:00:00	11.26	185.1	-20.3	-20.5	102.1	92.6
2011-01-01T09:00:00	10.89	184.8	-20.1	-20.3	102.1	94
2011-01-01T10:00:00	10.86	185.1	-19.5	-19.6	102.1	94.7
2011-01-01T11:00:00	10.83	185.1	-18.6	-18.7	102.2	95.4
2011-01-01T12:00:00	10.72	185.3	-17.7	-17.8	102.2	95.8
2011-01-01T13:00:00	10.48	184.4	-16.9	-17	102.2	96.1
2011-01-01T14:00:00	10.46	186.6	-16.1	-16.2	102.2	96.4
2011-01-01T15:00:00	10.25	189.3	-15.6	-15.7	102.2	96.1
2011-01-01T16:00:00	9.96	192.1	-15.4	-15.6	102.3	96
2011-01-01T17:00:00	9.76	195.4	-15.4	-15.6	102.4	96
2011-01-01T18:00:00	9.56	201.2	-15.2	-15.4	102.5	96

APPENDIX B – Code Scripts

B.1 – Aerodynamic Analysis

Data of the aerodynamic parameters lift and drag from the sources described in Chapter 3 are written in a CSV file named 'Aerodynamic_data.csv' and it is illustrated in Figure B.1.

The first column is the angle of attack in degrees, for the next columns, the headers have the following logic: first letter is 'd' of drag or 'l' of lift, next two letters are the first letters of each main author (i.e. Homolada et al. (2010) is 'ho') and last letters are 'ice' for the icing case of 'clean' of the clean case. As an example, the second column of the table, 'd_ho_ice' represents the drag coefficient of Homola et al. (2010) for the icing case.

angle	d_ho_ice	l_ho_ice	d_ho_clean	l_ho_clean	d_et_ice	l_et_ice	d_et_clean	l_et_clean	d_tu_ice	l_tu_ice	d_tu_clean	l_tu_clean	d_ga_ice	l_ga_ice	d_ga_clean	l_ga_clean	d_hu_ice	l_hu_ice	d_hu_clean	l_hu_clean
0	0.0390	0.4708	0.0260	0.4749	0.0171	0.3585	0.0052	0.4217	0.0450	0.4545	0.0099	0.5042	0.0106	0.4014	0.0087	0.4666	0.0300	0.3521	0.0150	0.3863
1	0.0403	0.5752	0.0284	0.5766	0.0195	0.4633	0.0060	0.5369	0.0394	0.5740	0.0104	0.6139	0.0143	0.4750	0.0106	0.5758	0.0326	0.4137	0.0162	0.4969
2	0.0417	0.6836	0.0290	0.6777	0.0218	0.5680	0.0065	0.6487	0.0394	0.6928	0.0108	0.7235	0.0179	0.5486	0.0125	0.6850	0.0355	0.4876	0.0174	0.6002
3	0.0445	0.7933	0.0332	0.7720	0.0242	0.6710	0.0069	0.7720	0.0412	0.8130	0.0113	0.8395	0.0216	0.6223	0.0145	0.7942	0.0382	0.5542	0.0188	0.7027
4	0.0481	0.8891	0.0373	0.8639	0.0267	0.7708	0.0075	0.8781	0.0460	0.9304	0.0119	0.9554	0.0252	0.6959	0.0164	0.9033	0.0410	0.6174	0.0201	0.8051
5	0.0517	0.9834	0.0414	0.9611	0.0311	0.8542	0.0081	0.9865	0.0493	1.0257	0.0127	1.0630	0.0289	0.7695	0.0184	1.0125	0.0453	0.6917	0.0226	0.8944
6	0.0561	1.0392	0.0480	1.0369	0.0319	0.9245	0.0091	1.0914	0.0568	1.1198	0.0135	1.1705	0.0388	0.7894	0.0218	1.1101	0.0495	0.7678	0.0254	0.9828
7	0.0606	1.0943	0.0546	1.1072	0.0409	0.9981	0.0099	1.1839	0.0741	1.1713	0.0150	1.2685	0.0488	0.8089	0.0252	1.2076	0.0538	0.8391	0.0278	1.0683
8	0.0662	1.1326	0.0628	1.1774	0.0451	1.0534	0.0103	1.2621	0.0915	1.2232	0.0164	1.3666	0.0587	0.8284	0.0286	1.3050	0.0565	0.8870	0.0325	1.1162
9	0.0722	1.1598	0.0713	1.2239	0.0498	1.0965	0.0113	1.3310	0.1124	1.2751	0.0179	1.4646	0.0687	0.8479	0.0321	1.4025	0.0589	0.9437	0.0371	1.1592
10	0.0932	1.1865	0.0798	1.2852	0.0639	1.1273	0.0149	1.3907	0.1266	1.3270	0.0193	1.5627	0.0787	0.8674	0.0355	1.5000	0.0741	0.9815	0.0460	1.2139

Figure B.1: Illustration of the CSV file for the aerodynamic parameters for the five references.

The following code, written in Python programming language, is repeated for each one of the five references, and the results of this code are the values written in Table 3.

```
import pandas as pd
import numpy as np

# Reading data from the CSV file #
file = pd.read_csv('Aerodynamic_data.csv')
# An array with Tip-to-speed ratio from 0 to 20 with 0.1 of variation #
lbda = np.arange(0,20.1,0.1)
Nb = 3 # Number of blades #
angle = file['angle'] # Angle of attack #

# Aerodynamic coefficients of Etemaddar et al. (2012) #
d_ice = file['d_et_ice'] # Drag for icing case
l_ice = file['l_et_ice'] # Lift for icing case
d_clean = file['d_et_clean'] # Drag for clean case
l_clean = file['l_et_clean'] # Lift for clean case
```

```
# Calculation of Cp,max for each combination of theoretical Cd/Cl
according to Wilson's equation #

# Icing case #

list_ice1 = []

for i in range(len(angle)):

    cp_max = (16/27)*lbda*( (Nb**(2/3) / (1.48 + (Nb**(2/3) -
    0.04)*lbda + 0.0025*(lbda**2))) -
    ((d_ice[i]/l_ice[i])*(1.92*Nb*lbda/(1+2*Nb*lbda))))

    list_ice1.append(cp_max) # Adding to list_ice1 the maximum power
    coefficient of the clean case of each angle #


list_ice2 = []

for i in range(len(list_ice1)):

    list_ice2.append(max(list_ice1[i])) # Adding to list2 the maximum
     power coefficient of the icing case of each angle #


# Looking for the maximum value in list_ice2 for the icing case #

a = round(max(list2),4) # Maximum power coefficient

b = list2.index(max(list2)) # In this case, the index of the maximum
value correspond to the angle

c = lbda[np.nanargmax(list1[b])] # Tip-to-speed ratio for the maximum
power coefficient


# Calculation of Cp,max for each combination of theoretical Cd/Cl
according to Wilson's equation #

# Clean Case #

list_clean1 = []

for i in range(len(angle)):

    cp_max_c = (16/27)*lbda*( (Nb**(2/3) / (1.48 + (Nb**(2/3) -
    0.04)*lbda + 0.0025*(lbda**2))) -
    ((d_clean[i]/l_clean[i])*(1.92*Nb*lbda/(1+2*Nb*lbda))))

    list_clean1.append(cp_max_c) # Adding to list3 the maximum power
coefficient of the clean case of each angle #


list_clean2 = []

for i in range(len(list_clean1)):

    list_clean2.append(max(list_clean1[i])) # Adding to list4 the
maximum power coefficient of the icing case of each angle #

# Looking for the maximum value in list_clean1 #

d = round(max(list4),4) # Maximum power coefficient
```

```
e = list4.index(max(list4)) # In this case, the index of the maximum
value correspond to the angle
f = lbda[np.nanargmax(list3[e])] # Tip-to-speed ratio for the maximum
power coefficient


# Non-optimized power coefficient for the icing case #
g = round(list_ice1[e][lbda.tolist().index(f)],4)


# Printing the results of the Clean case #
print('The maximum power coefficient for the clean case is Cp,clean = '
+ str(d) + ' when angle of attack is α,clean = ' + str(e) + '°' + ' and
tip-to-speed ratio is λ,clean = ' + str(round(f,1)))


# Printing the results of the Optimized case #
print('The maximum power coefficient for the icing case is Cp,opt = ' +
str(a) + ' when angle of attack is α,opt = ' + str(b) + '°' + ' and
tip-to-speed ratio is λ,opt = ' + str(round(c,1)))


# Printing the results of the non-optimized case #
print('Non-optimized power coefficient is Cp,non-opt = ' + str(g))
```

B.2 – Energy Yield

From this appendix B.2 to B.3, the next code depends on the previous, but they are separated for a better understanding of each step. The input files are those in Appendix A. For the energy production, we need to run the following code for each location:

```
import pandas as pd
import numpy as np
import matplotlib.pyplot as plt
import math
import seaborn as sns
from datetime import datetime
import sys, os

# Input the name of the CSV file with the weather data #
input1 = input('Complete Input File Name: ') # Name of the file #
input2 = input('Name of Location: ') # Name of the location #
df = pd.read_csv(input1)

# Wind speed series in an array
df['Date/time [UTC]']=pd.to_datetime(df['Date/time [UTC]']) #
Transforming the dates #
ws = np.asarray(df['Speed_50m [m/s]']) # Wind speed #
temp2 = np.asarray(df['Temperature_2m [degrees C]']) # Temperature #
press = np.asarray(df['Pressure_0m [kPa]']) # Pressure #
date = np.asarray(df['Date/time [UTC]']) # Date #
rh = np.asarray(df['RH_2m [%]']) # Relative Humidity #

# Constants for power coefficients for wind speed of 2.2, 3.2, 6.0, 7.3
and 19.2 m/s #
# Cp for clean case #
cp22_clean = 0.4755
cp32_clean = 0.4565
cp60_clean = 0.5126
cp73_clean = 0.4984
cp192_clean = 0.4173
# Cp for non-optimized case #
cp22_ice = 0.4157
```

```
cp32_ice = 0.3495
cp60_ice = 0.3821
cp73_ice = 0.3461
cp192_ice = 0.3829
# Cp for Optimized case #
cp22_opt = 0.4526
cp32_opt = 0.3848
cp60_opt = 0.4340
cp73_opt = 0.4078
cp192_opt = 0.4002


# Constants of turbine and environment #
pi = math.pi
R = 45


# Power coefficients are interpolated with the wind speed from weather
data and the calculated Cp #
# Power coefficients for Clean case #
cp_clean = []
for i in range(len(ws)):
    if ws[i] >= 3 and ws[i] <= 3.2:
        cp_n = (ws[i] - 2.2) * (cp32_clean - cp22_clean) / (3.2 - 2.2)
        + cp22_clean
    elif ws[i] > 3.2 and ws[i] <= 6:
        cp_n = (ws[i] - 3.2) * (cp60_clean - cp32_clean) / (6 - 3.2) +
        cp32_clean
    elif ws[i] > 6 and ws[i] <= 7.3:
        cp_n = (ws[i] - 6) * (cp73_clean - cp60_clean) / (7.3 - 6) +
        cp60_clean
    elif ws[i] > 7.3 and ws[i] <= 19.2:
        cp_n = (ws[i] - 7.3) * (cp192_clean - cp73_clean) / (19.2 -
        7.3) + cp73_clean
    cp_clean.append(cp_n)
# Power coefficients for non-optimized case #
cp_ice = []
for i in range(len(ws)):
    if ws[i] >= 3 and ws[i] <= 3.2:
```

```
        cp_b = (ws[i] - 2.2) * (cp32_ice - cp22_ice) / (3.2 - 2.2) +
        cp22_ice
    elif ws[i] > 3.2 and ws[i] <= 6:
        cp_b = (ws[i] - 3.2) * (cp60_ice - cp32_ice) / (6 - 3.2) +
        cp32_ice
    elif ws[i] > 6 and ws[i] <= 7.3:
        cp_b = (ws[i] - 6) * (cp73_ice - cp60_ice) / (7.3 - 6) +
        cp60_ice
    elif ws[i] > 7.3 and ws[i] <= 19.2:
        cp_b = (ws[i] - 7.3) * (cp192_ice - cp73_ice) / (19.2 - 7.3) +
        cp73_ice
    cp_ice.append(cp_b)
### Power coefficients for Optmized case ###
cp_opt = []
for i in range(len(ws)):
    if ws[i] >= 3 and ws[i] <= 3.2:
        cp_a = (ws[i] - 2.2) * (cp32_opt - cp22_opt) / (3.2 - 2.2) +
        cp22_opt
    elif ws[i] > 3.2 and ws[i] <= 6:
        cp_a = (ws[i] - 3.2) * (cp60_opt - cp32_opt) / (6 - 3.2) +
        cp32_opt
    elif ws[i] > 6 and ws[i] <= 7.3:
        cp_a = (ws[i] - 6) * (cp73_opt - cp60_opt) / (7.3 - 6) +
        cp60_opt
    elif ws[i] > 7.3 and ws[i] <= 19.2:
        cp_a = (ws[i] - 7.3) * (cp192_opt - cp73_opt) / (19.2 - 7.3) +
        cp73_opt
    cp_opt.append(cp_a)


# Air Density Calculation #
Rc = 0.287
rho_r = []
for i in range(len(temp2)):
    rho_i = press[i]/(Rc * (temp2[i] + 273.15))
    rho_r.append(rho_i)
# Pass the list of Values to arrays #
rho = np.asarray(rho_r)
cp_c = np.asarray(cp_clean) # clean
cp_i = np.asarray(cp_ice) # Icing
```

```
cp_o = np.asarray(cp_opt) # Optimized


# Calculating energy yield for 3 cases #
# Power for Clean Case #
power_clean = []
for i in range(len(ws)):
    if ws[i] <= 3:
        p = 0
        power_clean.append(p)
    else:
        p = (0.5 * rho[i] * pi * (R ** 2) * (ws[i] ** 3) *
        cp_c[i])/1000
        if p <= 1000:
            power_clean.append(p)
        else:
            p = 1000
            power_clean.append(p)

# Power non-optimized case #
power_ice = []
for i in range(len(ws)):
    if ws[i] <= 3:
        p_i = 0
        power_ice.append(p_i)
    else:
        p_i = (0.5 * rho[i] * pi * (R ** 2) * (ws[i] ** 3) *
        cp_i[i])/1000
        if p_i <= 1000:
            power_ice.append(p_i)
        else:
            p_i = 1000
            power_ice.append(p_i)

# Power curve for Optimized case #
power_opt = []
for i in range(len(ws)):
    if ws[i] <= 3:
```

```
        p_o = 0
        power_opt.append(p_o)
    else:
        p_o = (0.5 * rho[i] * pi * (R ** 2) * (ws[i] ** 3) *
        cp_o[i])/1000
        if p_o <= 1000:
            power_opt.append(p_o)
        else:
            p_o = 1000
            power_opt.append(p_o)
# Applying the conditions for atmospheric ice #
# Real power with no optimization #
power_real_nonopt = []
power_nonopt_clean = []
power_real = []
for i in range(len(ws)):
    if temp2[i] <= -4 and temp2[i] >= -20 and rh[i] >= 99:
        if ws[i] < 3:
            p = None
            power_real_nonopt.append(p)
            power_real.append(p)
            power_nonopt_clean.append(None)
        else:
            p = (0.5 * rho[i] * pi * (R ** 2) * (ws[i] ** 3) *
            cp_i[i])/1000
            if p < 1000:
                power_real_nonopt.append(p)
                power_real.append(p)
                power_nonopt_clean.append(None)
            else:
                p = 1000
                power_real_nonopt.append(p)
                power_real.append(p)
                power_nonopt_clean.append(None)
    else:
        if temp2[i] < -20:
            p = None
```

```
            power_real_nonopt.append(p)
            power_real.append(p)
            power_nonopt_clean.append(None)
        else:
            if ws[i] < 3:
                p = 0
                power_nonopt_clean.append(p)
                power_real.append(p)
                power_real_nonopt.append(None)
            else:
                p = (0.5 * rho[i] * pi * (R ** 2) * (ws[i] ** 3) *
                cp_c[i])/1000
                if p < 1000:
                    power_nonopt_clean.append(p)
                    power_real_nonopt.append(None)
                    power_real.append(p)
                else:
                    p = 1000
                    power_nonopt_clean.append(p)
                    power_real_nonopt.append(None)
                    power_real.append(p)

# Real power with optimization #
power_real_opt = []
power_optimized = []
power_opt_clean = []
for i in range(len(ws)):
    if temp2[i] <= -4 and temp2[i] >= -20 and rh[i] >= 99:
        if ws[i] < 3:
            p = None
            power_real_opt.append(p)
            power_optimized.append(p)
            power_opt_clean.append(None)
        else:
            p = (0.5 * rho[i] * pi * (R ** 2) * (ws[i] ** 3) *
            cp_o[i])/1000
            if p < 1000:
```

```
                power_real_opt.append(p)
                power_optimized.append(p)
                power_opt_clean.append(None)
            else:
                p = 1000
                power_real_opt.append(p)
                power_optimized.append(p)
                power_opt_clean.append(None)
    else:
        if temp2[i] < -20:
            p = None
            power_real_opt.append(p)
            power_optimized.append(p)
            power_opt_clean.append(None)
        else:
            if ws[i] < 3:
                p = 0
                power_opt_clean.append(p)
                power_optimized.append(p)
                power_real_opt.append(None)
            else:
                p = (0.5 * rho[i] * pi * (R ** 2) * (ws[i] ** 3) *
                cp_c[i])/1000
                if p < 1000:
                    power_opt_clean.append(p)
                    power_optimized.append(p)
                    power_real_opt.append(None)
                else:
                    p = 1000
                    power_opt_clean.append(p)
                    power_optimized.append(p)
                    power_real_opt.append(None)

# Plotting the power curve for this location #
sns.scatterplot(ws, power_opt_clean, label = 'Clean', s = 20)
sns.scatterplot(ws, power_real_opt, label = 'Optimized', color =
'#21DC0A', alpha = 1, s = 15)
```

```
sns.scatterplot(ws, power_real_nonopt, label = 'Non-optimized', color =
'#CD4E4E', alpha = 0.8, s = 15)

plt.ylabel('Power [kW]')

plt.xlabel('Wind Speed [m/s]')

plt.title(input2)

plt.legend()

plt.tight_layout()

plt.show()


# Creating a data frame with the results #

df1 = pd.DataFrame(list(zip(date, ws, temp2, rh, power_clean,
power_real, power_optimized)), columns = ['date', 'ws', 'temp20', 'rh',
'power_clean', 'power_real', 'power_optimized'])
```

B.3 – Power Losses

B.3.1 – Yearly Losses

With the final data frame from B.2 – Energy Yield

```
# Data series in an array #
df1['date']=pd.to_datetime(df1['date']) # Transform to date ytpe
ws = np.asarray(df1['ws'])
temp2 = np.asarray(df1['temp20'])
date = np.asarray(df1['date'])

# Transform date as index #
df1 = df1.set_index(['date'])
df1.index = pd.to_datetime(df1.index, unit='s')

# Group by month and year #
sumbymonth = df1.resample('M').sum()
sumbyyear = df1.resample('Y').sum()

p_clean_bymonth = sumbymonth['power_clean'] # Power grouped by month
for the clean case #

p_real_bymonth = sumbymonth['power_real'] # Power grouped by month for
the non-optimized case #

p_opt_bymonth = sumbymonth['power_optimized'] # Power grouped by month
for the optimized case #

p_clean_byyear = sumbyyear['power_clean'] # Power grouped by year for
the clean case #

p_real_byyear = sumbyyear['power_real'] # Power grouped by year for the
non-optimized case #
p_opt_byyear = sumbyyear['power_optimized'] # Power grouped by month
for the optimized case #
# Months #
m = ['Jan', 'Feb', 'Mar', 'Apr', 'May', 'Jun', 'Jul', 'Aug', 'Sep',
'Oct', 'Nov', 'Dec']
```

```
# Years #
y = ['2011', '2012', '2013', '2014', '2015', '2016', '2017', '2018',
'2019']
# Losses by year in a list #
# Non-optimized case #
loss_year = []
for i in range(len(p_clean_byyear)):
    loss = (1 - p_real_byyear[i]/p_clean_byyear[i])
    loss_year.append(loss)
loss_year_mean = sum(loss_year)/len(loss_year) # Average losses for the
non-optimized case #
# Optimized Case #
opt_year = []
for i in range(len(p_clean_byyear)):
    opt = (1 - p_opt_byyear[i]/p_clean_byyear[i])
    opt_year.append(opt)
opt_year_mean = sum(opt_year)/len(opt_year) # Average losses for the
optimized case #


# Plotting losses by year #
sns.set(style="darkgrid")
fig, ax = plt.subplots()
line1 = ax.plot(y, loss_year, label = 'Icing Losses', color =
'#CD4E4E')
line2 = ax.axhline(loss_year_mean, color='#CD4E4E', linestyle='--',
label = 'Mean Losses')
line3 = ax.plot(y, opt_year, label = 'Optimized Losses', color =
'#21DC0A')
line4 = ax.axhline(opt_year_mean, color='#21DC0A', linestyle='--',
label = 'Mean Losses')
ax.set_title(input2)
ax.set_ylabel('Mean Losses (%)')
vals = ax.get_yticks()
ax.set_yticklabels(['{:,.1%}'.format(x) for x in vals])
ax.legend()
plt.xticks(rotation=60)
plt.tight_layout()
plt.show()
```

B.3.2 – Monthly Mean Losses

With data from B.3.1 – Yearly Losses

```
# Losses by month in a list #
loss_month = []
for i in range(len(p_clean_bymonth)):
    loss = (1 - p_real_bymonth[i]/p_clean_bymonth[i])
    loss_month.append(loss)
# Optimization by month in a list #
opt_month = []
for i in range(len(p_clean_bymonth)):
    opt = (1 - p_opt_bymonth[i]/p_clean_bymonth[i])
    opt_month.append(opt)

# INDEXES FOR THE LOOP IN THE NEXT STEP #
# January #
a = 0
jan_index = [a]
for i in range(0,9):
    a = a + 12
    jan_index.append(a)
# February #
a = 1
feb_index = [a]
for i in range(0,9):
    a = a + 12
    feb_index.append(a)
# March #
a = 2
mar_index = [a]
for i in range(0,9):
    a = a + 12
    mar_index.append(a)
# April #
a = 3
```

```
apr_index = [a]
for i in range(0,9):
    a = a + 12
    apr_index.append(a)
# May #
a = 4
may_index = [a]
for i in range(0,9):
    a = a + 12
    may_index.append(a)
# June #
a = 5
jun_index = [a]
for i in range(0,9):
    a = a + 12
    jun_index.append(a)
# July #
a = 6
jul_index = [a]
for i in range(0,9):
    a = a + 12
    jul_index.append(a)
# August #
a = 7
aug_index = [a]
for i in range(0,9):
    a = a + 12
    aug_index.append(a)
# September #
a = 8
sep_index = [a]
for i in range(0,9):
    a = a + 12
    sep_index.append(a)
# October #
a = 9
```

```
oct_index = [a]
for i in range(0,9):
    a = a + 12
    oct_index.append(a)
# November #
a = 10
nov_index = [a]
for i in range(0,9):
    a = a + 12
    nov_index.append(a)
# December #
a = 11
dec_index = [a]
for i in range(0,9):
    a = a + 12
    dec_index.append(a)


 # Losses for each month in separated lists for NON-OPTIMIZED case #
jan_mm = []
for i in range(len(loss_month)):
    if i in jan_index:
        jan_i = loss_month[i]
        jan_mm.append(jan_i)
feb_mm = []
for i in range(len(loss_month)):
    if i in feb_index:
        feb_i = loss_month[i]
        feb_mm.append(feb_i)
mar_mm = []
for i in range(len(loss_month)):
    if i in mar_index:
        month_i = loss_month[i]
        mar_mm.append(month_i)
apr_mm = []
for i in range(len(loss_month)):
    if i in apr_index:
```

```
        month_i = loss_month[i]
        apr_mm.append(month_i)
may_mm = []
for i in range(len(loss_month)):
    if i in may_index:
        month_i = loss_month[i]
        may_mm.append(month_i)
jun_mm = []
for i in range(len(loss_month)):
    if i in jun_index:
        month_i = loss_month[i]
        jun_mm.append(month_i)
jul_mm = []
for i in range(len(loss_month)):
    if i in jul_index:
        month_i = loss_month[i]
        jul_mm.append(month_i)
aug_mm = []
for i in range(len(loss_month)):
    if i in aug_index:
        month_i = loss_month[i]
        aug_mm.append(month_i)
sep_mm = []
for i in range(len(loss_month)):
    if i in sep_index:
        month_i = loss_month[i]
        sep_mm.append(month_i)
oct_mm = []
for i in range(len(loss_month)):
    if i in oct_index:
        month_i = loss_month[i]
        oct_mm.append(month_i)
nov_mm = []
for i in range(len(loss_month)):
    if i in nov_index:
        month_i = loss_month[i]
```

```
        nov_mm.append(month_i)
dec_mm = []
for i in range(len(loss_month)):
    if i in dec_index:
        month_i = loss_month[i]
        dec_mm.append(month_i)

 # Losses for each month in separated lists for OPTIMIZED case #
jan_oo = []
for i in range(len(opt_month)):
    if i in jan_index:
        jan_o = opt_month[i]
        jan_oo.append(jan_o)
feb_oo = []
for i in range(len(opt_month)):
    if i in feb_index:
        feb_o = opt_month[i]
        feb_oo.append(feb_o)
mar_oo = []
for i in range(len(opt_month)):
    if i in mar_index:
        mar_o = opt_month[i]
        mar_oo.append(mar_o)
apr_oo = []
for i in range(len(opt_month)):
    if i in apr_index:
        apr_o = opt_month[i]
        apr_oo.append(apr_o)
may_oo = []
for i in range(len(opt_month)):
    if i in may_index:
        may_o = opt_month[i]
        may_oo.append(may_o)
jun_oo = []
for i in range(len(opt_month)):
    if i in jun_index:
```

```
        month_i = loss_month[i]
        jun_oo.append(month_i)
jul_oo = []
for i in range(len(opt_month)):
    if i in jul_index:
        month_i = loss_month[i]
        jul_oo.append(month_i)
aug_oo = []
for i in range(len(opt_month)):
    if i in aug_index:
        month_i = loss_month[i]
        aug_oo.append(month_i)
sep_oo = []
for i in range(len(opt_month)):
    if i in sep_index:
        month_i = loss_month[i]
        sep_oo.append(month_i)
oct_oo = []
for i in range(len(opt_month)):
    if i in oct_index:
        oct_o = opt_month[i]
        oct_oo.append(oct_o)
nov_oo = []
for i in range(len(opt_month)):
    if i in nov_index:
        month_i = opt_month[i]
        nov_oo.append(month_i)
dec_oo = []
for i in range(len(opt_month)):
    if i in dec_index:
        dec_o = opt_month[i]
        dec_oo.append(dec_o)


# Monthly losses for the non-optimized case #
monthly_loss = [jan_mm, feb_mm, mar_mm, apr_mm, may_mm, jun_mm, jul_mm,
aug_mm, sep_mm, oct_mm, nov_mm, dec_mm]
```

```
# Monthly mean losses for the non-optimized case #
loss_mm = []
for i in range(len(monthly_loss)):
    mm = sum(monthly_loss[i])/len(monthly_loss[i])
    loss_mm.append(mm)

# Monthly losses for the noptimized case #
monthly_opt = [jan_oo, feb_oo, mar_oo, apr_oo, may_oo, jun_oo, jul_oo,
aug_oo, sep_oo, oct_oo, nov_oo, dec_oo]
# Monthly mean losses for the noptimized case #
loss_oo = []
for i in range(len(monthly_opt)):
    oo = sum(monthly_opt[i])/len(monthly_opt[i])
    loss_oo.append(oo)

# Plotting the losses
x = np.arange(len(m))
width = 0.35 # width of the bars
fig, ax1 = plt.subplots()
rect1 = ax1.bar(x - width/2, loss_mm, width, label = 'Icing', color =
'#CD4E4E')
rect2 = ax1.bar(x + width/2, loss_oo, width, label = 'Optimized', color
= '#21DC0A')
ax1.set_ylabel('Mean Losses (%)')
ax1.set_title(input2)
ax1.set_xticks(x)
vals = ax1.get_yticks()
ax1.set_yticklabels(['{:,.1%}'.format(x) for x in vals])
ax1.set_xticklabels(m)
ax1.legend()
plt.tight_layout()
plt.show()
```